

UCSF

UC San Francisco Electronic Theses and Dissertations

Title

Identification and analysis of an asymmetrically localized determinant of cell fate in *Saccharomyces cerevisiae*

Permalink

<https://escholarship.org/uc/item/96j883nd>

Author

Sil, Anita,

Publication Date

1996

Peer reviewed|Thesis/dissertation

Identification and Analysis of an Asymmetrically Localized
Determinant of Cell Fate in Saccharomyces cerevisiae

by

Anita Sil

DISSERTATION

Submitted in partial satisfaction of the requirements for the degree of

DOCTOR OF PHILOSOPHY

in

Biochemistry

in the

GRADUATE DIVISION

of the

UNIVERSITY OF CALIFORNIA

San Francisco



DEDICATION

To my parents, Anil and Dipti Sil

ACKNOWLEDGEMENTS

The past six years have been a wonderful voyage of discovery, both personally and professionally. There are many people who have contributed in a multitude of ways to my life at UCSF. I am so grateful to Ira Herskowitz for creating an environment in which graduate students can flourish. His support, guidance, and friendship have been invaluable. I would also like to thank my thesis committee, Andrew Murray, Cori Bargmann, and Cynthia Kenyon, for always displaying the highest level of enthusiasm and interest in my project.

I might never have arrived at UCSF's doorstep were it not for Harold Varmus and Brenda Herschbach Jarrell, who opened the golden door of opportunity for me. That first long-ago summer at UCSF was made infinitely warmer by the friendship and advice of Peter Pryciak, Caroline Goutte, Dave Kaplan, and Jeanne Harris.

The intellectual environment at UCSF is a unique melange of informality and amiable intensity--and just plain enjoyment of the mysteries of biology. Interacting with people in the community has been a priceless asset and a great deal of fun. I would especially like to thank Ray Deshaies, Tim Stearns, Pat O'Farrell, and Dave Morgan for their attention and input. Our longtime neighbors, the O'Farrell lab, and our former neighbors, the Guthrie and O'Shea labs, have been an enormous resource. I thank Erin for generously allowing me to use her microscope equipment.

I am grateful to Sue Adams and Rachel Mozesson for always having a kind word, a smile, and excellent advice to smooth my path.

Many other friends have made the intervening years a very special time. I have always admired the intellect and insight of Heather Colbert.

Svetlana Shtrom has been a warm and selfless friend and an amazing example of true grit and determination. Phil Moore has taught me the power of the cosmic ridgehand, which is not to be underestimated, and given me the gift of his time and friendship.

I owe a great deal to both past and present members of the Herskowitz lab. Margareta Andersson, Nia Le, and Dora Ayala concocted the solutions, poured the plates, and ordered the reagents that made the work in this thesis possible. Warren Kruger showed me how to do the first of many pedigrees. I will always treasure the infectious enthusiasm of Craig Peterson and the noisy irreverence of Joe Ogas. Aaron Neiman and Janet Chenevert were excellent intellectual role models. Matthias Peter and Joe Gray are two of the people I most enjoyed talking to about science; I appreciate their infinite encouragement and support, for which I also thank Bruce Cree. Nicole Valtz has been a compatriot throughout interviews, lab choices, orals, and thesis writing. Flora Banuett devotes a great deal of her time to keeping the lab operational, for which we are all grateful. I thank Judy Shih and Seiko Ishida for the pleasure of introducing them to yeast. I am grateful to Mary Maxon for pursuing aspects of the *ASH1* project, and I hope she will glean as much from working on *HO* regulation as I have. I also thank all the "junior" members of the Herskowitz lab for setting a high standard that the rest of us try to live up to!

Special mention must be made of my baymates. Hay-Oak Park has been an ardent, unconditional supporter for the duration of my graduate career. Her guidance and experience will be sorely missed in *our* lab, but will make *her* lab an exciting and productive place to be. Sylvia Sanders has brought a great deal of laughter and happiness into my life. It's a good thing

we are leaving the lab at the same time, for I could not bear to be left behind. And what can I say about Ramon Tabtiang? We are all proud and lucky to be part of his present, and look forward to great things in his future. I will always prize my friendship with these three as being one of the highlights of graduate school.

UCSF has given me another great gift, the opportunity to meet my husband, Joachim Li. I have learned many valuable things from Joachim, most of them unrelated to yeast genetics. I admire his grace, perseverance, humor, intellect and dedication, but even more I admire his serene temperament, which will keep him standing through the roughest storms.

Penultimately, I thank my parents. It takes a great deal of courage to uproot oneself and travel to a foreign country in pursuit of a better future; my parents went through that transition twice in their lifetime. They are both dedicated, unselfish people whose attention to their work is unparalleled. If I ever achieve a tenth of what they have accomplished, I will consider myself lucky.

Finally, I thank Kim Nasmyth, for being a gracious communicator of results and ideas before publication, as well as a top-notch motivator.

A version of Chapter Two originally appeared as Sil and Herskowitz (1996), *Cell*, **84**: 711-722.

UNIVERSITY OF CALIFORNIA, SAN FRANCISCO

BERKELEY • DAVIS • IRVINE • LOS ANGELES • RIVERSIDE • SAN DIEGO • SAN FRANCISCO



SANTA BARBARA • SANTA CRUZ

ANITA SIL
DEPARTMENT OF BIOCHEMISTRY AND
BIOPHYSICS
SAN FRANCISCO, CALIFORNIA 94143-0448
(415)476-4985 FAX # (415)502-5145
E-MAIL: SIL@CGL.UCSF.EDU

August 7, 1996

Cell Press
1050 Massachusetts Avenue,
Cambridge, MA 02138
fax: 617-661-7061

To whom it may concern,

I would like permission from *Cell* to reprint the article "Identification of an Asymmetrically Localized Determinant, Ash1p, Required for Lineage-Specific Transcription of the Yeast *HO* Gene" (authored by myself and Ira Herskowitz) for my PhD thesis. The appropriate reference for this article is *Cell* 84 (711-722). University Microfilms, which will transfer my dissertation to microfilm, requests permission to supply single copies on demand. Please respond by fax to 415-502-5145.

Thank you for your consideration.

Sincerely,

Anita Sil

Anita Sil 8/14/96

vii

Permission granted subject to citation of the original manuscript, and notation that copyright is held by Cell Press. (Our permission is contingent on permission of the author.)

vii

**Identification and Analysis of an Asymmetrically Localized Determinant of
Cell Fate in *Saccharomyces cerevisiae***

Anita Sil

ABSTRACT

Asymmetric cell fate is a process fundamental to development. *Saccharomyces cerevisiae* is a single-celled organism that exhibits asymmetric determination of cell fate. Cell division yields a mother cell, which is competent to transcribe the *HO* gene and switch mating type, and a daughter cell, which is not. Thus, mother and daughter cells inherit a different transcriptional potential. I have isolated a mutant that disrupts the normal process of asymmetric cell fate in *S. cerevisiae*: mutant daughters transcribe *HO* and switch mating type. This mutation defines the *ASH1* (Asymmetric Synthesis of *HO*) gene. Deletion and overexpression of *ASH1* cause reciprocal cell-fate transformations: in *ash1Δ* strains, daughters switch mating type at the same high frequency as mothers. Conversely, overexpression of *ASH1* inhibits switching in mother cells. In wild-type cells, Ash1p function is limited to daughter cells via the localization of Ash1p to the incipient daughter nucleus of cells that have undergone nuclear division. Thus Ash1p is a cell-fate determinant that is asymmetrically localized to the daughter nucleus where it inhibits *HO* transcription. Analysis of the *ASH1* gene reveals that the 3' untranslated region (UTR) of the Ash1 messenger RNA is required for asymmetric localization of Ash1p. These data suggest that Ash1 RNA might be localized to the incipient daughter cell via its 3'UTR.

Furthermore, the localization of Ash1p is perturbed in cells that lack Bud8p, a protein that localizes to the distal pole of the daughter cell. I propose that Bud8p is a component of a landmark required for asymmetric localization of Ash1 RNA to the distal pole of the daughter cell.

Ira Herskowitz

TABLE OF CONTENTS

CHAPTER ONE	Introduction	1
CHAPTER TWO	Identification of Ash1p, an Asymmetrically Localized Regulator of Cell Fate in Yeast	42
CHAPTER THREE	Establishment of Asymmetric Localization of Ash1 Protein	100
CHAPTER FOUR	Conclusion	137
APPENDIX ONE	A High Copy Screen for Genes that Activate <i>HO</i> in Daughter Cells	144
APPENDIX TWO	The Effect of Vegetative Growth on the Switching Pattern	166
APPENDIX THREE	Regions of the <i>HO</i> Promoter Required for Mother/Daughter Regulation	178
APPENDIX FOUR	Miscellaneous Pedigrees	192
REFERENCES		197

LIST OF TABLES

- 2-1. Switching Behavior of Strains Lacking or Overproducing *ASH1* or Lacking *URS2*
- 2-2. Chapter Two Strain List
- 3-1. Chapter Three Strain List
- A1-1. The Pedigree of Death
- A1-2. Secondary Screens
- A1-3. The Effect of the High Copy Plasmids in the Four-Shmoo Microcolony Assay
- A1-4. Appendix One Strain List
- A2-1. The Switching Frequency of Various Strains
- A2-2. Switching Frequency of *HO ste3Δ* Strain Transformed with a *GAL-HO* Plasmid
- A2-3. Appendix Two Strain List
- A3-1. CEN-ARS *HO* Plasmids Bypass Mother/Daughter Regulation
- A3-2. CEN-ARS *HO* Plasmids Bypass the *SWI5* Requirement
- A3-3. Bypass of Mother/Daughter Regulation by Various *HO* Constructs
- A3-4. Bypass of *SWI5* by Minimal *HO* Promoter Construct Integrated at *URA3*
- A3-5. Bypass of *SWI5* by Minimal and Large *HO* Promoter Constructs
- A3-6. Appendix Three Strain List
- A4-1. Switching Frequency of Various *HO* Strains
- A4-2. Appendix Four Strain List

LIST OF FIGURES

- 1-1. Mechanisms of Localization of Cell-Fate Determinants
- 1-2. Regulation of Sporangium Development in *B. subtilis*
- 1-3. The Cell Cycle of *C. crescentus*
- 1-4. FlbE Localization in *C. crescentus*
- 1-5. Pole Differentiation in *C. crescentus*
- 1-6. Localization of Numb in *Drosophila* Neuroblasts
- 1-7. The First Embryonic Division of *C. elegans*
- 1-8. The Yeast Cell Cycle
- 1-9. Lineage-Specific Regulation of Mating-Type Switching
- 2-1. Mitotic Lineages of Yeast Cells are Stem-Cell Lineages
- 2-2. A Four-Shmoo Microcolony Indicates that both Mother and Daughter Cells have Switched Mating Type
- 2-3. *ash1-1* Daughters Transcribe *HO* RNA
- 2-4. Ash1p has Similarity to the GATA Zn Finger
- 2-5. Ash1p is Localized to One of Two Nuclei in the Majority of Large-Budded Cells
- 2-6. Color images of Ash1p Staining
- 2-7. Ash1p is Localized Asymmetrically in a/ α Cells
- 2-8. Ash1p is Localized to the Incipient Daughter Nucleus
- 2-9. Ash1p is Expressed in a Cell-cycle-Specific Manner
- 2-10. Overexpression of *ASH1* on a 2-micron Plasmid Results in Symmetric Staining
- 2-11. Expression of *HO* RNA in *URS2 Δ* Strains is Dependent on *SWI5* but Independent of *SWI4*
- 2-12. *ASH1* and *SWI5* have Reciprocal Effects on Cell Fate

- 3-1. Models for the Basis of Ash1p Asymmetry
- 3-2. The Bipolar Budding Pattern
- 3-3. Expression of *ASH1* on a Low-Copy Plasmid does not Disrupt Ash1p Asymmetry
- 3-4. Asymmetry of Ash1p Staining in Large-Budded Asynchronous Cells and in Cells After Release from Pheromone Arrest
- 3-5. Replacement of the *ASH1* Promoter with the *GAL* Promoter Results in Asymmetric Staining
- 3-6. The *ASH1* 3'UTR is Required for Ash1p Asymmetry
- 3-7. The Budding Pattern of Mutants Defective in the Bipolar Pattern
- 3-8. The Effect of Mutants Defective in the Bipolar Pattern on Ash1p Localization
- 3-9. *bud8Δ* Cells Display Symmetric Staining of Ash1p
- 3-10. A Distal Pole Landmark that Binds Ash1 RNA is Localized as a Consequence of Bud Growth
- A1-1. A Special Strain Couples Activation of *HO* to Growth Rate
- A1-2. Statistics from the High Copy Screen
- A1-3. Growth of Strains Carrying High Copy Plasmids on Glucose vs. Galactose
- A1-4. Comparison of the Ability of Different Plasmids to Confer Growth on Glucose
- A2-1. Transcription of *HO* Occurs at Normal Levels in *swi4Δ HOURS2Δ* Strains
- A3-1. CEN-ARS Plasmids Containing Different Amounts of *HO* Promoter DNA

CHAPTER ONE

INTRODUCTION

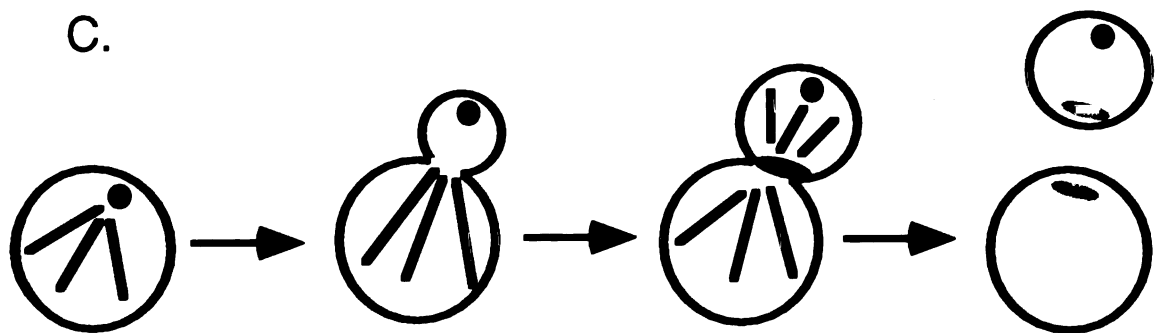
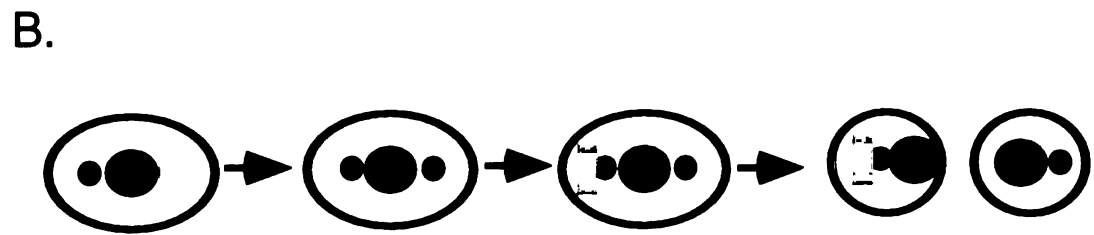
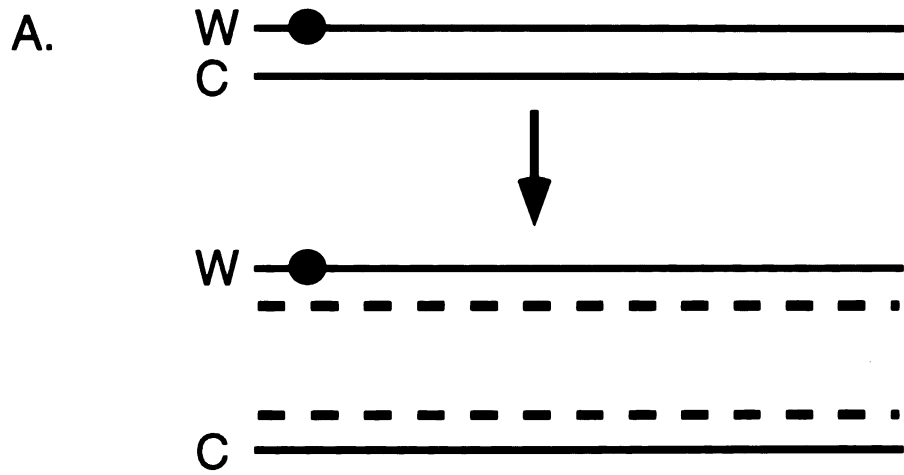
In 1961, Jacob and Monod wrote the following: "The fundamental problem of chemical physiology and of embryology is to understand why tissue cells do not all express, all the time, all the potentialities inherent in their genome." Their cogent words allude to the tantalizing mystery of asymmetric cell division: How does a cell divide to produce two genetically identical cells with fundamentally different fates? Thirty-five years later, the quest to understand the basis of asymmetric cell fate is still paramount.

During the development of a multicellular organism, a fertilized egg is miraculously transformed into a creature composed of cells with a variety of fates and functions; it is clear that asymmetric cell division is crucial for the generation of such diversity. The grand orchestration of asymmetric cell divisions that occurs during the development of multicellular organisms is mirrored on a simpler scale during the lifetime of many unicellular organisms. These systems provide an excellent opportunity to study the mechanism of asymmetric cell fate.

For both multicellular and unicellular organisms, asymmetric cell fate is a result of either "intrinsic" or "extrinsic" differences between sister cells (reviewed in Herskowitz and Horvitz, 1992). An intrinsic difference between sister cells is often generated in the pre-divisional mother cell that gives rise to the sister cells. The partitioning of a cell fate determinant--a molecule that is necessary and sufficient to direct cell fate--to one cell but not the other is the classic example of an intrinsically different division. In contrast, an extrinsic difference occurs when a cell divides to yield two equipotent sister cells that later adopt distinct fates due to external influences such as cell-cell signalling. I will focus mainly on examples of intrinsic asymmetric cell fate.

Intrinsic differences between sister cells often originate from the innate polarity of the pre-divisional mother cell. For example, mRNAs that localize to a particular region of an oocyte can act as determinants that ultimately induce the fate of cells in the resultant embryo (reviewed in St Johnston, 1995). The discrete localization or activation of determinants, whether at the RNA or protein level, can be accomplished by multiple means. What cellular elements can act as the basis of such polarity (see Figure 1-1)? First, DNA strands are inherently asymmetric. The Watson and Crick strands can be distinguished on the basis of nucleotide sequence, and temporal regulation of a modification such as methylation allows an old Watson strand to be distinguished from a new one. If, for example, the mother cell contains a transcriptional activator that can bind only to the old Watson strand, only one of two daughter cells will inherit a chromosome competent to transcribe the gene in question. Second, the two centrosomes are not equivalent. Since centrosome duplication is conservative, the pre-divisional cell contains one old and one new centrosome. Attachment of a cell-fate determinant to one or the other will result in segregation of such a molecule to one of two sister cells. Third, asymmetry can be caused by the process of cell growth itself. For example, a determinant might localize to a particular region of the pre-divisional mother cell via attachment to a molecular landmark. The landmark could be positioned in the pre-divisional cell as a consequence of the directed secretion or membrane deposition that occurs as the cell grows. Attachment of a determinant to such a landmark will result in its partitioning to one of the two sister cells after cell division, provided that the plane of cell division does not bisect the location of the landmark. Alternatively, such landmarks can be remnants of previous sites

Figure 1-1. Mechanisms of Localization of Cell-Fate Determinants. (A) A chromosome is shown on the top line. The Watson strand is designated with a W whereas the Crick strand is designated with a C. The red dot on the Watson strand represents a covalent modification such as methylation. The arrow indicates the process of DNA replication; the newly synthesized strands are indicated by dotted lines. Because the covalent modification machinery is temporally regulated, only one chromatid has a marked Watson strand. Each chromatid will segregate to one of two daughter cells; only one daughter cell will inherit the marked chromatid. (B) A cell is drawn on the left. The black dot in the center of the cell represents the nucleus. The red dot is the "old" centrosome. The second cell has undergone centrosome duplication to generate a "new" centrosome, drawn as a blue dot. The yellow rectangle in the third cell represents a determinant that localizes specifically to the "old" centrosome. After cell division, one daughter inherits the determinant but the other does not. (C) A round mother cell is shown on the left. The black lines represent the actin cytoskeleton, which is oriented toward one point on the cell surface. The red dot is a marker that is deposited at this spot as a function of targeted secretion as the daughter cell grows. At a certain point in the cell cycle, the cytoskeleton reorganizes toward the "neck" between the mother and daughter cells. This reorientation allows molecules necessary for cytokinesis to be targeted to the neck region. The pink oval in the last panel indicates a landmark left at the site of cell division as a result of directed secretion toward the neck of the pre-divisional cell.



of cell division. Finally, asymmetric positioning of the septum in the pre-divisional cell results in two sister cells of different size; this inherent size disparity can be exploited to generate cell fate differences.

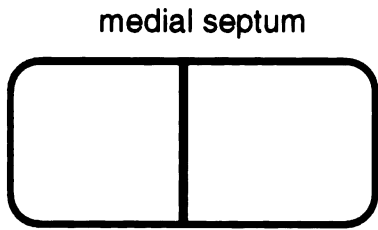
Studies of the basis of asymmetric cell fate often progress in a stepwise fashion. First, determinants of cell fate are identified. Once these molecules are in hand, it is possible to study both how these determinants dictate cell fate and how the pre-divisional cell brings about the segregation or activation of such determinants in one of two sister cells. The ultimate goal is to understand how the innate cellular polarity of the mother cell results in the asymmetric distribution or activity of the determinant. Recently, researchers in various systems have made distinct progress toward this goal. A review of the advances in cell fate asymmetry sets the stage for understanding the regulation of asymmetric cell division in the budding yeast *Saccharomyces cerevisiae*, the focus of this thesis.

Bacillus subtilis

Spore formation in the bacterium *Bacillus subtilis* (reviewed in Duncan et al., 1994; Jenal and Stephens, 1996) is a dramatic example of an asymmetric cell division that is thought to be regulated by an asymmetrically positioned cell septum. Vegetatively-growing *B. subtilis* cells choose a medial site of division. When cells are deprived of nutrients, however, the septum is placed at either of the two poles of the cell. This polar septation results in the formation of a sporangium, a two-celled compartment composed of a forespore and a mother cell (Figure 1-2). The forespore develops into the mature spore whereas the mother cell, which is approximately four times the size of the forespore, nurtures the forespore cell, engulfs it, and then is lysed upon maturation of the spore.

Figure 1-2. Regulation of Sporangium Development in *B. subtilis*. A

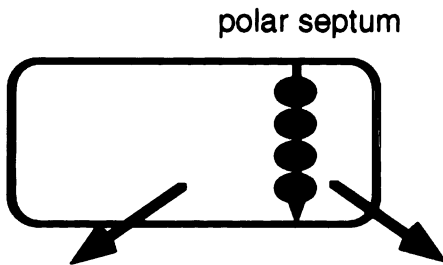
vegetative *B. subtilis* cell is shown at the top of the diagram. This cell chooses a medial site for septation. When these cells are deprived of nutrients, a polar site is chosen instead. SpoIIE, designated as a green oval, localizes to this polar site. The large mother cell compartment, shown on the left, contains σ F that is inactive because it is complexed with SpoIIAB. In the smaller forespore compartment on the right, SpoIIE dephosphorylates SpoIIAA, thereby allowing SpoIIAA to bind SpoIIAB. σ F is then free to activate forespore-specific genes.



Vegetative *B. subtilis*



Nutrient Deprivation



Sporulating *B. subtilis*

SpollAB- σ F
SpollAA-P

SpollAB-SpollAA
 σ F ON

● SpollE

The developmental program that is initiated during sporulation is dependent on the activation of a cascade of compartment-specific σ factors. The pivotal step in this cascade is activation of σ_F specifically in the forespore but not in the mother cell. This activation of σ_F , which occurs immediately after polar septation, triggers mother-specific activation of σ_E via signalling between the forespore and the mother cell. Both σ_F and σ_E specify transcription of other compartment-specific σ factors that induce the appropriate developmental program in each cell (reviewed in Stragier and Losick, 1990; Losick and Stragier, 1992).

How might polar septation stimulate activation of σ_F only in the smaller forespore cell? Inactive σ_F is distributed throughout both the pre-divisional and post-divisional sporangium. Thus, asymmetric σ_F activity is not accomplished by localization of the protein specifically to the forespore compartment. Rather, inhibition of σ_F activity is relieved in the forespore compartment but not in the mother cell. The activity of σ_F is controlled by SpoIIAA and SpoIIAB (Alper et al., 1994; Min et al., 1993; Diederich et al., 1994). SpoIIAB is an anti-sigma factor that binds σ_F and renders it inactive. If SpoIIAA binds SpoIIAB, however, SpoIIAB is effectively sequestered from binding σ_F , leaving σ_F free to activate forespore-specific genes and signal the mother cell to activate σ_E . Thus, the activation of σ_F in the forespore can be achieved by sequestering SpoIIAB in complexes with SpoIIAA rather than with σ_F . Two variables may influence the interaction between SpoIIAA and SpoIIAB. First, SpoIIAB is thought to bind adenosine nucleotides; the *in vitro* affinity of SpoIIAB for σ_F is enhanced in the presence of ATP whereas the interaction between SpoIIAB and SpoIIAA is favored in the presence of ADP. Thus a lower ATP/ADP ratio in the forespore cell compared to the

mother cell could account for the differential ability of the two cells to activate σF (Alper et al., 1994; Diederich et al, 1994). Second, SpoIIAB has been shown to be a serine protein kinase that can phosphorylate SpoIIAA. When SpoIIAA is phosphorylated, its affinity for SpoIIAB decreases, and SpoIIAB is free to bind and inactivate σF . Thus differential phosphorylation of SpoIIAA in the forespore and mother cells could result in differential activation of σF .

A crucial connection has recently been made between positioning of the polar septum and the phosphorylation state of SpoIIAA (Arigoni et al., 1995 and Duncan et al, 1995). SpoIIE, an integral membrane protein synthesized shortly before the asymmetric division of the sporangium, is required for activation of σF . SpoIIE localizes in a collar-like structure at the polar sites where the sporulation septum forms. Mutations in SpoIIE block σF activation but not septum formation. Duncan et al. (1995) show that SpoIIE is a serine phosphatase that specifically dephosphorylates SpoIIAA *in vitro*. Localization of SpoIIE to a polar site could result in a higher effective concentration of SpoIIE in the presumptive forespore cell due to the smaller volume of the forespore compartment. Thus, SpoIIAA would be shunted into its dephosphorylated form in the forespore compartment, resulting in binding of SpoIIAA to SpoIIAB and release of active σF . Thus the intrinsic difference between the forespore and mother cells could be determined by the polar site of cell division.

What cellular landmarks direct SpoIIE to the incipient polar site of cell division? The pattern of SpoIIE localization in the pre-divisional sporangium has been described by Arigoni et al. (1995). SpoIIE initially localizes to a polar site at each end of the cell before septum formation has occurred, thus suggesting the presence of an unknown molecular landmark

at the poles of the cell. SpoIIE then concentrates at same site where the sporulation septum forms; σ F activity in these cells is present at low levels. By the time σ F is maximally active in the forespore compartment, little or no SpoIIE remains at either pole. SpoIIE is likely to be following the localization of FtsZ, a tubulin-like protein required for cell division both during growth and during sporulation. FtsZ localizes to the medial septum in vegetative *B. subtilis* cells. In sporulating cells, however, FtsZ concentrates at both poles of the cell just prior to the formation of the polar septum (Levin and Losick, 1996). In cells that have formed an asymmetrically-positioned septum, FtsZ disappears from the septum but remains temporarily at the pole distal to the septum. This distal staining persists until σ F activation is complete. Although FtsZ localization is independent of SpoIIE, it has recently been shown that SpoIIE localization is dependent on FtsZ (Petra Levin, personal communication). Thus, in order to understand asymmetric cell division of *B. subtilis*, it is crucial to identify the molecules that direct FtsZ to polar sites.

Levin and Losick (1996) have shown that the Spo0A protein governs the ability of FtsZ to recognize polar sites rather than the vegetative medial site. Spo0A is necessary for sporulating cells to adopt the initial bipolar FtsZ staining and to position the septum asymmetrically. Furthermore, expression of a constitutively active Spo0A protein is sufficient to redirect FtsZ to the poles of vegetative cells. It is unclear if Spo0A is masking the medial site of cell division or activating latent sites at the poles. The polar sites that are active in sporulating cells are clearly present in vegetative cells, both because the constitutive Spo0A allele can activate their use in vegetative cells, and because mutations in the *min* genes alleviate the inhibition of polar

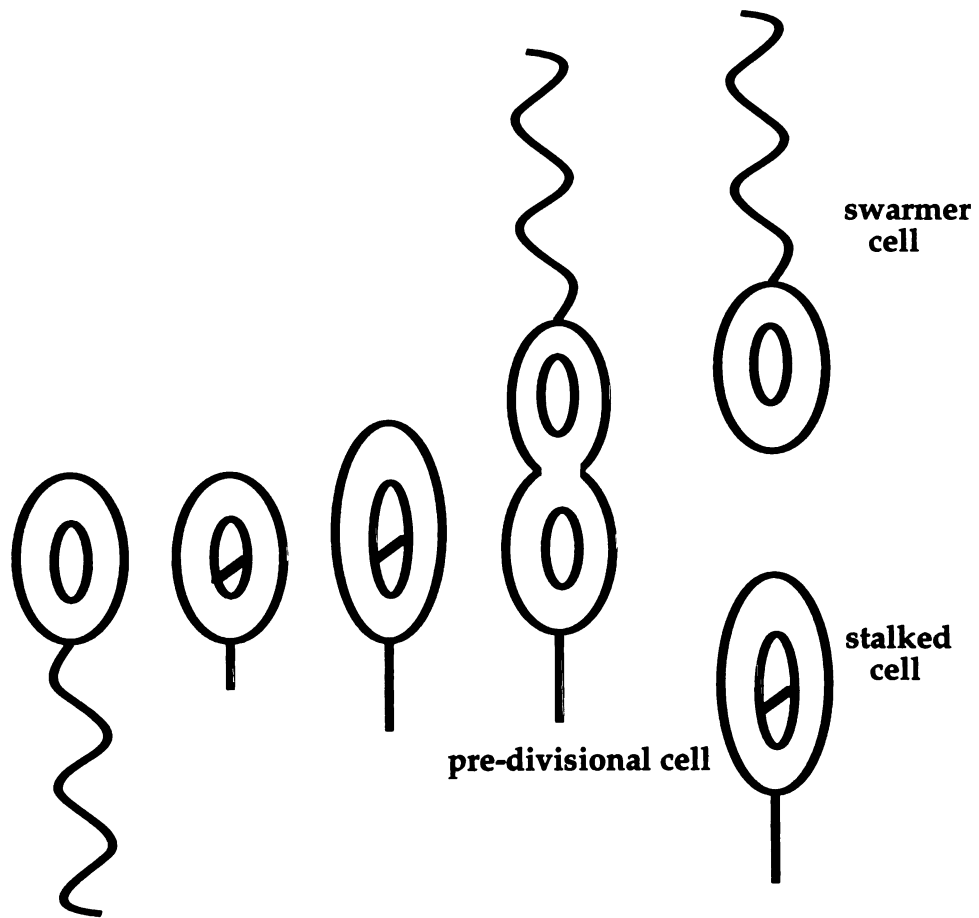
division sites in vegetative *B. subtilis* and *E. coli* cells (Adler et al, 1967; de Boer et al, 1989, 1992; Labie et al, 1990).

The fact that polar landmarks are responsible for asymmetric septum formation in sporulating cells seems incontrovertible. The nature of these landmarks, however, remains elusive. They may be remnants of previous cell divisions or may be positioned as a consequence of cell growth rather than cell division. Elucidating their identity is an essential step to understanding the underlying polarity of the pre-divisional sporangium that governs cell-fate differences in *B. subtilis*.

Caulobacter crescentus

Cell division in *Caulobacter crescentus* (reviewed in Gober and Marques, 1995; Marczyński and Shapiro, 1995; Jenal et al., 1995) generates two distinct cells: a motile swarmer cell and a sessile stalked cell (Figure 1-3). The swarmer cell is motile due to a single polar flagellum that emanates from the swarmer pole; a chemosensory apparatus localized to the swarmer pole allows the cell to respond to attractants and repellents in its environment. The swarmer cell is incapable of replicating its DNA or undergoing cell division until it differentiates into a stalked cell by ejecting the flagellum and growing a stalk in its place. The stalked cell can divide to produce an unlimited number of swarmer cells. As the stalked cell grows, it undergoes DNA replication and generates an asymmetric pre-divisional cell. This pre-divisional cell has a number of key asymmetric features. First, the two chromosomes resulting from DNA replication display very different sedimentation coefficients. The chromosome that segregates to the stalked pole is slow-sedimenting and can replicate immediately after cell division. The chromosome found at the incipient swarmer pole is fast-sedimenting

Figure 1-3. The Cell Cycle of *C. crescentus*. A motile swarmer cell is shown on the left of the diagram. This cell is unable to divide or replicate its DNA. Once this cell ejects its flagellum (curvy line) and grows a stalk (straight line) in its place, it can begin DNA replication. A pre-divisional cell containing a stalked pole and a swarmer pole is formed. This cell divides to yield a stalked cell and a swarmer cell. The latter initiates a new cell cycle immediately.



and cannot replicate until the swarmer cell differentiates into a stalked cell; at this point, the chromosome undergoes a rapid transition to the slow-sedimenting form. Second, flagellar components and proteins required for chemosensory function are targeted specifically to the incipient swarmer pole. Thus the predivisional cell divides to yield two asymmetric cells with different nucleoid properties and very distinct morphological structures at their poles.

The assembly of a flagellum specifically at the incipient swarmer pole is attained at least in part by differential transcription of flagellar genes at the two poles of the pre-divisional cell. (Differential transcription is also thought to be important for activation of DNA replication specifically in the stalked cell [reviewed in Gober and Marques, 1995]) Approximately 50 genes are estimated to be required for flagellar biosynthesis (reviewed in Gober and Marques, 1995; Marczyński and Shapiro, 1995). Transcription of these genes, which are divided into several classes (II, III, and IV), is coordinated by an elaborate regulatory hierarchy. Each promoter of a given class of genes shares a similar sequence organization and a similar spatial and temporal activation pattern. Class II genes encode early flagellar genes and are transcribed before Class III genes. Class III and IV genes encode late flagellar genes and are transcribed only at the swarmer pole after compartmentalization prevents diffusion between the incipient swarmer and stalked sections of the pre-divisional cell. Furthermore, the expression of all the genes in one class is dependent on the expression of the genes in the preceding class. For example, a mutation in any of a large number of class II genes results in the inability to transcribe class III genes. Since products of class II genes are assembled at the incipient swarmer pole, it is thought that the bacterial cell monitors the

assembly of these gene products before transcription of later classes is initiated (reviewed in Shapiro, 1995).

How are the flagellar gene products targeted to the incipient swarmer pole? It is thought that early components of the flagellum, such as the FliF protein, might have an intrinsic affinity for a morphogenetic landmark present at the incipient swarmer pole (Marczynski and Shapiro, 1995). Late flagellar components might then sequentially self-assemble onto the structure created by the early components in a manner analogous to bacteriophage morphogenesis. The fact that late flagellar genes are transcribed only at the swarmer pole of the pre-divisional cell limits flagellar proteins to the swarmer cell: a mutant that allows transcription of late flagellar genes at both the stalked and the swarmer poles results in accumulation of flagellin in the both the stalked and the swarmer progeny (Wingrove et al., 1993).

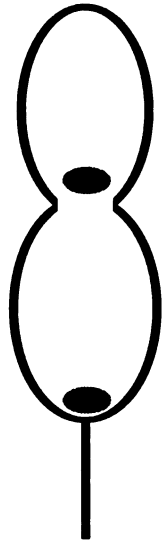
This polar regulation of late flagellar genes is modulated by FlbD, a transcription factor that activates late flagellar gene transcription (Wingrove et al., 1993; Wingrove and Gober, 1994). Although FlbD protein is distributed throughout the pre-divisional cell, its activity is limited to the swarmer compartment. Phosphorylation of FlbD occurs concomitantly with transcription of late flagellar genes. A constitutively active allele of FlbD that no longer requires phosphorylation activates transcription in both the swarmer and the stalked compartments of the pre-divisional cell. Thus, if phosphorylation of FlbD is limited to the swarmer cell compartment of the predivisional cell, activation of FlbD would be spatially constrained. Because FlbD is activated late in the cell cycle, it is possible that the assembly of early flagellar components could serve as a temporal and spatial landmark to activate the protein that phosphorylates FlbD. Interestingly, active FlbD also

serves as a repressor of early flagellar gene transcription at the swarmer pole (Wingrove and Gober, 1994).

Wingrove and Gober (in press) have recently identified FlbE, a protein kinase that is proposed to activate FlbD in the swarmer compartment. Purified FlbE protein can phosphorylate FlbD *in vitro*. The peak of FlbE kinase activity is coincident with the transcription of late flagellar genes. Furthermore, FlbE kinase has been localized to two sites in the pre-divisional cell (Figure 1-4): in the swarmer compartment at the medial site of cell division and at the stalked pole. Wingrove and Gober (in press) propose that a morphogenetic landmark at the site of cell division activates the FlbE kinase specifically in the swarmer compartment but that the FlbE kinase localized to the stalked pole might be sequestered in an inactive form. Alternatively, since the swarmer compartment is smaller than the stalked compartment, the higher effective concentration of FlbE in the swarmer compartment might result in localized phosphorylation of FlbD. This second model is analogous to the activation of SpoIIAA by SpoIIIE in the forespore cell of *B. subtilis*.

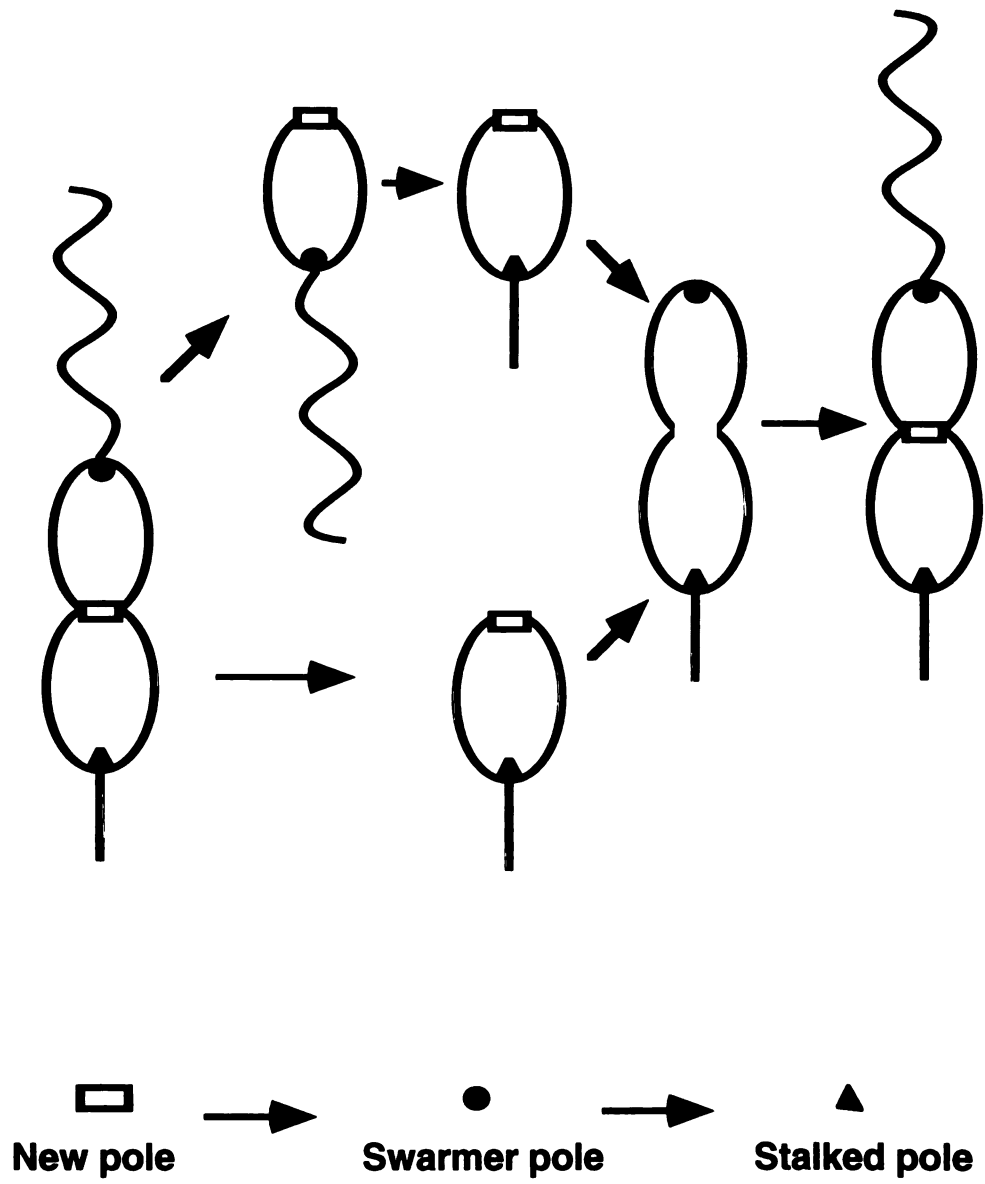
As in *B. subtilis*, the key to the mystery of *C. crescentus* asymmetry may lie at the poles of the pre-divisional cell. Jenal et al. (1995) give an excellent discussion of *Caulobacter* polar development. The pre-divisional *Caulobacter* cell has a stalked pole at one end and a swarmer pole at the other. When the cell divides, it creates two new poles at the medial site of cell division (Figure 1-5). Thus cell division results in a cell with a stalked pole at one end and a new pole at the other, and a second cell with a swarmer pole (marked by a flagellum) at one end and a new pole at the other. Once the cell cycle is reinitiated, each new pole goes on to become a swarmer pole. Since swarmer cells differentiate into stalked cells by losing the flagellum and growing a stalk

Figure 1-4. FlbE Localization in *C. crescentus*. An early pre-divisional cell that has not yet assembled a flagellum at the incipient swarmer pole is shown. FlbE localizes to two places in this cell: at the stalked pole, and in the incipient swarmer cell adjacent to the site of cell division (Wingrove and Gober, in press).



● **FibE**

Figure 1-5. Pole Differentiation in *C. crescentus*. This diagram is adapted from Jenal et al. (1995). There is a defined progression of polar development in *C. crescentus*. New poles (indicated by a rectangle) are formed at the site of cell division; these poles always become swarmer poles (indicated with a black dot) in the following cell cycle. The swarmer pole then becomes the stalked pole (indicated with a triangle) in the next cell cycle.



in its place, each swarmer pole subsequently becomes a stalked pole. Thus, polar development always proceeds in a stereotyped fashion: new pole to swarmer pole to stalked pole, with the latter representing the terminally differentiated cell pole. How does differentiation of these poles relate to cell asymmetry? There is likely to be a morphological marker at the incipient swarmer pole that targets the assembly of flagellar proteins. Since this pole develops from the new pole, a remnant laid down as a consequence of the previous cell division (when the new pole is formed) could serve as a landmark for targeting flagellar proteins in the next cell cycle. When a swarmer cell ejects the flagellum and differentiates into a stalked cell, a residual flagellar component at the pole could mark the location of the incipient stalk. The identification of polar markers, such as the proteins that bind and activate FlbE, will be instrumental to understanding the basis of *Caulobacter* asymmetry. As in *B. subtilis*, the poles of the cells clearly represent specialized structures involved in determination of cell fate.

Drosophila

The *Drosophila* Numb protein is a cell-fate determinant that is segregated to one of two sister cells in the developing nervous system (Rhyu et al., 1994). Numb is asymmetrically segregated during the division of several different cell types including cells of the embryonic peripheral nervous system (PNS), the central nervous system (CNS), and the adult PNS. Loss of *numb* function and overexpression of *numb* have reciprocal phenotypes, indicating that Numb is both necessary and sufficient for cell fate determination (Rhyu et al., 1994).

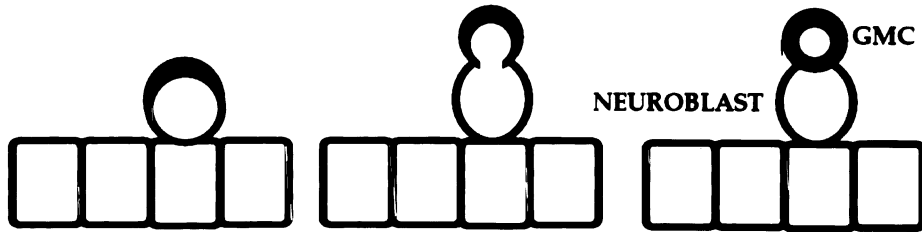
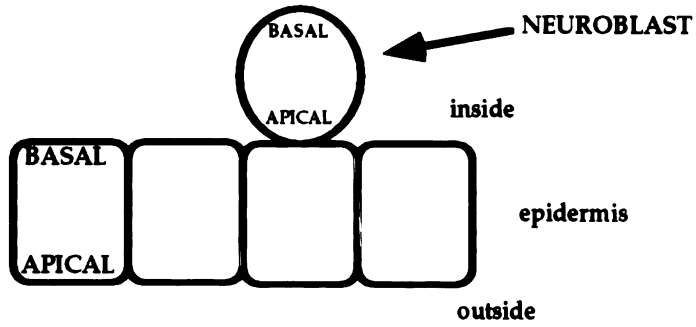
Numb, a membrane protein, has been shown to localize during mitosis of developing neuroblasts in the CNS (Knoblich et al., 1995), which

delaminate from epithelial cells. In interphase and early prophase, Numb protein is evenly distributed along the membrane. By late prophase, Numb forms a crescent over the centrosome nearest the interior of the embryo (the basal pole of the cell); all metaphase cells show the same tight crescent of localized protein on one side of the pre-divisional cell. In telophase, Numb is partitioned into the ganglion mother cell, the sister cell that forms toward the interior of the embryo (Figure 1-6A). After mitosis is completed, Numb is dispersed homogeneously along the membrane.

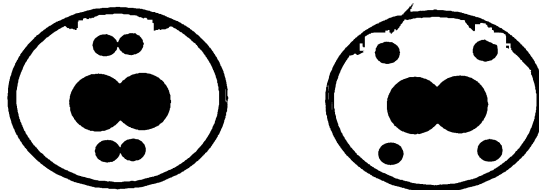
Since the Numb crescent always overlies one of the two centrosomes, it was desirable to know if localization of Numb is coordinated in some way with centrosome position. *pebble* mutant embryos are unable to undergo cytokinesis; hence mitosis yields cells with two nuclei and four centrosomes. The four centrosomes form two pairs of either closely associated or widely-spaced centrosomes on opposite sides of the cell from each other. The Numb protein again localizes in a crescent overlying the two centrosomes at the basal pole (Knoblich et al., 1995). In cells where this pair of centrosomes is widely separated, the Numb protein either concentrates in a single crescent between the two centrosomes or in two individual crescents, each over one of the two centrosomes (Figure 1-6B). Thus it seems likely that centrosome positioning and Numb localization are coordinated in some fashion. Interestingly, if the centrosomes are misoriented by treatment with colcemid, Numb protein localization is unaffected (Knoblich et al., 1995). Furthermore, centrosome position is independent of Numb localization. Thus it seems likely that a cellular landmark positions both the centrosome and Numb protein, but the location of each is independent of the other.

Figure 1-6. Localization of Numb in *Drosophila* Neuroblasts. (A) A layer of polarized epithelial cells is drawn in the top panel. The apical side of the epithelium faces the outside of the embryo, whereas the basal side is internal to the embryo. An oval neuroblast is shown delaminating from the epithelial cells. In the next panel, a yellow crescent of Numb localizes on the basal side of the neuroblast. The neuroblast divides to give rise to another neuroblast and a ganglion mother cell (GMC), which forms on the basal side of the dividing neuroblast cell. Numb is segregated into the GMC, and becomes distributed around its periphery. (B) A cell from a *pebble* mutant, which doesn't undergo cytokinesis. This cell has two pairs of centrosomes, drawn as black dots. The nuclei are represented by solid blue circles. If the centrosome pairs are close together, as drawn in the left cell, a single crescent of Numb protein forms on the basal side of the cell. If the centrosome pairs are far apart, as in the cell on the right, two crescents of Numb are formed on the basal side.

A.



B.



All pre-divisional cells that localize Numb protein are derived from polarized epithelial cells, suggesting that the maintenance of previously established epithelial polarity in the pre-divisional cell might underlie its asymmetry (Knoblich et al., 1995). The Inscuteable protein has recently been shown to be necessary both for Numb localization and for positioning the division axis via the centrosome (Kraut et al., in press). The function of Inscuteable with regards to the plane of division and to Numb localization has been most closely examined in two types of cells, the neuroblast cells described above and the cells of the procephalic neurogenic region (PNR) of the ectoderm. Neuroblasts and cells in the PNR divide perpendicular to the epithelial plane; thus the centrosomes of these cells are normally aligned along the apical/basal axis of the epithelial plane with the Numb protein crescent at the basal pole of the cell. In *inscuteable* mutants, the neuroblast centrosomes are no longer positioned along the apical/basal axis. Instead, the division plane is random with respect to the epithelial plane. Furthermore, Numb protein is not properly localized in the majority of these cells. In some cells, Numb is evenly distributed around the cell surface, whereas in others, Numb forms a crescent, but the position of the crescent is random with respect to the epithelial plane. There is no correlation between the position of the centrosomes and the localization of Numb in these mutants. In the PNR, wild-type cells initially position the spindle parallel to the epithelial plane and then rotate it so that the centrosomes are aligned along the apical/basal axis. In *inscuteable* mutants, the PNR spindles fail to rotate and remain parallel to the epithelial plane. Numb protein is evenly distributed along the membrane in these mutant cells and thus segregates to both daughter cells at division.

Kraut et al. (in press) show that Inscuteable protein localizes to the apical side of both neuroblast and PNR cells, on the opposite side of the cell from the Numb crescent. Inscuteable localizes in an apical crescent prior to the appearance of the basal Numb crescent. This localization, which is not dependent on Numb, persists through prophase and metaphase. By anaphase, Inscuteable is delocalized. Interestingly, ectopic expression of *inscuteable* is sufficient to reorient the spindle of cells that normally divide parallel to the epithelial plane. Ectopic expression of Inscuteable in these cells triggers localization of Inscuteable protein in an apical crescent and causes the spindle to rotate such that cells divide perpendicular to the epithelial surface. Ectopic Inscuteable expression is not sufficient, however, to localize Numb asymmetrically. Thus Inscuteable is necessary and sufficient for reorientation of the division plane, and is necessary but not sufficient for asymmetric localization of Numb.

The localization of Inscuteable to the apical pole of the cell may be a consequence of the apical/basal polarity of the epithelium (Kraut et al, in press). Understanding how the polarity of the epithelium sets up the asymmetry of the cells in question awaits the identification of molecules at the apical pole that are required for Inscuteable localization. It is also unclear how localization of Inscuteable at the apical pole of the cell orients the spindle and localizes Numb to the basal pole of the cell. Inscuteable seems to be required to position a landmark that influences Numb localization. Since the *pebble* mutants, which cannot undergo cytokinesis (described above), often display two Numb crescents at the basal pole, these cells seem to contain two discrete basal landmarks for Numb localization. These data suggest that one landmark is created per cell division cycle. Thus mutants that cannot

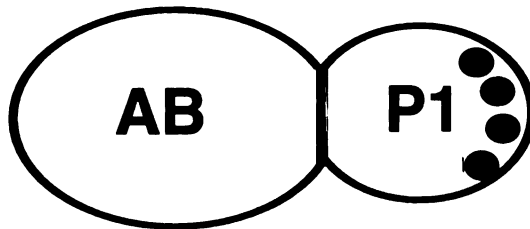
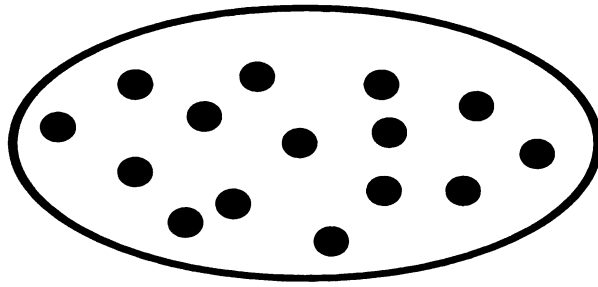
undergo cytokinesis will contain two landmarks--one from the previous cell cycle, when cytokinesis did not occur, and one from the current cell cycle. Somehow the Inscuteable protein, in conjunction with the process of cell division, positions a landmark that translates into cellular asymmetry.

Caenorhabditis elegans

Multiple asymmetric divisions occur during development of the *Caenorhabditis elegans* embryo (reviewed in Priess, 1994). It is thought that the asymmetry of the anterior/posterior (A/P) axis of the embryo is a result of intrinsic A/P asymmetry of the egg. In order to differentially segregate determinants that are laid down in a A/P gradient in the egg, embryonic cells must divide parallel to the A/P axis. Left/right and dorsal/ventral asymmetries, in contrast, are thought to arise extrinsically, from cell-cell interactions. For example, in the very early embryonic divisions, cells that result from divisions that are parallel to the A/P axis are intrinsically different, whereas cells that result from divisions perpendicular to the A/P axis are initially equivalent at birth but manifest different fates due to interaction with a particular cell. Thus regulating the division plane is an essential component of proper development.

The first division of the fertilized egg occurs along the A/P axis to generate the anterior AB blastomere and the posterior P1 blastomere (Figure 1-7). AB and P1 differ both in terms of size and in terms of cell fate: only the P1 cell can give rise to pharyngeal cells, muscle cells, and intestinal cells, for example. Concomitant with this first cell cycle, P granules, cytoplasmic bodies that are distributed uniformly throughout the egg, are localized to the posterior pole and then partitioned into the P1 cell. In the second cell cycle, AB and P1 undergo stereotyped divisions. In both the AB and P1 cells, the

Figure 1-7. The First Embryonic Division of *C. elegans*. The top panel shows an unfertilized *C. elegans* egg. P granules, indicated by black ovals, are distributed evenly throughout the egg. After fertilization, the first division of the embryo occurs along the anterior/posterior axis to generate an anterior blastomere, AB, and a posterior blastomere, P1. The P granules are segregated to the posterior of the P1 cell.



● P granules

spindle aligns perpendicular to the A/P axis. The P1 cell spindle, however, then rotates an additional 90° so that it is parallel to the A/P axis. Thus, the AB division generates two sister cells that are initially equipotent, whereas the P1 division generates an anterior and a posterior cell that are inherently asymmetric. The P granules again segregate to the posterior daughter.

The *par* genes are necessary for maintenance of A/P polarity in the early embryo and for the spindle alignment events described above (Cheng et al., 1995; Kemphues, 1989, Kemphues et al, 1988; Morton et al, 1992). In *par* mutants, AB and P1 are the same size, P granules are mislocalized, and other aspects of asymmetry and cell fate determination are perturbed. I will focus specifically on the spindle orientation defects of *par-2* and *par-3* mutants in the second embryonic cell cycle (Cheng et al., 1995). In *par-2* mutants, the P1 spindle fails to rotate; thus both AB and P1 divide orthogonal to the A/P axis. In *par-3* mutants, both the AB and the P1 spindles rotate; thus both AB and P1 divide parallel to the A/P axis. Interestingly, in the *par-2 par-3* double mutant, both spindles rotate. These data suggest that PAR-3 functions to prevent spindle rotation in the AB cell and that PAR-2 limits the function of PAR-3 to the AB cell, thus allowing spindle rotation only in the P1 cell. Etemad-Moghadam et al. (1995) have recently shown that PAR-3 protein displays a distinct localization in the early embryo: it is concentrated at the anterior pole of the fertilized egg. In the second cell cycle, PAR-3 is distributed uniformly around the periphery of the AB cell in all two-cell embryos. In P1 cells that are in interphase, PAR-3 protein either is not observed, or the staining is present only at the extreme anterior of the cell. In later two-cell embryos, PAR-3 is concentrated at the anterior third of the P1 cell. In *par-2* mutant embryos, however, PAR-3 stains the periphery of both AB and P1 at

the two-cell stage. The fact that localization of PAR-3 is limited to the periphery of wild-type AB cells and the anterior of wild-type P1 cells is consistent with the idea that PAR-3 prevents spindle rotation in the AB cell only. In the absence of PAR-2, however, PAR-3 is mislocalized over the periphery of the P1 cell where it inappropriately inhibits spindle rotation.

The means by which PAR-3 prevents spindle rotation in the AB cell is unclear. Etemad-Moghadam et al. (1995) postulate that PAR-3 acts to stabilize the AB spindle, thereby preventing it from responding to a cortical site that has been shown to be necessary for spindle rotation (Hyman, 1989; Hyman and White, 1987). Furthermore, the intrinsic asymmetry of the egg that sets up the anterior localization of PAR-3 protein is far from being understood. A complete understanding of establishment of A/P polarity in the worm is dependent on elucidating the mechanism of PAR-3 localization. PAR-2 protein is known to localize to the posterior periphery of the egg and to the posterior periphery of the P1 cell (Boyd et al., in press). Hence, PAR-2 and PAR-3 are essentially found at opposite poles of the cell, much like the Inscuteable and Numb proteins in *Drosophila*. Interestingly, the localization of PAR-2 and PAR-3 is interdependent (Etemad-Moghadam et al., 1995; Boyd et al., in press). Finally, the initial A/P polarity of the egg, which is likely to be responsible for the graded distribution of PAR-2 and PAR-3, is established by the sperm entry point, which defines the posterior pole of the cell. It is possible that the process of fertilization places a landmark at the sperm entry point. The cytoplasmic streaming that follows fertilization might then establish the innate A/P polarity of the zygote with respect to this marked posterior pole.

Saccharomyces cerevisiae

The examples cited above illustrate how intrinsic cell fate differences are traced back to the innate asymmetry of the pre-divisional cell. The goal of this work is to identify determinants required for asymmetric cell fate in the budding yeast *S. cerevisiae* and to then study how yeast cell polarity might drive the localization of such determinants.

The regulation of mating-type switching in mother and daughter cells of budding yeast is a classic example of asymmetric cell-fate determination. A single genetic locus determines the mating type, either \underline{a} or α , of haploid yeast cells. Strains that undergo mating-type switching convert their mating type from \underline{a} to α and vice versa. Only cells that have budded previously (mother cells) are able to switch their mating type; newly born yeast cells (daughter cells) are not able to switch mating type (Hicks and Herskowitz, 1976; Strathern and Herskowitz, 1979; Strathern et al., 1979). Each cell-division cycle yields a mother cell and a newly-born daughter cell (Figure 1-8), thus producing two cells with asymmetric switching capabilities (Figure 1-9). Once the daughter cell has gone through one cell cycle, it becomes a mother cell and gains the ability to switch mating type.

Molecular studies have shown that the ability to switch mating type correlates with the ability to transcribe the *HO* gene (Nasmyth, 1983); *HO* encodes an endonuclease that initiates replacement of the information at the mating-type locus with information copied from one of two silent mating-type cassettes (reviewed in Herskowitz, 1989; Herskowitz and Oshima, 1981). *HO* transcription is limited to the late G1 phase of the cell cycle and is repressed in \underline{a}/α diploids. Significantly, *HO* transcription occurs only in mother cells but never in daughters. Ectopic expression of *HO* in daughter

Figure 1-8. The Yeast Cell Cycle. An unbudded mother cell (M) is drawn in green at the top of the diagram. This cell grows a red bud, or daughter cell (D). Once the newly born daughter cell forms a daughter of its own, it becomes a mother cell.

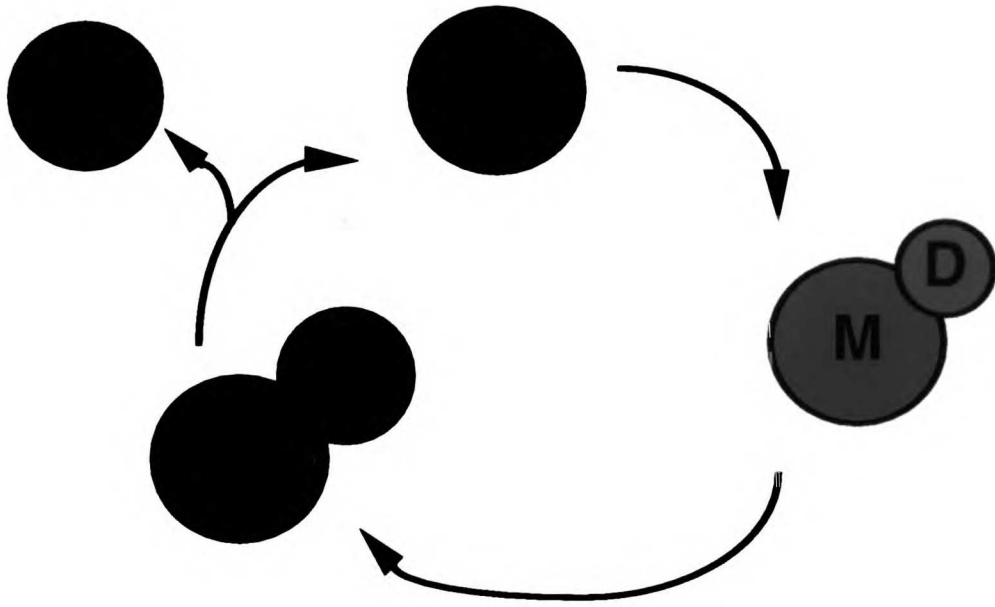
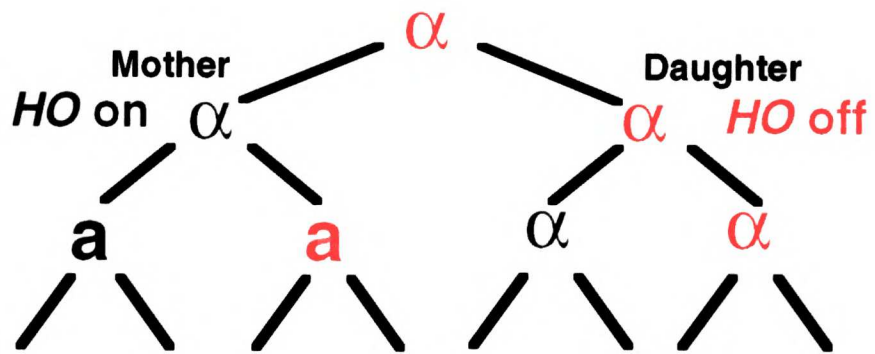


Figure 1-9 Lineage-Specific Regulation of Mating-Type Switching. A typical lineage of switching yeast cells is shown. At each division, mother cells (in green) are drawn to the left whereas daughter cells (in red) are drawn to the right. Only the mother cell inherits the ability to transcribe *HO* and switch mating type.



cells is sufficient to induce mating-type switching (Jensen and Herskowitz, 1984; Nasmyth, 1987), confirming that the inability of wild-type daughters to switch is due solely to their inability to transcribe *HO*. The exclusive expression of *HO* in mother cells has been a provocative mystery for quite some time. The objective of this work is to understand how a yeast cell divides asymmetrically to produce a mother cell that can transcribe *HO* and a daughter cell that cannot.

An analysis of the asymmetric regulation of *HO* transcription requires an understanding of the *HO* promoter. A rudimentary dissection of the upstream region of the *HO* gene reveals two promoter elements that modulate control of *HO* transcription (Nasmyth, 1985a). The upstream region, which is unusually large for *S. cerevisiae*, contains two regulatory blocks, URS1 and URS2, each approximately 1 kilobase in length. Deletion of URS2 results in altered cell cycle expression of *HO* (Nasmyth, 1985a), indicating that URS2 is necessary for the proper timing of transcription. Deletion of URS1 inactivates the promoter; however, replacement of URS1 with a 330 bp fragment containing the UAS of the *GAL1-10* promoter results in *HO* transcription that is galactose-dependent, cell-cycle regulated, and haploid-specific. Interestingly, activation of this hybrid promoter is no longer limited to mother cells (Nasmyth, 1987). These data indicate that URS2 is necessary and sufficient for proper cell-cycle regulation of the *HO* promoter whereas URS1 is necessary for UAS activity and proper mother/daughter specificity.

At least ten positive regulators (*SWI1-10*) of *HO* transcription have been identified (Haber and Garvik, 1977; Stern et al., 1984; Breeden and Nasmyth, 1987). Several lines of evidence implicate one of these proteins,

Swi5p, in proper mother/daughter regulation. First, Swi5p, a Zn-finger transcriptional activator, binds to two sites in URS1, the region of the promoter required for mother/daughter regulation (Tebb et al., 1993; Stillman et al., 1988). Second, mutations that bypass the need for Swi5p-dependent activation of *HO* transcription allow mating-type switching in both mother and daughter cells (Nasmyth et al., 1987b; Sternberg et al., 1987; Breeden and Mikesell, 1991; A.S. unpublished observations) Thus daughters contain all of the machinery necessary to transcribe *HO* except functional Swi5. Third, subtle perturbations in *SWI5* transcriptional regulation are sufficient to alter mother/daughter regulation (Nasmyth et al., 1987a; Lydall et al., 1991). Specifically, although Swi5p is needed in G1 for *HO* transcription, it is transcribed only during the S, G2, and M phases of the previous cell cycle (Nasmyth et al., 1987a). Constitutive expression of *SWI5* throughout G1, however, is sufficient to cause daughters to switch (Nasmyth et al., 1987a; Lydall et al., 1991). Finally, the instability of Swi5p is required to keep daughter cells from transcribing *HO* (Tebb et al, 1993). Swi5p is cytoplasmic until anaphase, when it enters mother and daughter nuclei (Nasmyth et al., 1990). Once Swi5p enters the nucleus, it becomes unstable and is rapidly degraded with a half-life of approximately ten minutes. Alleles of *SWI5* that encode a stabilized Swi5 protein allow daughter cells to switch mating type. These data are consistent with Swi5p being limiting in wild-type daughter cells in terms of amount or activity.

I propose two models to explain the mechanism of mother/daughter regulation. Both models ascribe the inability of daughters to transcribe *HO* to a lack of Swi5p activity, either at the right time or in the right place. The crux of the timing model is that the length of G1 in mothers is shorter than the

length of G1 in daughters. Daughter cells must linger in G1 until they have attained the minimum size required for progression through the cell cycle; mothers, on the other hand, have met this size requirement in prior cell cycles and hence have a significantly shorter G1 than daughter cells. Swi5p enters the nucleus in early G1 (Nasmyth et al., 1990), but *HO* is not transcribed until late G1, when Swi4p and Swi6p, which act on consensus sequences present in URS2, are activated (Breedon and Nasmyth, 1987; Nasmyth, 1985b; Andrews and Herskowitz, 1989a, 1989b). Since G1 is significantly longer in daughter cells and since Swi5p is unstable, it is possible that by the time Swi4p and Swi6p are activated in late G1, daughter cells no longer contain active Swi5p protein; thus, *HO* is not transcribed in daughters. *SWI5* is not transcribed during G1 and thus cannot be replenished during this window of time. This model assumes that Swi5p cannot perform its function until Swi4p/6p is active; however, the execution point of Swi5p function has not been determined experimentally. An argument against the timing model has been made experimentally: if mother cells are arrested in late G1 for long periods of time, they are still competent to transcribe *HO* immediately after the arrest (Tebb et al., 1993). Hence it has been argued that the length of G1 cannot play a role in inhibiting *HO* expression in daughter cells. However, if the late G1 arrest employed in this experiment is after the Swi5p execution point, the experiment does not exclude the timing model.

The asymmetric regulator model states that *HO* is transcribed only in mothers because either an activator of *HO* transcription segregates only to the mother cell or an inhibitor of *HO* transcription segregates only to the daughter cell. It was once thought that Swi5p itself might be segregated only to the mother cell, thus allowing *HO* transcription only in mothers; however,

immunofluorescence studies indicate that Swi5p protein enters both mother and daughter nuclei in late anaphase (Nasmyth, 1990). Since mother/daughter regulation is exquisitely sensitive to Swi5p levels, an asymmetric determinant could influence Swi5p activity. Thus, the asymmetric regulator model can be modified as follows: either (1) an activator of Swi5p function is segregated only to the mother or (2) an inhibitor of Swi5p function is segregated only to the daughter. The timing model and asymmetric regulator model are not mutually exclusive; the actual mechanism of mother/daughter control may involve aspects of both models.

Finally, if it is possible to identify an asymmetrically distributed regulator of cell fate in budding yeast, the ultimate aim is to understand how the innate polarity of the budding yeast cell is translated into the localization of a determinant to the mother or to the daughter cell. The study of asymmetric cell fate in yeast presents a remarkable opportunity to use molecular genetics to unlock one outstanding mystery of developmental biology. Chapter Two describes the identification of a cell-fate determinant that localizes predominantly to the daughter cell where it inhibits transcription of *HO*. Chapter Three describes experiments that address the question of how the yeast cell localizes this determinant to the daughter cell.

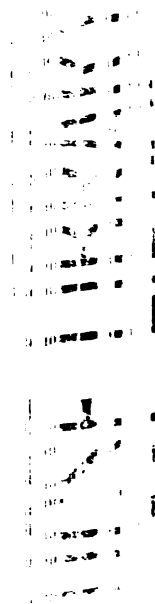
CHAPTER TWO

IDENTIFICATION OF Ash1p, AN ASYMMETRICALLY LOCALIZED REGULATOR OF CELL FATE IN YEAST

A version of Chapter Two originally appeared as Sil and Herskowitz (1996),
Cell, **84**: 711-722.

ary

Saccharomyces cerevisiae cells exhibit asymmetric determination of cell fate. Cell division yields a mother cell, which is competent to transcribe the *HO* gene and switch mating type, and a daughter cell, which is not. We isolated a mutant in which daughters transcribe *HO* and switch mating type. This mutation defines the *ASH1* (Asymmetric Synthesis of *HO*) gene. Deletion and overexpression of *ASH1* cause reciprocal cell-fate determinations: in *ash1Δ* strains, daughters switch mating type at the same frequency as mothers. Conversely, overexpression of *ASH1* inhibits switching in mother cells. Ash1p has a zinc-finger motif related to those found in the GATA family of transcriptional regulators. Ash1p is localized to the daughter nucleus in cells that have undergone nuclear division. Thus Ash1p is a cell-fate determinant that is asymmetrically localized to the daughter nucleus where it inhibits *HO* transcription.



Introduction

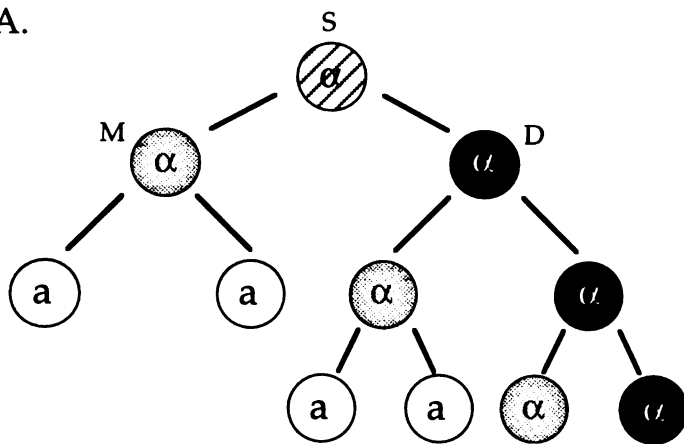
Asymmetric cell division is fundamental to development. The transformation from egg to organism involves multiple cell divisions that generate cells of specialized fate and function. The budding yeast *Saccharomyces cerevisiae* also exhibits asymmetric cell fate. In this case, yeast cells display lineage-specific regulation of a genetic rearrangement event known as mating type switching (Strathern and Herskowitz, 1979).

Haploid yeast cells exhibit either a or α mating type; strains carrying the *HO* gene undergo mating-type switching at high frequency and convert from a to α and vice versa (Herskowitz, 1988; Nasmyth, 1993). Only cells that have budded previously (mother cells) exhibit the ability to undergo mating-type interconversion; newly born yeast cells (daughter cells) and spore cells are not capable of switching mating type (Strathern and Herskowitz, 1979). Daughter cells and spore cells become mother cells once they have gone through one cell-division cycle; at that point they acquire the ability to switch mating type. Thus each cell division cycle of a daughter cell gives rise to a mother cell and to a newly-born daughter cell (derived from the bud), thereby producing two cells with different switching capabilities. The succession of daughter cells constitutes a stem-cell lineage (Figure 2-1A).

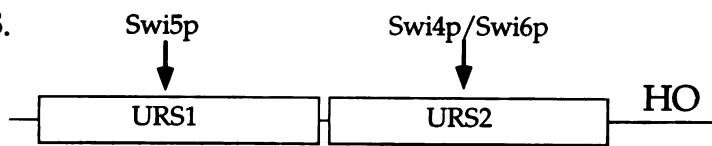
Molecular studies have shown that the asymmetric regulation of mating-type switching (mother/daughter regulation) results from asymmetric transcription of the *HO* gene (Nasmyth, 1983). *HO* codes for an endonuclease that initiates replacement of the information at the mating-type locus with information copied from one of two silent mating-type cassettes (reviewed in Herskowitz, 1988. *HO* transcription is limited to the late G1

Figure 2-1. Mitotic Lineages of Yeast Cells are Stem-Cell Lineages. (A) A typical lineage of switching cells. The striped cell that starts the lineage is a spore cell (S). At each division, daughter cells (D) are drawn to the right and mother cells (M) to the left. α daughter cells are drawn in black. Daughter cells are not able to switch mating type but instead divide to yield a mother cell and a new daughter; these daughter cells comprise a stem-cell lineage. α mother cells are shaded gray. Mother cells switch mating type at a frequency of 60-80%. A switch from α to a is manifested by cell-cycle arrest and altered morphology in the presence of α -factor. (B) The *HO* promoter. The upstream regulatory region of *HO* contains two segments, URS1 (-1950 to -1000) and URS2 (-900 to -150). Swi5p has two binding sites in URS1 (Tebb et al., 1993) and Swi4p/6p binds to ten sites in URS2 (Nasmyth, 1985, 1987; Andrews and Herskowitz, 1989).

A.



B.



phase of haploid mother cells, does not occur in daughter cells, and is thought not to occur in spore cells (Breedon and Nasmyth, 1987; Nasmyth, 1983, 1985). Ectopic expression of *HO* in daughter cells is sufficient to induce mating-type interconversion, confirming that the inability of wild-type daughters to undergo mating-type switching is due to their inability to transcribe *HO* (Jensen et al., 1983; Nasmyth, 1987).

At least ten proteins have been identified that regulate *HO* transcription (reviewed in Herskowitz et al., 1992; Nasmyth, 1993). The Swi4p/Swi6p complex has ten binding sites in the URS2 segment of the *HO* upstream regulatory region; URS2 restricts *HO* transcription to late G1 (Figure 2-1B) (Nasmyth, 1985b, 1987; Andrews and Herskowitz, 1989a). Swi5p, a zinc-finger protein, binds to two sites within the URS1 segment of the *HO* upstream regulatory region and is implicated in asymmetric regulation of *HO* transcription (Nasmyth, 1993; Nasmyth and Shore, 1987; Tebb et al., 1993).

Several lines of evidence (reviewed in Nasmyth, 1987, 1993) indicate that *SWI5* is limiting in wild-type daughter cells. First, perturbations in the timing of *SWI5* transcription allow mating-type switching in daughter cells. Although Swi5p is needed some time between anaphase and late G1 for *HO* transcription, *SWI5* is transcribed only during the S, G2, and M phases of the previous cell cycle (Nasmyth et al., 1987a). Constitutive expression of *SWI5* allows daughters to switch (Nasmyth et al., 1987a; Lydall et al., 1991). Similarly, alleles of *SWI5* that produce a stabilized protein allow daughters to switch mating type (Tebb et al., 1993). Finally, mutations that allow *HO* transcription in the absence of *SWI5* also permit switching in daughters and spores as well as mother cells (Nasmyth et al., 1987b; Sternberg et al., 1987). Though it was initially hypothesized that Swi5p might be asymmetrically

distributed to the mother cell and absent from the daughter cell, Swi5p is localized to both mother and daughter nuclei after anaphase (Nasmyth et al., 1990). Thus, Swi5p is present in the daughter nucleus but is limiting in terms of amount or activity. The temporal separation between entry of Swi5p into the nucleus at anaphase and transcription of *HO* in late G1 might provide a window of time in which Swi5p activity is modulated in daughters.

One attractive explanation for why Swi5p activates *HO* transcription only in mother cells and not in daughter cells is the existence of an asymmetrically distributed regulator, for example, an activator of *HO* expression that localizes preferentially to the mother cell or an inhibitor of *HO* expression that localizes preferentially to the daughter cell. To search for such a regulator, we screened for mutants in which daughter cells switch mating type. Using a microcolony assay for mating-type switching, we isolated a mutant, *ash1-1*, with this behavior. Characterization of *ASH1* and its gene product indicate that Ash1p is a negative regulator of the *HO* gene that is asymmetrically localized to daughter cells.

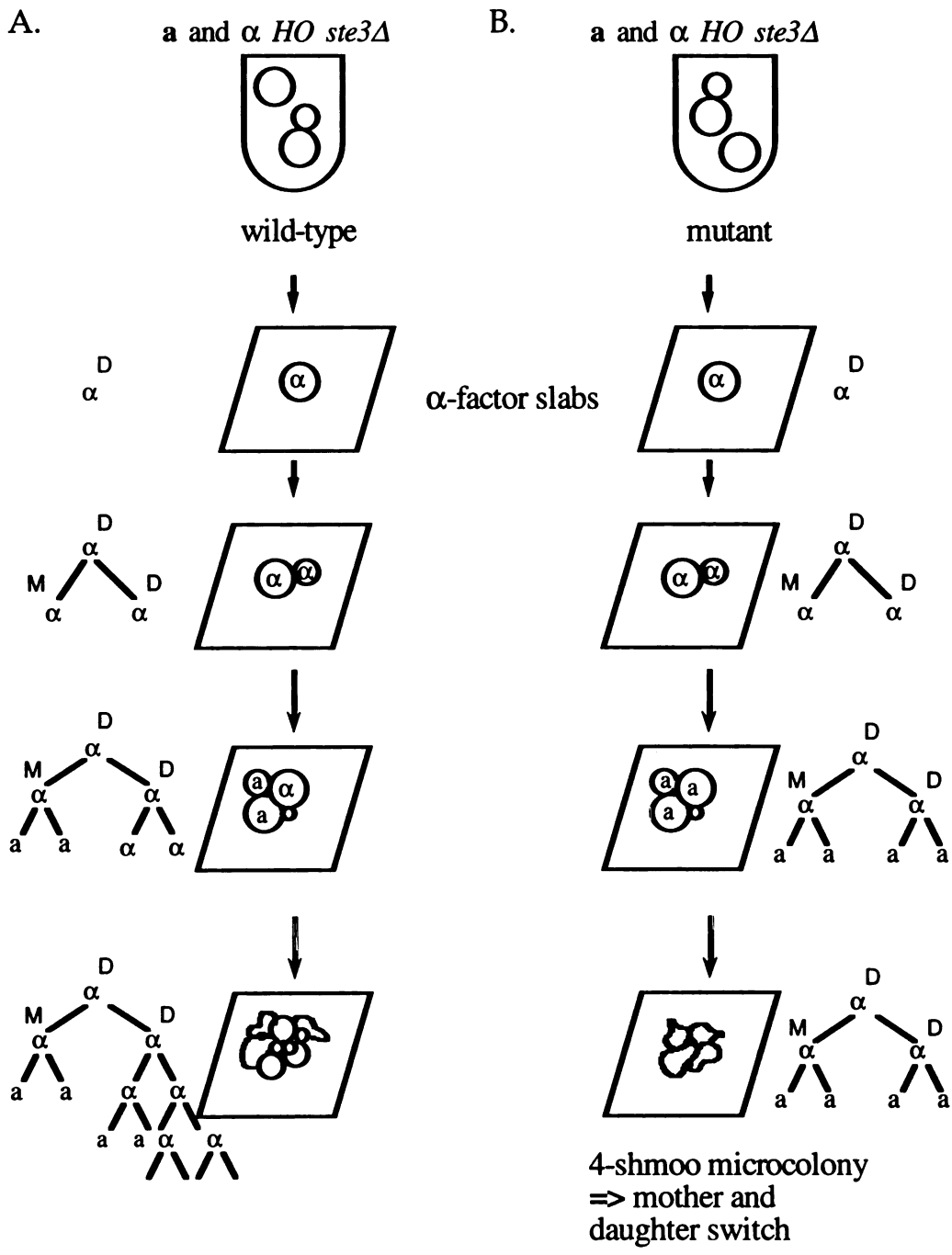
Results

Isolation of a Mutant Defective in Mother/Daughter Regulation of Mating-Type Switching

A mutant whose daughter cells switch mating type was identified using a microcolony assay for mating-type switching. To isolate such a mutant, it was necessary to assay mating-type switching in vegetative haploid cells using a special strain. Vegetative growth of wild-type *HO* cells yields both **a** and α cells, which then mate to form an **a**/ α diploid that no longer expresses *HO*. In contrast, an *HO* strain defective in the *STE3* gene, which encodes the **a**-factor pheromone receptor (Nakayama et al., 1985; Hagen et al., 1986), can switch back and forth between a *HO ste3 Δ* and α *HO ste3 Δ* . Since the α cells are unable to mate, **a**/ α diploids are not formed.

This *HO ste3 Δ* strain was used as the parent in a screen for mutants altered in mother/daughter regulation (Figure 2-2). As noted above, this strain grows into a population containing both **a** and α cells. The **a** cells respond to the pheromone α -factor by arresting in G1 and exhibiting the characteristic "shmoo" morphology. The α cells in the population are unaffected by α -factor and continue to bud and divide. Switching of an α cell to **a** is scored as a change in the ability of a cell to respond to α -factor. After two cell divisions, a wild-type α daughter cell forms a microcolony containing two **a** and two α cells (Figure 2-2). In the presence of α -factor, the **a** cells arrest and shmoo, whereas the α cells continue to divide, resulting in a large microcolony of budding and shmooing cells. In contrast, a mutant strain whose daughters have the ability to switch mating type can yield a distinctive

Figure 2-2. A Four-Shmoo Microcolony Indicates that both Mother and Daughter Cells have Switched Mating Type. An *HO ste3Δ* strain (YAS131) was used to screen for mutants whose daughters switch mating type. The strain was mutagenized, and then individual cells were grown in the presence of α -factor on agar slabs. (A) shows the fate of a wild-type α daughter; (B) shows the fate of a mutant α daughter. Lineages that begin as α mothers, **a** mothers, or **a** daughters are not shown. The **a** mothers and daughters form microcolonies made up of one or two shmoos. If a mutant α daughter does not switch in its first division, it divides to yield an α mother and daughter. If both these cell switch in their next division, four shmoos result. M, mother; D, daughter.



microcolony consisting of four *a* cells, all of which arrest and shmoo in response to pheromone, yielding a four-shmoo microcolony (Figure 2-2).

A mutant defective in mother/daughter regulation was identified by visual observation of microcolonies formed on α -factor slabs. The parent *HO ste3 Δ* strain was mutagenized and subsequently transferred to agar slabs containing α -factor. Approximately 86,000 microcolonies were screened in total from 20 independent cultures. Sixty-one four-shmoo microcolonies were identified; of these, 33 recovered from pheromone arrest and were rescreened individually by the microcolony assay. The majority of the isolates behaved identically to the wild-type parent strain. Two isolates gave intermediate numbers of four-shmoo microcolonies and were not studied further. One of the isolates gave a consistently high number of four-shmoo microcolonies (50-100) per 1000 microcolonies and was designated mutant *ash1-1* (Table 2-1, line 2).

Mutation in *ASH1* Allows Daughter Cells to Switch Mating Type

Lineage studies (pedigree analyses) were performed to determine if the four-shmoo microcolony phenotype of the *ash1-1* mutant was due to mating-type switching by daughter cells. Single cells were followed over multiple divisions in the presence of α -factor to observe switches from α to *a*. Since mother cells are larger than their daughters and generally bud before them, mother and daughter cells can be easily distinguished (Hicks and Herskowitz, 1976). Pedigree analysis of wild-type *HO ste3 Δ* cells showed that 71% of mothers switched mating type whereas less than 1% of daughters switched (Table 2-1, line 1). In contrast, the *ash1-1 HO ste3 Δ* mutant exhibited 77% switching by mothers and 47% switching by daughters (Table 2-1, line 2).

Table 2-1. Switching Behavior of Strains Lacking or Overproducing *ASH1* or Lacking *URS2*

Strain	Four-shmoo microcolonies *	Switching Frequency	
<i>ash1-1</i> Mutant		%M	%D
1. <i>HO ste3Δ</i> (YAS131)	3	71% (64/90)	<1% (0/77)
2. <i>HO ste3Δ ash1-1</i> (YAS132)	95	77% (86/111)	47% (46/97)
3. <i>HO ste3Δ ash1-1 swi5Δ</i> (YAS135)	4	<1% (0/114)	1% (1/85)
4. <i>HO ste3Δ ash1-1 swi5Δ / pSWI5</i>	90	N.D.	
5. <i>HO ste3Δ / pSWI5</i>	2	N.D.	
<hr/>			
<i>ash1</i> Deletion		%S(2)	%D1(2)
6. <i>ASH1 HO</i> (YAS143)		72% (73/102)	<1% (0/97)
7. <i>ash1Δ HO</i> (YAS144)		95% (103/108)	94% (100/106)
<hr/>			
<i>ASH1</i> Overexpression		%M	%D
8. <i>HO ste3Δ / 2μ vector</i> (YAS131)		66% (73/111)	<1% (0/89)
9. <i>HO ste3Δ / 2μ ASH1</i> (YAS131)		8% (9/110)	<1% (0/80)
<hr/>			
<i>HO URS2Δ</i>		%M	%D
10. <i>HO</i> (IH1879)		70% (70/98)	<1% (0/88)
11. <i>HO URS2Δ</i>		71% (141/200)	30% (57/189)

* The number of four-shmoo microcolonies per 1000 microcolonies (n=1000).

M: mother; D: daughter.

Lines 6-7: S is the spore cell that begins a lineage, S(2) is the first mother cell derived from the spore, and D1(2) is the first daughter of the S cell.

Line 11: Data from four different *HO URS2Δ* strains (YAS45-2A, YAS45-2B, YAS45-4C, and YAS65-6B) were pooled.

Because the efficiency of mating-type switching in lineages that originate from vegetatively growing wild-type cells is lower than the efficiency of switching observed in lineages that begin as spore cells (AS, unpublished observations), we also examined the efficiency of switching in *ash1-1* lineages that begin as spore cells. In these experiments, 84% (26/31) of *ash1-1* mothers and 76% (22/29) of *ash1-1* daughters switched mating type. The *ash1-1* mutation does not allow spores to switch: none of 51 spores switched mating-type in the first division after germination.

Since mutations that bypass the need for Swi5p in *HO* transcription allow daughters to switch mating type (Sternberg et al., 1987; Nasmyth et al., 1987b; Kruger, 1991), we determined if *ash1-1* mutants exhibit *HO* expression in the absence of *SWI5*. The *SWI5* gene was deleted in the *ash1-1* mutant, and the ability of this strain to switch mating type was determined (Table 2-1, line 3). Both the four-shmoo microcolony assay and pedigree analysis indicated that the phenotype of *ash1-1* is dependent on *SWI5*: the number of four-shmoo microcolonies in the *ash1-1 swi5Δ* double mutant was approximately equivalent to the number of four-shmoo microcolonies in the wild-type *HO ste3Δ* parent (Table 2-1, lines 1 and 3). Providing the *ash1-1 swi5Δ* strain with the *SWI5* gene on a plasmid restored the daughter-switching phenotype (Table 2-1, line 4). None of 114 mothers and only one of 85 daughters were observed to switch mating type by pedigree analysis in the *ash1-1 swi5Δ* double mutant (Table 2-1, line 3). These observations demonstrate that the daughter-switching phenotype of *ash1-1* mutants was dependent on *SWI5*.

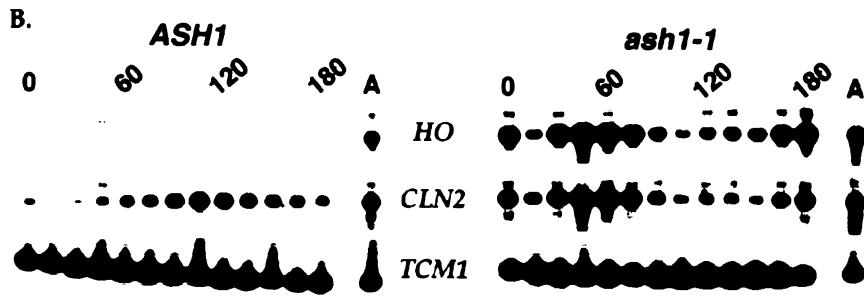
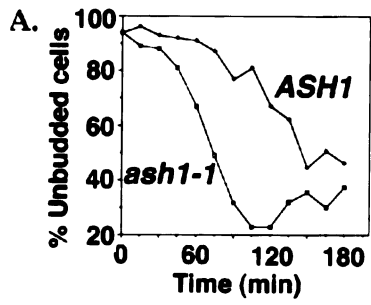
ash1-1* Daughter Cells Transcribe *HO

Since the asymmetry of mating-type switching in wild-type cells is due to the asymmetric synthesis of *HO* (Nasmyth, 1983), it was important to determine if *ash1-1* daughters transcribe *HO de novo* rather than, for example, inherit a stabilized *HO* protein. Early G1 daughters of the *ash1-1* strain and its wild-type parent were isolated by centrifugal elutriation at 4°C and then allowed to progress through the cell cycle at 30°C. Samples were taken every 15 minutes, and the percentage of unbudded cells was calculated to ascertain progress through the cell cycle (Figure 2-3A). Northern analysis of RNA isolated from the same samples revealed that, unlike wild-type daughters, *ash1-1* daughters transcribe *HO* (Figure 2-3B). Since wild-type mothers normally transcribe *HO* in late G1, we marked late G1 in daughter cells by following transcription of *CLN2*, which encodes a G1 cyclin (Hadwiger et al., 1989). The timing of *HO* and *CLN2* transcription was coincident, indicating that daughter cells transcribed *HO* at the correct time in the cell cycle. Differences in cell cycle progression between the wild-type and mutant were due to variance in the elutriation procedure (see Experimental Procedures).

***ASH1* Encodes a Protein Related to the GATA Family of Transcriptional Regulators**

To clone the gene defective in the *ash1-1* mutant, we first determined that the *ash1-1* mutation is recessive, as described in Experimental Procedures. Upon backcrossing the *ste3Δ::LEU2 HO ash1-1* strain to a *STE3 HO* strain in the same background, it became readily apparent that *ash1-1* was tightly linked to *STE3*: the daughter-switching phenotype cosegregated with leucine prototrophy in 30 of 30 tetrads. Since *STE3* is on chromosome XI, a

Figure 2-3. *ash1-1* Daughters Transcribe *HO* RNA. Early G1 daughters were isolated from *ASH1 HO ste3Δ matΔ* (YAS138) and *ash1-1 HO ste3Δ matΔ* (YAS139) strains by centrifugal elutriation at 4°C. Cells were transferred to 30°C medium and followed through the cell cycle. Timepoints were taken every 15 minutes. (A) The percent unbudded cells was determined. (B) RNA from the same samples in (A) were subjected to Northern analysis. A corresponds to an RNA sample isolated from an asynchronous population of the same cells. Each sample was probed for *HO*, *CLN2*, and *TCM1* RNA. The latter is constant over the cell cycle and served as a loading control (Schultz and Friesen, 1983).



sequenced chromosome (Dujon et al., 1994), we tested candidate open reading frames (ORFs) in the vicinity of *STE3* for complementation of the four-shmoo microcolony phenotype. Eleven candidate ORFs, each with at least 800 base-pairs of flanking sequence, were amplified from genomic DNA using the polymerase chain reaction and cloned into an integrating vector. DNA encoding each ORF was integrated into the *ash1-1* mutant at its own chromosomal locus, and resulting strains were assayed for the four-shmoo microcolony phenotype. DNA encoding ORF YKL185w complemented both the four-shmoo microcolony phenotype of the *ash1-1* mutant (see Experimental Procedures) and a slight growth defect displayed by this mutant (data not shown). YKL185w has homology to the GATA family (Orkin, 1992) of transcriptional regulators (Figure 2-4).

Ash1p Localizes Asymmetrically to the Daughter Nucleus After Anaphase

Since *ASH1* is required to prevent *HO* transcription in daughters, we determined if Ash1p is localized asymmetrically to the daughter cell. For this purpose, we have constructed a myc-epitope tagged version (Kolodziej and Young, 1991) of Ash1p which is carried in single copy at the *ASH1* locus. Asynchronous cultures of a *ho* strains exhibited Ash1p staining (detected by indirect immunofluorescence with the 9E10 monoclonal antibody (Kolodziej and Young, 1991) in large-budded and unbudded cells. Ash1p is predominantly present in one of the two nuclei in large-budded cells that have undergone nuclear division; three examples of such cells are shown in Figure 2-5. The stained nucleus appeared to be the nucleus in the bud (the incipient daughter cell). Untagged cells, in contrast, did not show any nuclear staining, although a slight cytoplasmic haze could be observed (Figure 2-5).

Figure 2-4. Ash1p has Similarity to the GATA Zn Finger. (A) The Ash1p protein sequence, as predicted by the yeast genome sequencing project (Dujon et al., 1994). The putative zinc finger is underlined. (B) Comparison of zinc finger regions from various GATA proteins. Residues identical to Ash1p are shaded. The amino acid sequence numbers are shown. The SWISSPROT accession numbers for *GLN3* (a yeast gene involved in nitrogen regulation), *elt-1*, and *GATA-1* are as follows: *GLN3* (P18494), *elt-1* (P28515), and *GATA-1* (P15976). S.c. : *Saccharomyces cerevisiae*; C.e.: *Caenorhabditis elegans*; H.s.: *Homo sapiens*.

A.

```

1  MSSLYIKTPL HALSAGPDSH ANSSYYDNLL LPSFSNLSSN ISRNNITTDN NINSASPRKY 60
61  SFHSLNVSPI LSPISLANEI LGKKSNTAPA SPHHMDYNPI SSLTPGNSPE FNKASLSQIS 120
122  FTNPLNYGSG LGFSSNSQFR LPLDLRLSSV SLSKRPERPQ QSLFSLRHLQ LLPSPLLQEN 180
181  AARFPDTSKF TSNWKTDLTH WCKDTNYQDY VKIREEVAHF KPLSIFNLTN NQNNDSFNYG 240
241  KELESTRSSK FHSPSKESFD RTKLIPSILE AKDQFKOLSN NAW SITPPVT PPMSPPTNRT 300
301  MERTTLRGVE ASFFEGKSSN NDSIFNPIIS EKLQEVKHQ RQLRGNSFPM PNASHKKTNS 360
361  FKALQIKKLL ANRDILSHNS KSNVRKPSKN KISKQASNVF GNTARQLVMK LDNASYSSVS 420
421  ASSSPSPSTP TKSGKMRSRS SSPVRPKAYT PPSRSPNYHR FALDSPQSP RRSNNSITK 480
481  KCSRSSGSS PTRHTTTCVYCV SCHSSDSPEW RPSWSPRKOD OLCNSCGLRY KKTHTRCLND 540
541  LCRKIPTKGE INIMKSNGLD KEFVPERNCE IEGYRCLFCN YITETVEN 588

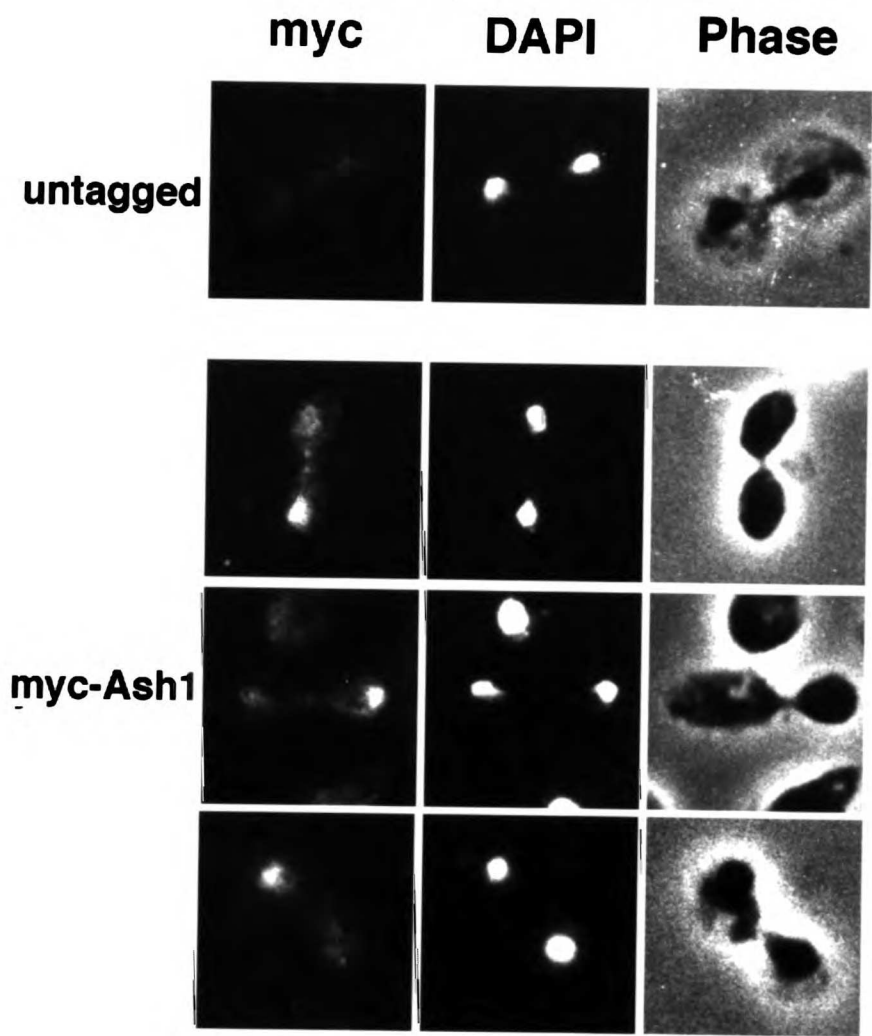
```

B.

S. cer. ASH1	497	RVCVSCSSD	SPC	WPSWSP	RKQDQ	LCNS	GLRY	531
C.elegans elt-1	215	RECVNCGVHN	TPL	WRRDGS	...	NYLCNAE	GLYF	246
Human GATA-1	202	RECVNCGATA	TPL	WRRDRTG	...	HYLCNAE	GLYH	233
S. cer. GLN3	304	IQCFNCKTFK	TPL	WRRSPEG	...	NTLCNAE	GLFO	335
Consensus		--C--C----	-P-WR-----	-----	LCN-	GL--R		

Figure 2-5. Ash1p is Localized to One of Two Nuclei in the Majority of Large Budded Cells. Cells from a Ash1-myc (YAS141) and untagged (YAS140) strains were grown to early log phase, fixed, and processed for indirect immunofluorescence staining with 9E10 antibodies, which recognize the myc epitope. Ash1-myc staining, DAPI staining, and a phase image is shown for each of three cells. The Ash1p and DAPI photographs were taken in the same focal plane. The top row depicts an image of cells from the untagged strain (YAS140), photographed and processed under the same conditions as the tagged strains.

Ash1p Localization

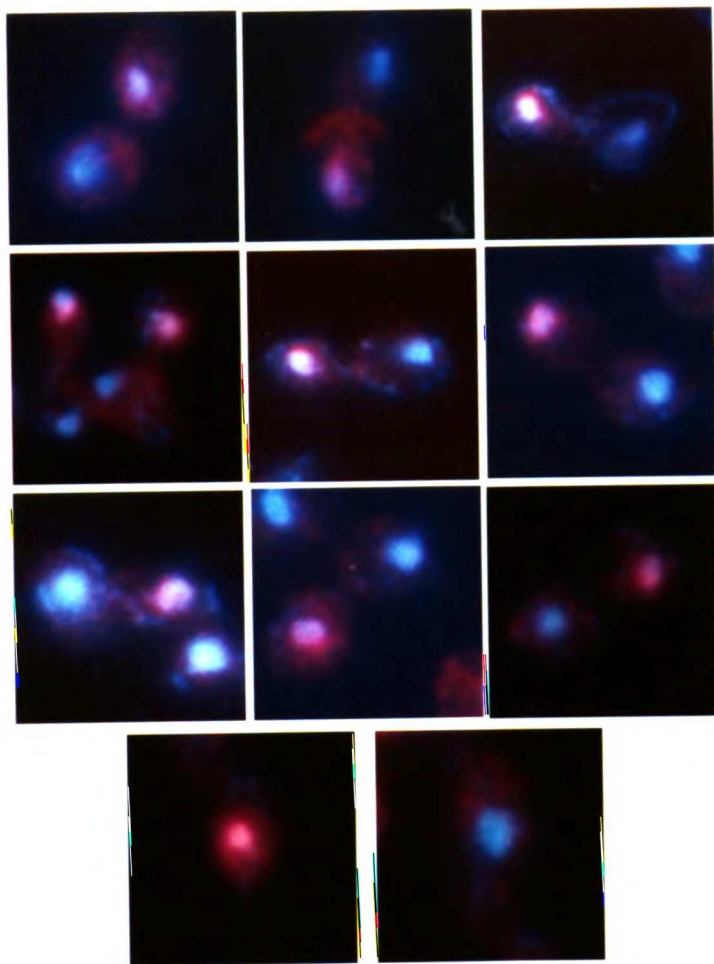


Ash1p is also present in the nucleus of 50-60% of unbudded cells. Superimposed DAPI (blue) and rhodamine (red) images of cells are displayed in Figure 2-6. Nuclei that contain Ash1p were pink, due to superimposed DAPI and rhodamine (to detect the 9E10 antibody) signals, whereas nuclei without Ash1p staining were blue. Localization of Ash1p to one of the two nuclei in large-budded a/α cells was also observed (Figure 2-7).

To determine definitively if the nucleus containing Ash1p is the daughter nucleus, we marked the mother cells morphologically by arresting a cells with α -factor and allowing them to shmoo in response to the pheromone. After removal of α -factor, the shmoo-shaped cells re-entered the cell cycle synchronously. Samples were taken every 10 minutes and examined for immunofluorescence staining. Ash1p was first visible 50 minutes after release from pheromone arrest, coincident with the appearance of large-budded, post-anaphase cells (data not shown). The cells in Figure 2-8 were present 60 minutes after release from arrest. Since all the mothers were shmoo-shaped but their counterpart daughter buds were round, mothers and daughters could be unambiguously distinguished. Ash1p preferentially stained the nucleus in the round, budded cell after anaphase (Figure 2-8). Thus Ash1p is localized predominantly to the daughter nucleus.

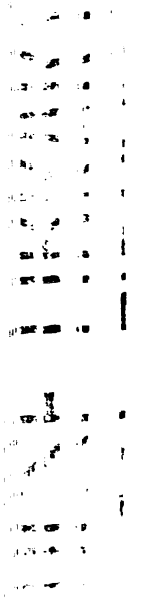
In asynchronous populations, 73% of the large-budded cells that had undergone nuclear division had visible Ash1p in the daughter nucleus only ($n=200$). 15% of large-budded cells showed Ash1p staining predominantly in the daughter nucleus with an intermediate amount of staining in the mother nucleus. The remaining 12% of large-budded cells that had undergone anaphase displayed equivalent levels of Ash1p in both the mother and daughter nuclei. Ash1p staining was not observed in the nucleus of cells

Figure 2-6. Color images of Ash1p staining. Superimposed DAPI (to detect DNA) and rhodamine (to detect the myc antibody) images of a Ash1-myc (YAS141) cells were photographed in the same focal plane. Nuclei that contain Ash1p were pink, due to superimposed blue (DAPI) and red (rhodamine) signals. Other nuclei were blue due to the DAPI staining. The bottom row shows two unbudded cells, one with Ash1p staining (on the left), one without (on the right).



LIBRARY

Figure 2-7. Ash1p is Localized Asymmetrically in a/ α cells. a/ α Ash1-myc (YAS142) cells were grown to early log phase, fixed, and processed for indirect immunofluorescence staining with 9E10 antibodies, which recognize the myc epitope. Ash1p staining, DAPI staining, and phase contrast images are shown for a group of cells. Unbudded cells (at the top) with and without nuclear staining and a large-budded cell with asymmetric staining are visible.



Ash1-myc **DAPI** **Phase**

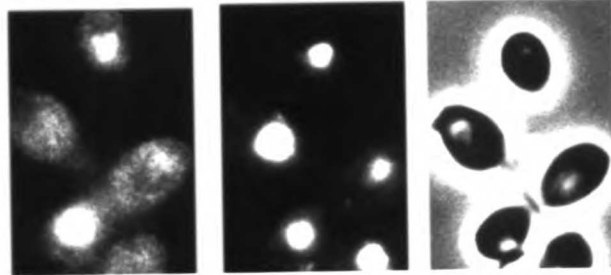
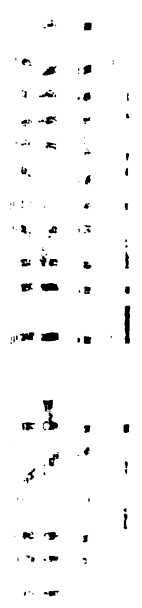


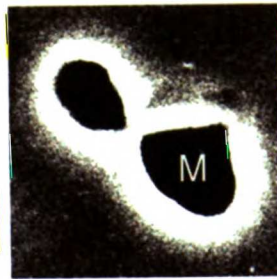
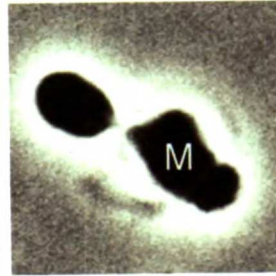
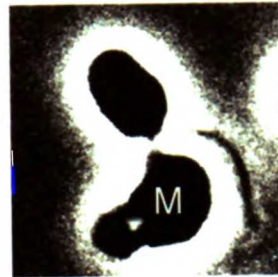
Figure 2-8. Ash1p is Localized to the Incipient Daughter Nucleus. α -factor was used to induce shmoo formation in YAS141 cells, which were then released into YEPD in the absence of pheromone and allowed to bud. The buds (incipient daughter cells) were round, whereas the mother cells (M) were shmoo-shaped. Each row shows Ash1p staining, DAPI staining, and phase contrast images for a different mother/daughter pair.



Ash1-myc

DAPI

Phase



undergoing mitosis. Finally, we examined synchronous populations of cells generated from α -factor arrest as described above and from *cdc15-2* arrest (Tebb et al., 1993) in search of a transient population of large-budded cells with strong Ash1p staining in both mother and daughter nuclei. Such a transient staining intermediate was not observed (data not shown). Since even untagged strains display a low background level of cytoplasmic staining, we could not determine if the analogous cytoplasmic haze seen in tagged strains represented actual Ash1p staining. Preliminary immunoblot experiments indicated, however, that the Ash1p protein was present only at times in the cell cycle when nuclear localization was observed (Figure 2-9).

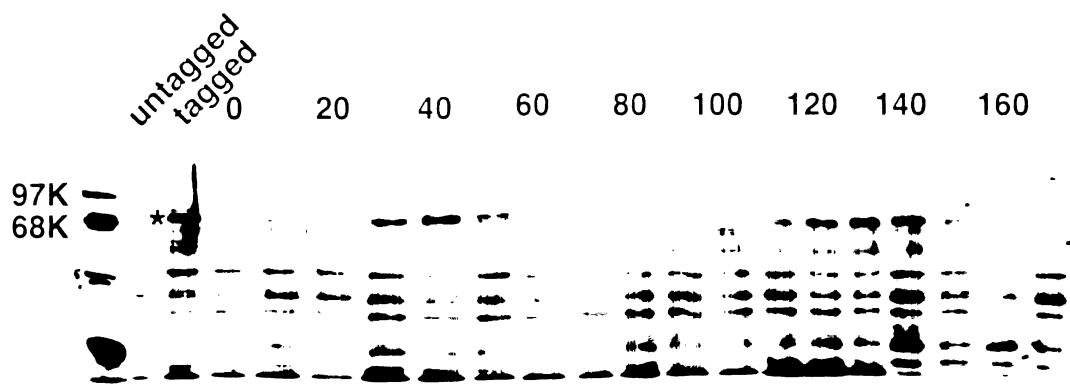
Daughter Cells Switch as Efficiently as Mother Cells in the *ash1* Δ Mutant

To determine the phenotype of an *ash1* null mutant, we replaced the entire *ASH1* ORF with the *LEU2* gene. We deleted one copy of the *ASH1* gene in an a/α *HO/HO* diploid and sporulated this strain to obtain *ash1* Δ *HO* segregants. The *ash1* Δ strains, identified by leucine protrophy, were viable. To study the effect of *ash1* Δ on mating-type switching, we sporulated congenic a/α *HO/HO* *ash1* Δ /*ash1* Δ and a/α *HO/HO* *ASH1* /*ASH1* strains and subjected spores to pedigree analysis (Table 2-1, lines 6-7). No daughter cells were observed to switch in *ASH1* strains whereas 94% of *ash1* Δ daughters switched mating type. Deletion of the *ASH1* gene clearly allowed daughters to switch mating type as efficiently as mothers, which switched at a frequency of 95% in the *ash1* Δ strain (see below). *ash1* Δ spores did not switch mating type: none of 105 spores switched in the first division after germination.

Not all wild-type mother cells switch mating type; these cells generally switch at a frequency of 60-80% (Strathern and Herskowitz, 1979). Since 27%

Figure 2-9. Ash1p is Expressed in a Cell-cycle-Specific Manner. *cdc15-2*

ASH1-myc (YAS150) cells were grown to mid-log phase and arrested as large-budded cells in late anaphase at the non-permissive temperature. These cells were then transferred to fresh medium at the permissive temperature and followed through the cell cycle. Samples were taken every 10 minutes after release from arrest and subjected to immunoblot analysis to detect Ash1-myc protein. The position of the 97kD and 68kD markers is indicated at the left of the blot. The first sample lane consists of protein from asynchronous cells of an isogenic untagged strain (YAS147); the next lane is an asynchronous sample from YAS150. Ash1-myc is indicated by an asterisk. It is visible 30, 40, and 50 minutes after release; these timepoints occur before the large-budded cells that accumulate during the arrest undergo their first division. Ash1-myc is seen again 110-150 minutes after release in late anaphase cells during the next round of the cell cycle. Ash1p is detected by immunofluorescence only at the identical timepoints as the Western analysis (data not shown).



of large-budded cells show some Ash1p staining in the mother nucleus as well as the daughter nucleus, it is possible that these mother cells do not switch mating type because of Ash1p. If so, deletion of the *ASH1* gene should allow mother cells to switch at higher frequency. We compared switching in lineally equivalent mothers from *ASH1* and *ash1Δ* strains. Specifically, we examined the switching frequency of the S(2) mother, the first mother arising from a spore cell (see diagram in Table 2-1, lines 6-7). 72% of *ASH1* S(2) mothers switched mating type in contrast to 95% of *ash1Δ* S(2) mothers. We conclude that *ash1Δ* mothers do switch more efficiently than *ASH1* mothers. This result indicates that when present, Ash1p may be able to inhibit *HO* expression in mothers as well as daughters.

Overexpression of *ASH1* Inhibits Mating-type Switching in Mother Cells

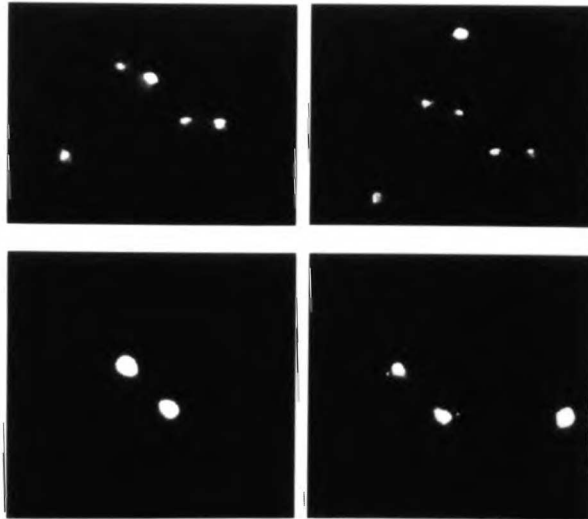
Because *ash1Δ* daughters switch mating type, it is clear that Ash1p is required to inhibit *HO* expression in daughter cells. We wished to know if overexpression of the *ASH1* gene would inhibit mating-type switching in mother cells, presumably by entering the mother nucleus and inhibiting *HO* expression. The *HO ste3Δ* strain was thus transformed with 2μ*ASH1* or control plasmids and mating-type switching was compared. 66% of mothers carrying the control vector switched mating type whereas only 8% of mothers carrying the 2μ*ASH1* plasmid switched (Table 2-1, lines 8-9). Since the 2μ*ASH1* plasmid inhibits mating-type switching in mother cells, we determined if Ash1p was localized to mother nuclei when *ASH1* was thus overexpressed. A 2μ plasmid containing the myc-tagged *ASH1* gene was used to localize Ash1p (Figure 2-10). A significant percentage (75%) of large-budded, post-anaphase cells showed intense staining in both mother and

Figure 2-10. Overexpression of *ASH1* on a 2-micron Plasmid Results in Symmetric Staining. YAS140 cells carrying 2 μ *ASH1-myc* were grown to early log phase, fixed, and processed for indirect immunofluorescence staining with 9E10 antibodies. Ash1p staining and DAPI staining in three large-budded cells is shown.

2 micron ASH1-myc

myc

DAPI



daughter nuclei (n=50). Cells carrying an untagged 2 μ *ASH1* plasmid showed no staining (data not shown).

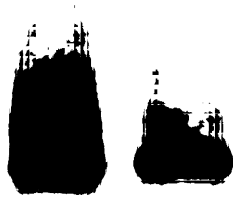
An Intact *HO* Promoter is Required for Mother/Daughter Regulation

Limiting the timing of *HO* transcription to late G1 might play a role in mother/daughter regulation. As mentioned earlier, Swi5p enters the nucleus just after anaphase, but *HO* transcription is restricted to late G1 due to the URS2 segment of the *HO* promoter. Postponing *HO* transcription from anaphase until late G1 might ensure that Ash1p, which localizes to daughter nuclei after nuclear division, can counteract Swi5p function in daughter cells. We used an *HO* promoter lacking URS2 to shift the transcription of *HO* to just after anaphase (Nasmyth, 1985b; Nasmyth et al., 1990). Four different *HO* *URS2* Δ strains were examined by pedigree analysis, and the results were pooled (Table 2-1, lines 10-11). Mothers switched at 71% and daughters switched at 30% in these strains. None of 58 spores were observed to switch in the first division following germination. These results indicate that URS2 is required for proper mother/daughter regulation.

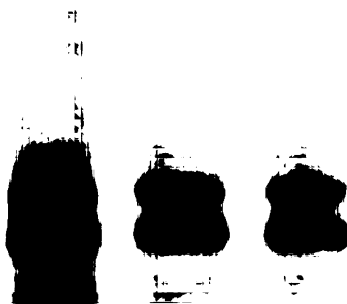
To verify the properties of the *HO* *URS2* Δ strain, we examined its dependence on *SWI5* and *SWI4*. Transcription from the *HO* *URS2* Δ promoter is known to be dependent on Swi5p, but independent of Swi4p/Swi6p (Nasmyth, 1987; Breeden, 1987). We confirmed that our *HO* *URS2* Δ strains are regulated by *SWI4* and *SWI5* in the expected manner (Figure 2-11).

Figure 2-11. Expression of *HO* RNA in *URS2Δ* Strains is Dependent on *SWI5* but Independent of *SWI4*. Primer extension was used to detect *HO* and *URA3* transcripts in RNA made from *HO URS2Δ*(IH1997), *swi4Δ HO URS2Δ*(YAS46-17B), and *swi5Δ HO URS2Δ* (YAS62-2C) strains.

HO URS2Δ
swi4Δ HO URS2Δ
swi5Δ HO URS2Δ



HO



URA3

Discussion

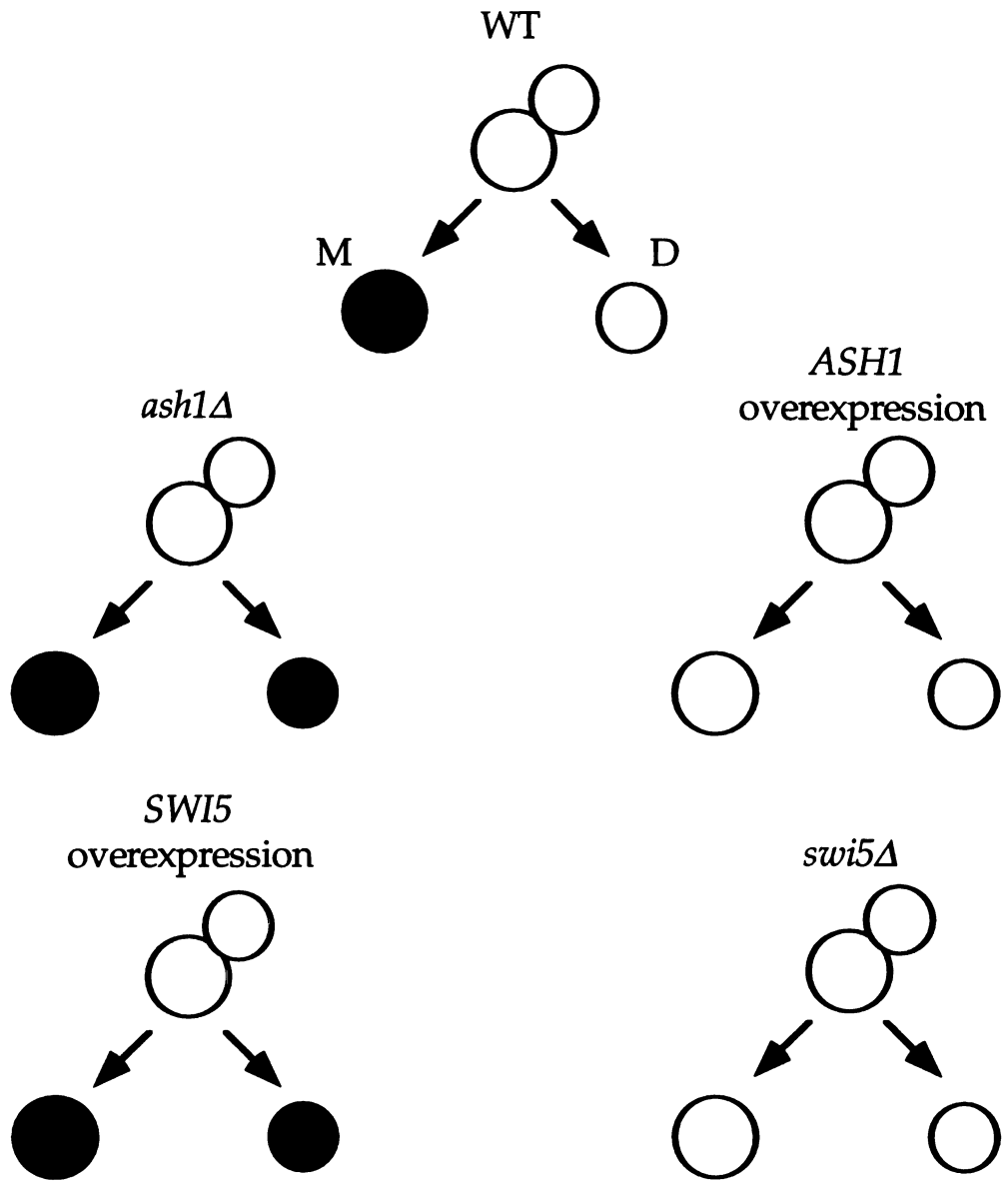
S. cerevisiae mother and daughter cells exhibit a striking difference in cell fate: mother cells are able to transcribe the *HO* gene and switch mating type whereas daughter cells are not. We have identified a gene, *ASH1*, that is required to prevent daughter cells from transcribing *HO* and switching mating type. *ASH1* has been independently identified as a regulator of *HO* by a strategy completely different from ours (Bobola et al., 1996). We have shown that daughter cells that lack *ASH1* are able to switch mating type at high efficiency. Furthermore, overexpression of *ASH1* inhibits mating-type switching in mother cells. Ash1p is asymmetrically localized to the incipient daughter nucleus in large-budded cells that have undergone nuclear division. These observations indicate that Ash1p functions in daughter cells to inhibit *HO* transcription.

Ash1p is a Key Determinant of a Stem Cell Lineage

S. cerevisiae daughter cells divide to yield a differentiated mother cell, which can switch mating type, and a pluripotent daughter cell, which cannot. Thus the mitotic yeast lineage can be viewed as a stem cell lineage. We have shown that Ash1p is required to maintain this lineage pattern; in its absence, daughter cells adopt the mother cell fate (Figure 2-12). Overexpression of *ASH1* inhibits mating-type switching in mother cells, indicating that ectopic expression of *ASH1* is sufficient to induce the majority of mother cells to adopt the daughter cell fate. Thus *ASH1* is necessary and sufficient for determining cell fate.

Swi5p, which is required for mother cells to express *HO* and switch mating type, plays an opposing role to Ash1p (Figure 2-12). In the absence of

Figure 2-12. *ASH1* and *SWI5* have Reciprocal Effects on Cell Fate. Five types of lineage are shown, each starting with a predivisional large-budded cell that divides to give rise to a mother (M) and a daughter (D). Cells that transcribe *HO* are black.



Swi5p, mother cells adopt the daughter cell fate (non-switching) (Stern et al., 1984). Overexpression of *SWI5* or stabilization of Swi5p allows daughter cells to transcribe *HO* and switch mating type (Lydall et al., 1991; Nasmyth et al., 1987a; Tebb et al., 1993). The ability of *ash1* mutant daughters to switch mating type is dependent on *SWI5*, indicating that *swi5* is epistatic to *ash1*. These data suggest that, in daughter cells, *ASH1* acts upstream of *SWI5* to inhibit *HO* expression. The patterns of regulation by *ASH1* and *SWI5* are analogous in several respects to cell-fate determination by *numb (nb)* and *tramtrack (ttk)* in the developing *Drosophila* nervous system (Rhyu et al., 1994; Guo et al., 1995; Knoblich et al., 1995). As with *ASH1* and *SWI5*, loss of function of *nb* or *ttk* causes opposite transformations of cell-fate determination. Ectopic expression of *nb* or *ttk* also has reciprocal effects on cell fate. Finally, *ttk* is epistatic to *nb*. Genetic and immunocytochemical analyses indicate that *nb* is required in neuronal cells to inhibit *ttk* expression so that these cells do not become support cells. Similarly, Ash1p appears to antagonize Swi5p function in daughter cells, rendering them unable to switch mating type.

Although *ash1* is not the only mutation that allows switching in daughter cells, *ASH1* plays a distinctive role in cell-fate determination. Mutations in the genes *SIN1* or *SIN3* also permit daughter cells to switch mating type, but in addition allow spore cells to switch (Sternberg et al., 1987; Nasmyth et al., 1987b; Kruger, 1991). *sin1* and *sin3* mutations bypass the need for *SWI5* in both mothers and daughters (Nasmyth et al., 1987b; Sternberg et al., 1987). In contrast, switching in *ash1* mutants is dependent on *SWI5*, indicating that Swi5p is able to function in daughter cells only in the absence of Ash1p. Thus Ash1p is a unique lineage determinant.

Distribution or Perdurance of Ash1p May be Responsible for Other Aspects of the Mitotic Cell Lineage

Our observations indicate that Ash1p affects not only all daughter cells but some mother cells as well. The first indication that Ash1p might play a role in mother cells came from immunofluorescence experiments which reveal that approximately 27% of mothers contain an Ash1p signal that is comparable to that in the daughter cell. This Ash1p could arise from perdurance of Ash1p (*i.e.* failure of the daughter predecessor to degrade Ash1p) or failure of a predivisional (large-budded) cell to distribute all Ash1p to the daughter cell. The observation that deletion of *ASH1* allows mother cells to switch at increased frequency provides evidence that Ash1p can affect switching in mother cells (Table 2-1, lines 6-7).

All mother cells, with the exception of the S(2) cell (see diagram in Table 2-1, lines 6-7), are derived from daughter cells. Examination of Ash1p localization in synchronous populations revealed that Ash1p is present in unbudded daughter cells but is not visible once cells have undergone bud emergence (data not shown). Thus Ash1p is present predominantly in daughter cells during G1, the proper time in the cell cycle to inhibit *HO* transcription. After this point, we presume that Ash1p is degraded, allowing the daughter cell to acquire competence to transcribe *HO* when it becomes a mother cell. Inappropriate perdurance of Ash1p might be partially responsible for the failure of wild-type mother cells to switch mating type at 100% efficiency.

Strathern and Herskowitz (1979) reported that mother cells of different generations switch at different frequencies; we propose that Ash1p may also

be responsible for these differences. In particular, S(2) cells (see diagram in Table 2-1, lines 6-7) switch at higher frequency than mother cells later in the mitotic lineage. In contrast to later mother cells, the S(2) cell is derived from a spore cell. Unlike daughters, spores do not require Ash1p to inhibit *HO* transcription and may not contain Ash1p. S(2) cells thus may be the only mother cells unable to inherit residual Ash1p from their precursor cell. Hence, the S(2) cells may constitute a specialized cell type primed to switch mating type after spore cell germination and division. Even S(2) cells, however, do not switch mating type at 100% efficiency, again due to Ash1p (Table 2-1, lines 6-7). Failure of the S(2) cell to switch may result from inability of the S cell to localize all of the Ash1p to D1(2) (see diagram in Table 2-1, lines 6-7).

The high efficiency of switching by *ash1Δ* mutants provides a measure of the preferential switching to the opposite mating type cassette, that is, the directionality of mating-type interconversion (Strathern and Herskowitz, 1979). The ability of *ash1Δ* S(2) α cells to switch mating type to a at 95% efficiency indicates that the fidelity of directional switching is exquisitely high.

Mechanisms for Generating Ash1p Asymmetry

Ash1p is present predominantly in the daughter nucleus. How is this asymmetry generated? In principle, Ash1p or *ASH1* RNA might be synthesized in a predivisional cell and be distributed preferentially into the bud. Preliminary immunoblot data from synchronous samples indicate that Ash1p is present in cells only at the same times in the cell cycle when it is localized (AS, unpublished observations). It is thus unlikely that Ash1p is synthesized early in the cell cycle and then distributed to the bud. Another

possibility is that synthesis of *ASH1* RNA or protein is limited to the bud. For example, *ASH1* transcription might be confined to the incipient daughter nucleus in large-budded cells that have undergone nuclear division. A similar situation is found in the predivisional *Caulobacter* cell in which the *flgK* gene appears to be differentially transcribed in one of two nucleoids in the predivisional cell (Gober et al., 1991). If *ASH1* is transcribed only in the incipient daughter nucleus, Ash1p must then be restricted to the daughter cell in some manner. These models suggest that there exists a second factor other than Ash1p that confers asymmetric properties to the two nuclei in the predivisional yeast cell. In any event, the asymmetric localization of Ash1p is likely to reflect an intrinsic difference between mother cells and their buds.

Possible Mechanisms of Ash1p Function

Ash1p is related to the family of transcriptional regulators known as GATA factors, which were first identified as regulators of hematopoietic lineages in mammals (Orkin, 1992). These proteins share a zinc-finger consensus and are known to function as both activators and repressors of transcription. Of the five previously identified fungal GATA proteins, at least two, Dal80p and urbs1p (Cunningham and Cooper, 1991; Voisard et al., 1993), are negative regulators of transcription. Several GATA factors have been implicated in development of multicellular eukaryotes; for example, the *Drosophila* GATA factor *pannier* inhibits expression of the basic HLH proteins *achaete* and *scute* in a tissue-specific manner (Romain et al., 1993).

In principle, Ash1p might inhibit *HO* expression by binding to *HO* promoter DNA, to Swi5p, or to another regulatory protein. GATA factors are known to bind the sequence GATA, among others. GATA sites in the

vicinity of the two Swi5p binding sites in the *HO* promoter could be Ash1p binding sites. Ash1p could exploit these sites to compete with Swi5p for access to the *HO* promoter. Alternatively, Ash1p might bind directly to Swi5p and sequester it from the *HO* promoter. A domain in Swi5p that governs its stability (Tebb et al., 1993) might be a binding site for Ash1p since deletions of this domain allow daughter cells to switch mating type.

Asymmetric Inhibition of *HO* Expression May Depend on Temporal and Spatial Information

Although the URS1 region of the *HO* promoter confers regulation by Swi5p and is necessary for mother/daughter regulation (Nasmyth, 1987), we have observed that the URS2 region is also required for mother/daughter regulation. *HO URS2Δ* cells, which transcribe *HO* shortly after anaphase rather than in late G1, exhibit a substantial loss of cell-fate asymmetry (Table 2-1, lines 10-11). Our data differ from those reported previously (Nasmyth, 1987). We have therefore confirmed that our *HO URS2Δ* strain exhibits proper regulation by *SWI5* and *SWI4*.

The phenotype of *HO URS2Δ* strains is similar to that of *ash1* mutants in two key ways. First, neither *HO URS2Δ* nor *ash1* spores are able to switch mating type. Furthermore, mating-type switching in these mutant daughter cells is dependent on *SWI5*. Thus the basis by which *HO URS2Δ* daughters switch mating type may be the same as for *ash1* mutants, that is, bypassing inhibition of *HO* by *ASH1*. Deletion of URS2 might allow daughters to switch mating type for several reasons. We cannot exclude the possibility that URS2 contains a subset of binding sites for Ash1p and that their removal allows switching in some, but not all, daughter cells. We favor the explanation,

however, that the altered timing of *HO* transcription displayed by *HO URS2Δ* strains is responsible for their loss of mother/daughter regulation. *HO* is transcribed shortly after Swi5p enters the nucleus in these strains (Nasmyth, 1985b; Nasmyth et al., 1990). We suggest that Swi5p activates transcription of *HO* in daughter cells of *HO URS2Δ* mutants before Ash1p can block Swi5p function. Thus, in wild-type strains, restricting *HO* transcription to late G1 might provide Ash1p with a window of opportunity to inhibit *HO* expression in daughter cells. We propose that a temporal signal imposed by URS2 and a spatial signal due to Ash1p are integrated to repress the *HO* promoter in daughter cells.

Ash1p Might Regulate Genes Other than *HO*

Ash1p function may not be limited to regulating *HO* transcription. This possibility is suggested by the observation that Ash1p is localized asymmetrically to what we presume is the daughter nucleus in *a/α* diploids. Since *HO* is repressed in *a/α* diploid cells by *a1-α2* (Jensen et al., 1983), Ash1p is not required to inhibit *HO* in *a/α* daughter cells. Ash1p may be fortuitously localized in these cells due to the nature of the mechanism that generates its asymmetry, or Ash1p could have daughter-specific targets (other than *HO*) which are not limited to haploid cells. The original *ash1-1* mutant exhibited a modest growth defect; in addition, overexpression of *ASH1* also caused slight growth inhibition (AS, unpublished observations). These data are consistent with regulation of target genes other than *HO* by Ash1p.

Mothers and daughters display several asymmetries in addition to *HO* expression which might be regulated by Ash1p. Such processes include segregation of ARS plasmids (Murray and Szostak, 1983) and the budding

pattern of a/ α diploids (Chant and Herskowitz, 1991; Chant and Pringle, 1995). Whether these processes are regulated by *ASH1* remains to be determined.

Asymmetric Cell Division and Cell Fate

One genetic criterion for a determinant of asymmetric cell fate is that underproduction and overproduction of the product lead to opposite fates (Horvitz and Herskowitz, 1992). This requirement is satisfied for the cell fate decisions controlled by the *numb* and *tramtrack* proteins of *Drosophila* (Guo et al., 1995; Knoblich et al., 1995; Rhyu et al., 1994) and by the *SpoIIE* protein of *Bacillus subtilis* (Duncan et al., 1995; Arigoni et al., 1995; Richard Losick, personal communication). Although both *SWI5* and *ASH1* satisfy this criterion, *Swi5p* is not asymmetrically localized whereas *Ash1p* is. In the case of the *Drosophila numb* protein, its localization to the ganglion mother cell results from asymmetric localization in the predivisional neuroblast cell (Rhyu, 1994). This asymmetry may originate from preexisting asymmetry in the neuroblast; the basis of such asymmetry is yet to be determined (Knoblich, 1995). Similarly, the asymmetric cells generated in *B. subtilis* sporulation are produced by positioning of a septum at a polar position in the predivisional cell. Although we do not yet know the basis for asymmetric localization of *Ash1p* to daughter cells, it is expected that its localization ultimately can be traced to the inherent asymmetry of the cell division process of budding yeast. The *numb*, *SpoIIE*, and *Ash1* proteins provide a link between asymmetric cell division and cell fate decisions.

Experimental Procedures

Genetic and Molecular Biological Methods

DNA manipulations were as described in Sambrook et al., 1989. Yeast genetic methods were as described in Rose et al., 1990.

Strains and Plasmids

Strains are described in Table 2-2, at the end of this chapter. YAS131-139 and YAS144 are derivatives of IH1879 (Hicks and Herskowitz, 1976). YAS140-142 are derivatives of K699 (a W303 strain from Kim Nasmyth (IMP, Vienna)). YAS45-2A, 45-2B, 45-4C, and 65-6B are derivatives of IH1879 and IH1997. IH1997 was obtained from Kim Nasmyth and contains the *HO URS2Δ* allele designated 229.102, which is missing nucleotides -145 to -901 of the *HO* promoter (Nasmyth, 1985b). The *ste3Δ::LEU2* strains were constructed by one-step gene replacement (Rothstein, 1991) using plasmid pSL376 (Hagen et al., 1986) and confirmed by colony polymerase chain reaction (PCR). The *swi5Δ::HISG* strains were constructed by one-step gene replacement using plasmid M596 from David Stillman (University of Utah) and confirmed by Southern blotting. The *matΔ::URA3* strains were constructed by one-step gene replacement using pKSW37 from the laboratory of James Broach (Princeton University).

Deletion of *ASH1* The *ash1Δ* construct replaced the entire *ASH1* coding sequence with the *LEU2* gene. A DNA fragment containing *ASH1* and several hundred base pairs of 5' and 3' flanking DNA was cloned into the vector Bluescript (Stratagene). A portion of this plasmid was amplified by

PCR using divergent primers that hybridized just upstream of the *ASH1* start codon and just downstream of the stop codon. The resulting linear fragment was cleaved at a restriction site introduced by the primers and circularized, yielding a plasmid that contained the *ASH1* flanking regions separated by this restriction site. The *LEU2* gene was then introduced into this site to form pAS171. The resulting disruption fragment was excised from pAS171 with *SacI* and *XhoI* and used to replace the chromosomal *ASH1* gene by one-step gene replacement (Rothstein, 1991). The presence of the *ash1* deletion was confirmed by colony PCR.

ASH1-myc construction and complementation analysis A unique *Bam*HI site was introduced into pAS151-A (see below) just downstream of the *ASH1* start codon using PCR, resulting in pAS151-B. Expand Long Template Polymerase from Boehringer Mannheim was used for the PCR. Plasmid pKK-1 encoding a multimerized epitope (Glu-Gln-Lys-Leu-Ile-Ser-Glu-Glu-Asp-Leu-Asn) from the *myc* oncogene (Kolodziej and Young, 1991) was obtained from Daniel Kornitzer and Steve Kron (MIT). Sequence encoding three copies of this epitope was excised from pKK-1 with *Bam*HI and introduced in the appropriate orientation into the *Bam*HI site of pAS151-B, resulting in pAS158. pAS158 was linearized with *NheI* and used to replace the chromosomal *ASH1* gene by two-step gene replacement (Rothstein, 1991). When pAS158 was linearized and integrated into YAS132 at the *ASH1* locus, it complemented the four-shmoo microcolony phenotype of the parent strain. Complementation of the daughter-switching phenotype of *ash1Δ* strains was also examined. pAS151-A and pAS158 were linearized in the *URA3* gene of the plasmid with *PstI* and integrated at the *ura3* locus of YAS158-1A. The resultant a/α diploids were sporulated and subjected to pedigree analysis.

ash1Δ ura3::ASH1 mothers switched at a frequency of 60% (76/127) whereas daughters were not observed to switch (0/107). *ash1Δ ura3::ASH1-myc* mothers switched at a frequency of 43% (41/96) whereas the corresponding daughters were not observed to switch. Clearly, *ASH1-myc* is sufficient to prevent daughter switching, and, if anything, inhibits switching somewhat in mother cells when present at the *URA3* locus. *ASH1-myc* was also integrated at the *ASH1* locus: pAS158 was linearized with NheI and integrated at the *ASH1* locus of YAS157. The resultant a/α diploid was sporulated and subjected to pedigree analysis. Mothers switched at a frequency of 60% (88/146) whereas no daughters were observed to switch (0/125).

Plasmids pSWI5 (Table 2-1, lines 4-5) is plasmid BD19 (Stern, 1985), which contains the *SWI5* gene in YCp50. pAS151-A results from insertion of a PCR product (see below, in Cloning of *ASH1*) encoding the *ASH1* ORF (YKL185w) into integrating vector pRS306 (Sikorski and Hieter, 1989). pAS152 is the analogous plasmid encoding YKL183w. 2μ *ASH1* (pAS174) consists of *ASH1* and several hundred base pairs of 5' and 3' flanking DNA from pAS151-A inserted into pRS426 (Sikorski and Hieter, 1989). The 2μ *ASH1-myc* plasmid (pAS163) is identical to pAS174 with the exception of sequence encoding the triple-myc epitope which is inserted just downstream of the start codon of *ASH1*.

Mutant Isolation

Early log phase *HO ste3Δ* cells of YAS131 were mutagenized with 2% ethylmethanesulfonate (EMS) to 5-15% survival, split into pools, and grown for 24-36 hours to bias against dying cells. These cells were then transferred to YEPD agar slabs containing α -factor. After approximately 10-12 hours, four-

cell microcolonies containing four shmoos were identified. These microcolonies were moved with a dissecting needle to a fresh agar slab lacking α -factor and allowed to recover from pheromone arrest. Each mutant isolate was grown to early log phase and retested in the microcolony assay. Of 86,000 microcolonies screened, one mutant, *ash1-1*, was obtained (see Results).

Cloning of *ASH1*

Dominance/recessivity Test Since the *HO* gene is repressed in a/ α diploids, we constructed a *mat Δ /MAT α ash1-1/ASH1 ste3 Δ /ste3 Δ HO/HO* diploid to test if *ash1-1* is dominant or recessive. We first transformed Y132 (*HO ste3 Δ ash1-1*) with a pGAL-STE3 plasmid (obtained from the laboratory of George Sprague). The transformed cells were mated with Y138 (*mat Δ ASH1 HO ste3 Δ*) in the presence of galactose. Zygotes were isolated by micromanipulation, grown to early log phase, and assayed by pedigree analysis. 70% (94/134) of mothers and 3% (4/122) of daughters were observed to switch mating type. Since the *ash1-1* mutation was complemented by *ASH1* in these strains, we concluded that *ash1-1* was recessive.

Cloning *ASH1* Genetic analysis indicated that the *ash1-1* mutation was within approximately 2 cM of the *STE3* gene (see Results), which is on a sequenced chromosome (Dujon et al., 1994). In order to identify the *ASH1* gene, we used PCR to amplify candidate genes in the vicinity of *STE3* using genomic DNA from IH1879 as template. We amplified DNA corresponding to 11 individual ORFs, each with at least 500 base pairs of 5' sequence and 300 base pairs of 3' sequence. Each ORF was amplified three independent times using Expand Long Template Polymerase from Boehringer Mannheim Biochemicals. The resulting linear fragment was cleaved at a restriction site

introduced by the primers and cloned into the integrating vector pRS306 (Sikorski and Hieter, 1989). Each of the resulting 33 clones was linearized at a unique site and integrated at the corresponding genomic locus in the *ash1-1* mutant strain (YAS132). All of the clones but one set of three were also integrated at the *URA3* locus in YAS132. The four-shmoo microcolony assay was performed on one to four transformants from each of the resulting strains. Only the gene encoding ORF YKL185w (Dujon et al., 1994) complemented the *ash1-1* mutant phenotype. The number of four-shmoo microcolonies per 1000 microcolonies (n=1000) was as follows: YAS131: 2; YAS132/integrated vector: 110; YAS132/integrated YKL185w: 3; YAS132/integrated YKL183w: 122. These data show that the DNA encoding YKL185w (from pAS151A) does complement the *ash1-1* defect whereas the DNA encoding YKL183w (from pAS152) does not.

ASH1 Sequence Confirmation

The *ASH1* gene was sequenced as part of the Yeast Genome Project (Dujon et al., 1994). The majority of the gene (corresponding to all but the first 109 amino acids and the last 25 amino acids) has been sequenced independently by M.E. Cusick (GenBank Accession #M88605); this latter sequence is identical to that of the Yeast Genome Project. We have confirmed that the sequences encoding the first 15 amino acids and the last 16 amino acids are correct.

Mating-type Switching Assays

Four-shmoo Microcolony Assay Cells were grown to early log phase in YEPD, sonicated, and transferred to 4% agar YEPD slabs containing 25 µg/ml α -factor. These slabs were incubated at 30°C for 10-14 hours and the resultant

microcolonies were examined under 250X magnification. The number of four-shmoo microcolonies per 1000 microcolonies was counted.

Pedigree Analysis: The starting cells for lineage studies were usually spore cells. **a**/ α diploids were sporulated and the resultant tetrads were dissected using conventional protocols. Each tetrad was dissected in close proximity to a wall of α cells that produced α -factor for the duration of the experiment. Mothers and daughters could be distinguished on the basis of size. A switch from α to **a** was scored as the acquired ability to respond morphologically to α -factor. When the starting cells for pedigrees were vegetative cells, as for the *ste3 Δ* strains, cells were grown to early log phase in YEPD, sonicated, and placed proximal to a wall of α cells. In the case of the 2 μ ASH1 experiments, early log phase cells were grown under selection for the auxotrophic marker on the plasmid. These cells were then sonicated and placed on 4% agar YEPD slabs for the remainder of the experiment.

RNA Analysis

Northern Blot Analysis. RNA preparation and sample analysis was performed as described previously (Cross and Tinkelenberg, 1991). The *HO ste3 Δ ash1-1* and *HO ste3 Δ ASH1* strains give rise to **a**/ α cells at a low frequency (AS, unpublished observations). To avoid any such diploidization, we deleted the *MAT* loci in the *ste3 Δ HO ash1-1* and *ASH1* strains; once the *MAT* locus is deleted, the cells can no longer switch mating type and are stably haploid. The probes used were all gel-purified DNA restriction fragments labeled by random-prime labeling using a Prime-it kit (Stratagene). The fragments used were as follows: *HO*: a 2.1 kb HindIII-EcoRV fragment that spans the entire coding sequence; *CLN2*: a 0.9 kb XhoI-HindIII fragment

containing coding sequence for amino acids 86-378 (Hadwiger and Reed, 1990); *TCM1* (Schultz and Friesen, 1983): a 0.8 kb HpaI-SalI fragment from pAB309Δ. Primer extension. RNA isolation and primer extensions were done as described previously (Ogas et al., 1991). The primer used to assay the *HO* transcript was 5'GGGATCTAACCTACCAGGTTCCACC. The primer used to assay the *URA3* transcript was 5'CGTGTCATGATATTAATAGC.

Immunoblot Analysis

Whole cell extracts were made from an equal number of cells from each sample as follows: Cells were collected by centrifugation, washed with water, and resuspended in 50 mM TRIS pH 7.5, 1% SDS, 5 mM DTT, 1 mM EDTA, and 1 mM PMSF. Samples were heated to 95°C, mixed with glass beads, and vortexed three times for 30 s. Protein from the same number of cells was then fractionated using 10% SDS polyacrylamide mini-gels and transferred to nitrocellulose filters in 150 mM glycine, 20 mM TRIS pH 7.5, 20% methanol. Filters were blocked for 1-16 hours in TBS containing 0.1% Triton-X 100 and 10% non-fat dry milk and decorated with a 1:1000 dilution of 9E10 monoclonal antibody (Kolodziej and Young, 1991) provided by Joachim Li (UCSF). Ash1-myc protein was then visualized using the Amersham ECL protein detection kit.

Immunofluorescence

The protocol used was essentially that described by Pringle et al., 1991. Cells were grown to early or mid-log phase and fixed with formaldehyde for 1-3 hours. The cells were washed with phosphate buffer and then spheroplasted. Cells were applied to polylysine-coated slides and treated with methanol and

acetone. The 9E10 antibody (Kolodziej and Young, 1991) was provided by Joachim Li (UCSF) and was used at a 1:200 dilution. The secondary antibody was a rhodamine-conjugated goat anti-mouse antibody from Jackson Immunoresearch and was used at a 1:100 dilution. The mounting medium was Fluoromount-G from Southern Biotechnology Associates, Inc.

Printing and Photography

Cells were visualized with an Olympus BX60 microscope. Black and white pictures were taken with TMAX 400 35 mm film at ASA 800. Images were printed on Rapitone P1-4 paper. Color pictures were taken with Kodak Gold Ultra 400 film. In Figure 2-7, DAPI and rhodamine images were photographed on the same frame of film. Figures were arranged and labeled in Adobe Photoshop.

Cell Synchrony Experiments

Elutriation Centrifugal elutriation was performed as described in Schwob and Nasmyth (1993) with the following modifications. 2 l cells at OD₆₀₀ 1-2 were grown overnight in YEP-raffinose (3% raffinose) and collected by filtration through Whatman cellulose nitrate filters, pore size 0.8. Approximately 0.2 l small G1 daughter cells at OD₆₀₀ 0.2-0.3 were collected by elutriation at 4°C. These daughter cells were collected by filtration and resuspended in 30°C YEP-raffinose. Several variables, especially the OD₆₀₀ of cells at the initial collection phase, affected the synchrony of the early G1 daughters after elutriation. The *ash1-1* samples in Figure 2-3 were an example of a synchronous release from G1. The *ASH1* samples, in contrast, did not exit G1 quite as synchronously, as evidenced by the trailing *CLN2* peak and the

kinetics of bud emergence. Variability in the budding index profile between different *ash1-1* experiments (data not shown) indicates that the synchrony difference is a reflection of the synchrony protocol rather than a genetic difference between the *ash1-1* and *ASH1* strains. In all experiments, *ash1-1* daughters transcribed *HO* whereas *ASH1* daughters did not. Calcofluor staining, which stains bud scars on the surface of mother cells, was used to ascertain the purity of the elutriated population shown in Figure 2-3. 92% of the *ASH1* cells and 98% of the *ash1-1* cells (n=200) had no bud scars, confirming that daughter cells were isolated.

α-factor Arrest and Release 0.15 l of a *ASH1-myc* cells were grown to OD₆₀₀ 0.3 at 25°C and arrested with 20 µg/ml *α*-factor for 3-3.5 hours. Cells were collected by filtration and washed twice with 0.15 l of 30°C YEPD. Cells were resuspended in 0.15 l of 30°C YEPD and allowed to re-enter the cell cycle. 10 ml samples were taken every ten minutes; 5 ml were processed for indirect immunofluorescence and 5 ml were used to make cell extracts for immunoblot analysis (data not shown).

cdc15 Arrest and Release 0.15l of *cdc15-2 ASH1-myc* (YAS150) cells were grown to OD₆₀₀ 0.5 at 25°C and arrested in late anaphase by shifting to 36°C for 3 hr. The cells were then returned to 25°C by mixing them with an equal volume of fresh YEPD at 14°C. 10 ml samples were taken every ten minutes; 5 ml were processed for indirect immunofluorescence and 5 ml were used to make cell extracts for immunoblot analysis.

Acknowledgments

We are indebted to Fred Cross, who generously allowed us to do the elutriation experiments in his lab and to Bert Oehlen for detailed instruction

on these experiments. We thank Erin O'Shea for use of the Olympus BX60 microscope, David Stillman, Betsy Ferguson, Daniel Kornitzer, Lisa Szeto, Linda Riles and Joachim Li for plasmids; Joachim Li for the 9E10 antibody; and Kim Nasmyth for strains. We are grateful to Ramon Tabtiang, Sylvia Sanders, Hay-Oak Park, Matthias Peter, Cori Bargmann, Andrew Murray, and Joachim Li for helpful comments on the manuscript and useful discussions. We acknowledge Ray Deshaies, Joachim Li, Craig Peterson, Joe Ogas, Tim Stearns, Warren Kruger, and Peter Sorger whose input at the inception of this project was invaluable. We thank Ramon Tabtiang for help with the figures and Flora Banuett for synthesis of oligonucleotides. Finally, we are grateful to Kim Nasmyth for communicating results before publication.

This work was supported by an NIH research grant (AI18738) to IH. We also gratefully acknowledge support from an NIH National Research Service Award in Genetics, the Markey Program in Biological Sciences, the Herbert W. Boyer Fund, and the University of California Chancellor's Fellowship.

Table 2-2. Chapter Two Strain List

<u>Strain name</u>	<u>Relevant Genotype</u>	<u>Source</u>
YAS131	a and α HO <i>ste3Δ::LEU2</i>	This study
YAS132	a and α HO <i>ste3Δ::LEU2 ash1-1</i>	"
YAS135	a and α HO <i>ste3ΔLEU2 ash1-1 swi5Δ::HISG</i>	"
YAS138	<i>matΔ::URA3 ASH1 HO ste3Δ::LEU2</i>	"
YAS139	<i>matΔ::URA3 ash1-1 HO ste3Δ::LEU2</i>	"
YAS140	a <i>ho ASH1</i>	Kim Nasmyth (K699)
YAS141	a <i>ho ASH1-myc</i>	This study
YAS142	a/ α <i>ho/ho ASH1-myc/ASH1</i>	This study
IH1879	a/ α HO/HO	Hicks and Herskowitz, 1976
YAS144	a/ α HO/HO <i>ash1Δ::LEU2/ash1Δ::LEU2</i>	This study
YAS147	a <i>cdc15-2</i>	Ray Deshaies
YAS150	a <i>cdc15-2 ASH1-myc</i>	This study
YAS157	a/ α HO/HO <i>ura3/ura3 ASH1/ASH1</i>	Kim Nasmyth (K4709)
YAS158-1A	a/ α HO/HO <i>ura3/ura3 ash1Δ/ash1Δ</i>	This study
YAS45-2A	a/ α HO URS2 Δ	"
YAS45-2B	a/ α HO URS2 Δ	"
YAS45-4C	a/ α HO URS2 Δ	"
YAS65-6B	a/ α HO URS2 Δ	"
IH1997	a HO URS2 Δ <i>hmla</i>	Kim Nasmyth
YAS46-17B	a and α HO URS2 Δ <i>swi4Δ</i>	This study
YAS62-2C	a HO URS2 Δ <i>swi5Δ</i>	"

YAS131, 132, 135, 138, 139, 144, and IH1879 are isogenic
YAS140-142, 147, 150, 157, 158-1A are isogenic (W303 background)
IH1879 and IH1997 are the parents of the remaining strains

CHAPTER THREE

ESTABLISHMENT OF ASYMMETRIC LOCALIZATION OF ASH1 PROTEIN

Abstract

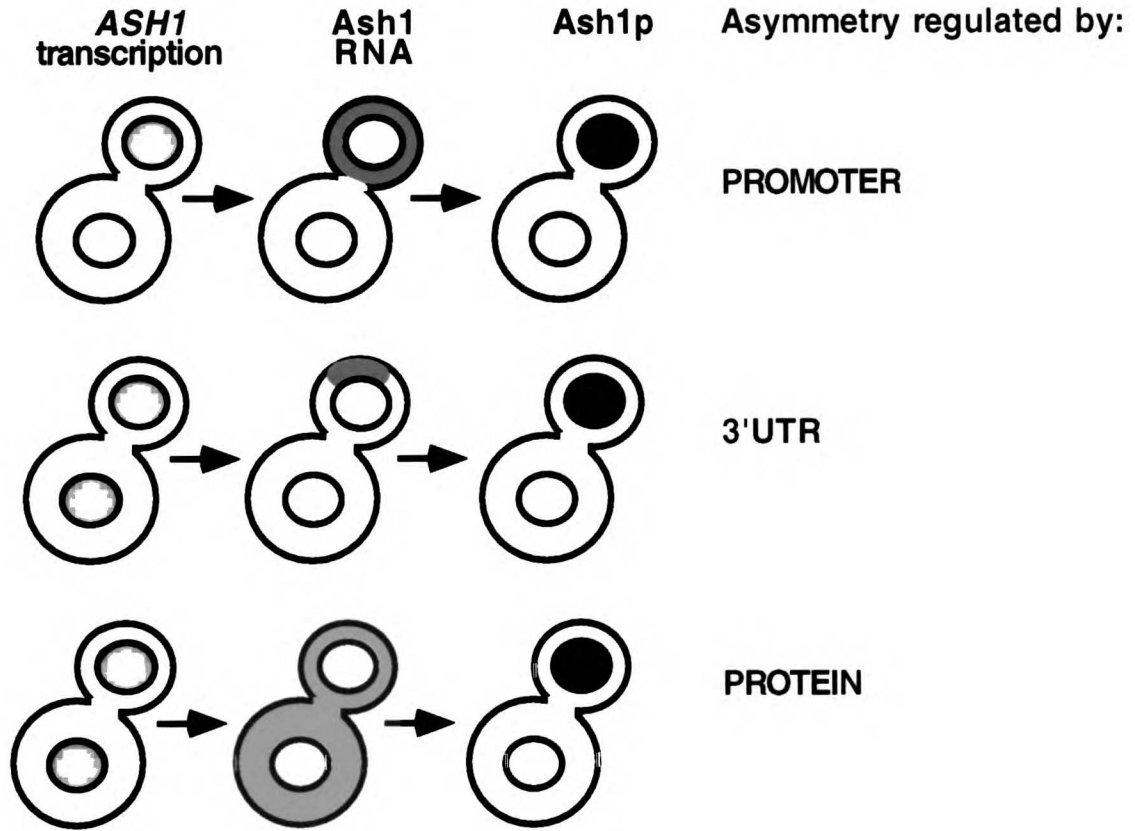
Ash1 protein is a key regulator of cell-fate determination in budding yeast. Ash1p localizes predominantly to the incipient daughter nucleus in large-budded cells that have undergone anaphase. After cell division, these cells yield a mother cell with little or no detectable Ash1p staining and a daughter cell with a significant amount of nuclear Ash1p staining. In this chapter, I show that the promoter and 5' untranslated region (UTR) of the *ASH1* gene are not necessary to achieve asymmetry of Ash1 protein. In contrast, deletion of the 3'UTR reveals a clear requirement for this region in the asymmetric localization of Ash1 protein, suggesting that Ash1 RNA localization may precede and cause protein localization. Furthermore, I have discovered that *BUD8*, a gene that regulates budding pattern, is required for Ash1p asymmetry. The Bud8 protein has been shown to localize to the distal pole of the daughter cell (Heidi Harkins and John Pringle, personal communication). I propose that a complex of proteins, including Bud8p, is required to localize Ash1 RNA via its 3'UTR at the distal pole of the daughter cell.

Introduction

In Chapter Two, I discussed the identification of Ash1p, an asymmetrically localized protein that is necessary and sufficient for specifying cell fate. As discussed in Chapter One, a complete dissection of asymmetric cell fate necessitates identification of cell fate determinants followed by an investigation of how the inherent polarity of the pre-divisional cell establishes the asymmetry of the determinant. The simplicity and versatility of *S. cerevisiae* make it an ideal system for ascertaining the link between cell polarity and asymmetry.

Ash1p is localized asymmetrically to the incipient daughter nucleus; the protein is synthesized and localized to the nucleus after nuclear division has occurred. There are many possibilities for how its localization might be regulated (Figure 3-1). For example, it is possible that only the incipient daughter nucleus is competent to transcribe *ASH1*. Such an example of differential transcription is analogous both to regulation of *HO* (only the mother cell, but not the daughter, is competent to transcribe *HO*) and to targetting of flagellar gene products to the swarmer pole in *Caulobacter* (see Chapter One). If *ASH1* asymmetry were controlled by its transcription, one would predict that the *ASH1* promoter would be required for asymmetry. Alternatively, *ASH1* RNA could be localized to the daughter cell. There are many examples of determinants that are localized via sequences in their RNA (reviewed in St Johnston, 1995); identification of such a molecule in yeast would allow an extensive analysis of the mechanism of this type of localization. In other systems, the region of the RNA most often implicated in its localization is the 3'UTR; thus, it is important to determine whether the *ASH1* 3'UTR is required for asymmetry. Finally, the asymmetry of Ash1

Figure 3-1. Models for the Basis of Ash1p Asymmetry. Three models are presented for the basis of Ash1p asymmetry. For each model, three large-budded post-anaphase cells and their nuclei are depicted. In the first line, *ASH1* is differentially transcribed in the incipient mother and daughter nuclei; only the incipient daughter nucleus is able to transcribe *ASH1*, as indicated by the yellow spot in one nucleus. Ash1 RNA is then exported out of the daughter nucleus, and is present mostly in the cytoplasm of the bud where it is translated. Because most of the Ash1 protein is made in the bud, the majority of the protein (drawn in red) will end up in the daughter nucleus for reasons of proximity. Hence, asymmetry is regulated by the *ASH1* promoter in this model. In the second line, *ASH1* is transcribed in both the mother and daughter nuclei, as indicated by the yellow spot in both nuclei. Ash1 RNA, however, gets localized to a pole of the incipient daughter cell. This localization results in localized translation and subsequent protein import into the daughter nucleus for reasons of proximity. In this model, asymmetry is dependent on a signal in the RNA; in many other systems, signals for RNA localization lie in the 3'UTR of the message. In the third line, *ASH1* is transcribed in both nuclei, the RNA is present throughout the cytoplasm, but Ash1p is either selectively stabilized in the daughter nucleus, selectively destabilized in the mother nucleus, or selectively imported into the daughter nucleus. In this final model, the signal for asymmetry would be in the protein sequence.



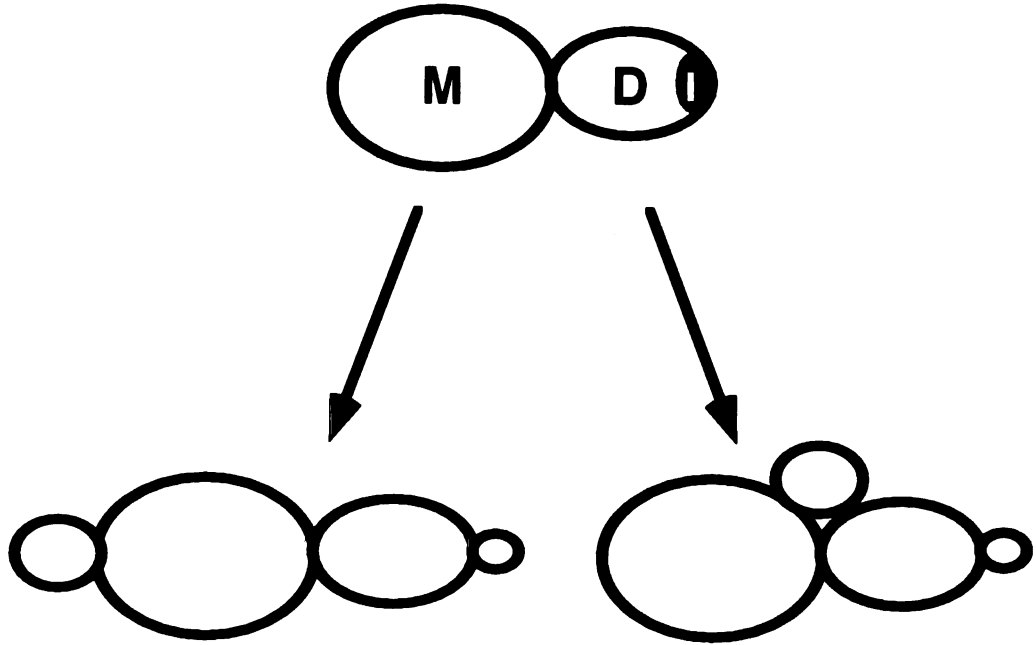
could be regulated at the protein level. Perhaps Ash1p is selectively stabilized in the daughter nucleus, or destabilized in the mother nucleus.

Alternatively, Ash1p might be differentially imported into the daughter but not the mother nucleus. This final model predicts that a signal in the Ash1 open reading frame (ORF) would be necessary for Ash1 asymmetry.

Obviously, these various models are not mutually exclusive.

Determining the regions of the *ASH1* gene that are necessary for asymmetry will identify the signal that the cell exploits to bring about localization of the protein. How might the cell utilize this signal to establish localization? One model predicts that Ash1 RNA or protein could be concentrated in the presumptive daughter cell late in the cell cycle; if so, a landmark required for localization must be placed in the growing bud. Recent work from Zahner et al. (1996) defined several proteins that are candidates for daughter-specific landmarks; these proteins are required to specify budding pattern in *S. cerevisiae*. Budding yeast exhibit a genetically programmed pattern of polarized cell growth (Freifelder, 1960; Hicks et al., 1977; Sloat et al., 1981; Chant and Herskowitz, 1991). *a* or α haploid cells bud in an "axial" pattern: both mother and daughter cells bud adjacent to the site of the previous cell division. *a*/ α diploid cells, in contrast, bud in a bipolar pattern; as the name implies, these cells show evidence of budding from either pole of the cell (Figure 3-2). Mother cells bud either at the pole opposite their previous daughter cell or at the pole adjacent to the daughter cell. Daughter cells, in contrast, place their first bud almost exclusively at their distal pole--the pole of the cell opposite the mother cell (Chant and Pringle, 1995). Daughter cells are hardly ever observed to place their first bud at the proximal pole--the pole of the cell adjacent to the mother cell. In subsequent

Figure 3-2. The Bipolar Budding Pattern. A mother and daughter pair are shown in the top line of the diagram. A purple spot marks the "distal pole" of the daughter cell. In the next cell cycle, the mother cell will go on to bud either away from the daughter cell (drawn on the left) or toward the daughter cell (drawn on the right). The daughter cell, in contrast, buds almost exclusively from the distal pole (away from the previous site of cell division).



cell cycles, however, these cells bud at either pole. Thus the bipolar budding pattern is another example of a cell fate difference between mothers and daughters--mothers exhibit a choice in bud location whereas daughters are limited to the distal pole. These data strongly suggest that a landmark at the distal pole directs placement of a daughter cell's first bud. This pole is essentially the target of the secretion and cell growth machinery during bud emergence, suggesting that simply the process of growing a bud provides the cell with a mechanism to insert a landmark protein at this location.

Mutations in genes required specifically for the axial budding pattern cause haploid cells to utilize the bipolar budding pattern (Chant and Herskowitz, 1991; Fujita et al., 1994; Halme et al., 1996; Roemer et al., 1996; Sanders and Herskowitz, 1996). Thus the bipolar landmarks must also be deposited at the poles of haploid cells. The axial landmarks, however, normally prevail over the bipolar landmarks with respect to budding pattern in wild-type haploid cells.

Zahner et al. (1996) identified several genes required for the bipolar budding pattern. One of these genes, *BUD8*, is required specifically for utilization of the distal pole; *bud8* mutant daughters, in marked contrast to wild-type daughters, no longer bud at the distal pole. Bud8p localizes to the distal pole of the daughter cell, making it an ideal candidate for the distal pole landmark (Heidi Harkins and John Pringle, personal communication). I show that the asymmetry of Ash1p localization is dependent on *BUD8*. I propose that a complex of proteins including Bud8p is placed at the distal pole of the daughter cell as a consequence of bud emergence; this complex is required to establish localization of Ash1p.

Materials and Methods

Genetic and Molecular Biological Methods

DNA manipulations were as described in Sambrook et al., 1989. Yeast genetic methods were as described in Rose et al., 1990.

Strains and Plasmids

Strains are described in Table 3-1, at the end of this chapter. YAS140, 141, 209, and 211 are derivatives of K699 (a W303 strain from Kim Nasmyth (IMP, Vienna)). YAS209 was constructed by linearizing pAS188 (see below) with EcoNI and integrating it at the *ASH1* locus of YAS140. YAS211 was constructed by linearizing pAS202 (see below) with NheI and integrating it at the *ASH1* locus of YAS140.

Plasmids pAS175 (CEN-ARS *ASH1-myc*) was constructed by inserting a XhoI/SacI fragment containing a tagged version of the *ASH1* gene from pAS158 (see Chapter 2) into pRS316 cut with XhoI and SacI. pAS163 (2 μ *ASH1-myc*) is described in Chapter 2. pAS188 (integrating *GAL-ASH1-myc*) was derived from pAS151-B (see Chapter 2). pAS151-B has a XhoI site at the 5' end of *ASH1* and a BamHI site precisely downstream from the *ASH1* ATG. The XhoI/BamHI fragment of pAS151-B was replaced with a SacI/BamHI fragment containing the *GAL1-10* promoter from pRD53 (from Ray Deshaies) to make pAS180. This plasmid contains a unique BamHI site at the position normally just downstream of the *ASH1* ATG. An oligo containing an ATG and a BamHI site was introduced at the unique Bam site to form pAS183. Plasmid pKK-1 encoding a multimerized epitope (Glu-Gln-Lys-Leu-Ile-Ser-Glu-Glu-Asp-Leu-Asn) from the *myc* oncogene (Kolodziej and Young, 1991) was obtained from Daniel Kornitzer and Steve Kron (MIT). Sequence

encoding three copies of this epitope was excised from pKK-1 with BamHI and introduced in the appropriate orientation into the BamHI site of pAS183, resulting in pAS188. pAS202 was constructed by replacing the SphI/SacI fragment of pAS158 (*ASH1-myc*; see Chapter 2) with a PCR product that spanned the *ASH1* ORF but did not include the 3'UTR. Specifically, the *ASH1* coding sequence was amplified with Expand Long Template Polymerase from Boehringer Mannheim. The PCR product was digested with SphI, which cuts near the 5' end of the coding sequence, and SpeI, which was introduced directly after the *ASH1* stop codon from the PCR primer. This fragment was used to replace the *ASH1* coding sequence and 3' UTR of pAS158.

α -factor Arrest and Release Experiments

0.15 l of cells were grown to OD₆₀₀ 0.3 (in YEPD for YAS141 and in SD-ura for 2 μ *ASH1-myc* transformants of YAS140) at 25°C and arrested with 20 μ g/ml α -factor for 3-3.5 hours. Cells were collected by filtration and washed twice with 0.15 l of 30°C YEPD. Cells were resuspended in 0.15 l of 30°C YEPD and allowed to re-enter the cell cycle. 10 ml samples were taken every ten minutes for three hours and processed for indirect immunofluorescence. Ash1p staining appeared in large-budded post-anaphase cells about 50 minutes after release from arrest.

Immunofluorescence

The protocol used was essentially that described by Pringle et al., 1991. Cells were grown to early or mid-log phase and fixed with formaldehyde for 1-3 hours. The cells were washed with phosphate buffer and then spheroplasted.

Cells were applied to polylysine-coated slides and treated with methanol and acetone. The 9E10 antibody (Kolodziej and Young, 1991) was provided by Joachim Li (UCSF) and was used at a 1:300 dilution. The secondary antibody was a rhodamine-conjugated goat anti-mouse antibody from Jackson Immunoresearch and was used at a 1:100 dilution. The mounting medium was Fluoromount-G from Southern Biotechnology Associates, Inc. An affinity-purified polyclonal antibody to Spa2p was provided by Nicole Valtz (UCSF) and used at a 1:8 dilution. In this case, the secondary antibody was a fluorescein-conjugated goat anti-rabbit antibody from Jackson Immunoresearch.

Printing and Photography

Cells were visualized with an Olympus BX60 microscope. Black and white pictures were taken with TMAX 400 35 mm film at ASA 800. Images were printed on Rapitone P1-4 paper. Figures were arranged and labeled in Adobe Photoshop.

Results

Overexpression of *ASH1* Disrupts Asymmetric Localization of Ash1p

Understanding the basis of Ash1p asymmetry begins with an analysis of known situations that disrupt Ash1p localization. In Chapter Two, I showed that overexpression of *ASH1* on a 2-micron plasmid results in symmetric staining of Ash1 protein. To determine if symmetric staining was a consequence of increased levels of *ASH1* or of insufficient regulatory regions on the 2-micron plasmid, I constructed a centromere-based (low-copy) plasmid containing the identical region of *ASH1*. Yeast transformants

bearing the low-copy plasmid exhibited largely asymmetric staining of *ASH1* (Figure 3-3). These data indicate that both the high-copy and low-copy plasmids contain regions of the *ASH1* gene that are sufficient for asymmetric localization.

Asymmetric accumulation of Ash1p in wild-type cells is a result of (1) asymmetric localization of Ash1p and (2) degradation of Ash1p in unbudded cells. Failure to degrade Ash1p each cell cycle would result in inappropriate persistence of the protein in mother cells. Overexpression of *ASH1* could overwhelm the asymmetric localization machinery or titrate out the degradation machinery. To distinguish between these two possibilities, I used the mating pheromone α -factor to arrest cells in G1. All Ash1p staining disappears during the arrest period; thus Ash1p from previous cell cycles is degraded. I then washed out the pheromone and followed *de novo* Ash1p staining in large-budded cells (Figure 3-4). In cells expressing only the endogenous *ASH1*, 12% of asynchronous large-budded cells showed symmetric staining of Ash1p. After release from α -factor, 3% of large-budded cells showed symmetric staining. Thus, only 3% of wild-type cells bypass the localization machinery; the remaining 9% that give symmetric localization in asynchronous populations (to give a total of 12%) may result from perdurance of Ash1p. In contrast, 69% of large-budded asynchronous cells carrying the 2-micron *ASH1* plasmid showed symmetric staining whereas 33% of these cells were symmetric in the first cell-cycle after release from α -factor. When the same cells were monitored in the second cell cycle after α -factor release when synchrony is lost, 61% of the large-budded cells showed symmetric staining. These data indicate that the asymmetric localization machinery is being bypassed in at least 33% of the large-budded cells when

Figure 3-3. Expression of *ASH1* on a Low-Copy Plasmid does not Disrupt *Ash1p* Asymmetry. YAS140 cells carrying CEN-ARS *ASH1-myc* (pAS175) were grown to early log phase, fixed, and processed for indirect immunofluorescence staining with 9E10 antibodies. *Ash1p* staining and DAPI staining in two large-budded cells (one at the top left of the photograph, and one at the top right) is shown. *Ash1p* staining in an unbudded cell can be seen at the bottom of the photograph.

CEN-ARS ASH1-myc

myc

DAPI

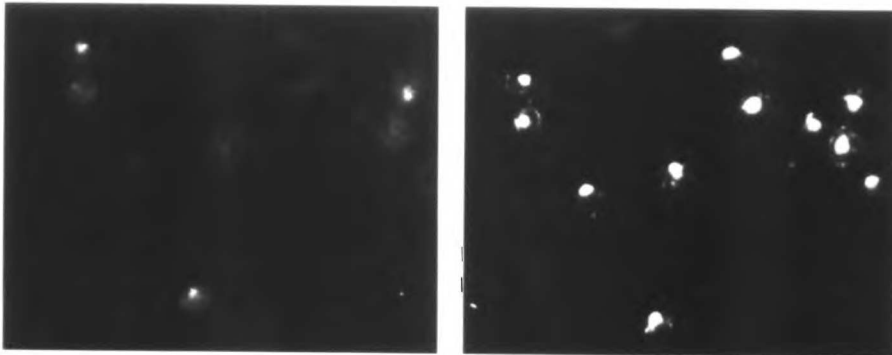
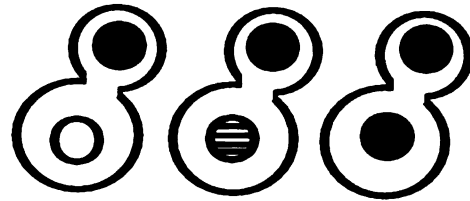


Figure 3-4. Asymmetry of Ash1p Staining in Large-Budded Asynchronous Cells and in Cells After Release from Pheromone Arrest. a *ASH1-myc* cells (YAS141) carrying no plasmid ("WT") or a *ASH1* (YAS140) cells carrying 2μ *ASH1-myc* (" 2μ *ASH1*") were subjected to DAPI staining and indirect immunofluorescence staining with 9E10 antibodies. Cells were either prepared from asynchronous samples (lines 1 and 3) or were released from α -factor arrest. Three categories of large-budded post-anaphase cells were counted. Ash1 staining was either completely asymmetric (1st column), partially symmetric (second column), or completely symmetric (3rd column). n=100 for each sample.



WT Asynchronous	73	15	12
WT Pheromone Release	80	17	3
2μASH1 Asynchronous	16	13	69
2μASH1 Pheromone Release			
1st cell cycle	31	36	33
2nd cell cycle	20	19	61

ASH1 is overexpressed. The remaining 36% of the cells that show symmetric staining in an asynchronous population may do so as a result of titration of the degradation machinery.

The *ASH1* Promoter and 5'UTR are Not Required for Ash1p Asymmetry

If Ash1p asymmetry were due to differential transcription in the daughter cell, the *ASH1* promoter should be required for proper localization of the protein. I replaced the *ASH1* promoter and the 5'UTR with the inducible *GAL1-10* promoter (pAS188), and integrated this GAL-*ASH1-myc* construct at the *ASH1* locus. Detection of the tagged protein was dependent on growth in galactose. The majority of large-budded cells showed asymmetric Ash1p staining (Figure 3-5). These data indicate that the promoter and 5'UTR are not required for asymmetric localization.

The *ASH1* 3'UTR is Necessary for Ash1p Asymmetry

There are many examples of determinants that are localized via their RNA; localization in these cases is often mediated by the 3'UTR (reviewed in St Johnston, 1995). To determine if the *ASH1* 3'UTR is necessary for localization of Ash1p, I constructed an allele of *ASH1* that lacked its 3'UTR. This 3'UTR Δ construct was integrated at the *ASH1* locus and assayed for protein localization (Figure 3-6). The 3'UTR Δ strain showed largely symmetric staining: 80% of large-budded cells had equivalent staining in mother and daughter nuclei whereas only 4% of wild-type cells displayed this staining pattern. These data indicate that the 3'UTR is necessary for asymmetric localization of Ash1p.

***BUD8* is required for Ash1p Asymmetry**

Localization of Ash1p to the incipient daughter cell may depend on a daughter-specific landmark. Since this type of landmark is required for the

Figure 3-5. Replacement of the *ASH1* promoter with the *GAL* promoter results in asymmetric staining. YAS209 cells (*GAL-ASH1-myc* is integrated at the *ASH1* locus of YAS140) were grown to early log phase in raffinose, washed twice with water, and shifted to galactose medium for various lengths of time (30, 60, 90, or 120 minutes). Cells were harvested and subjected to indirect immunofluorescence staining with 9E10 antibodies. Ash1-myc and DAPI staining are shown for four large-budded post-anaphase cells.

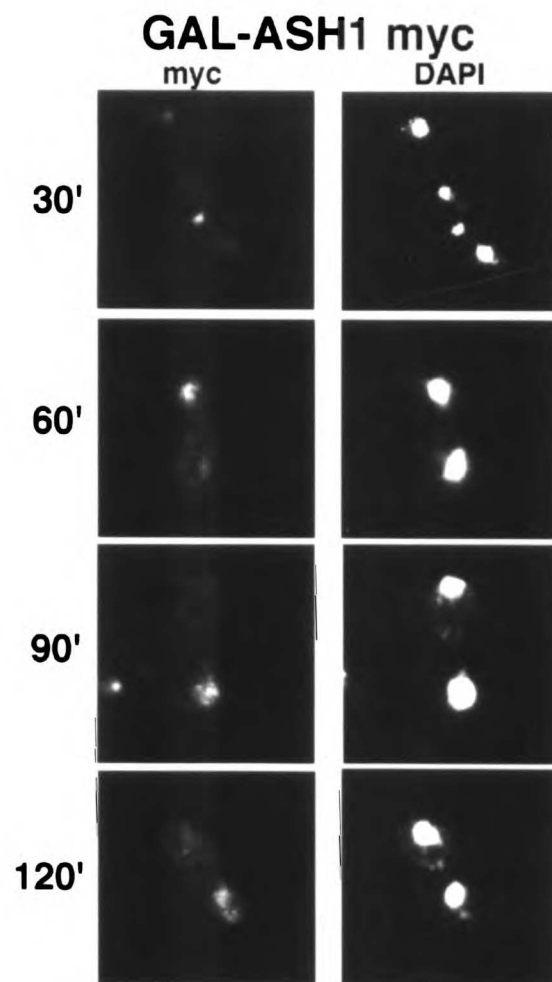
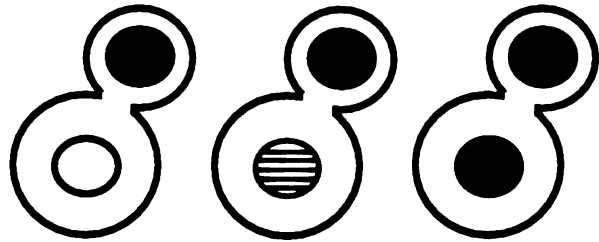


Figure 3-6. The *ASH1* 3'UTR is Required for Ash1p Asymmetry. a *ASH1-myc* cells (YAS141) or a *ASH1::ASH1 3'UTRΔ-myc* cells (YAS211) were grown to early log phase, harvested, and subjected to DAPI staining and indirect immunofluorescence staining with 9E10 antibodies. YAS141 cells are designated "WT" whereas YAS211 cells are designated "3'UTRΔ". Three categories of large-budded post-anaphase cells were counted. Ash1 staining was either completely asymmetric (1st column), partially symmetric (second column), or completely symmetric (3rd column). n=200 for each sample; percentages of cells in each category are shown.



WT

77

19

4

3'UTR Δ

15

5

80

bipolar budding pattern, I examined Ash1p localization in four mutants defective in this pattern. Specifically, wild-type daughter cells always bud from the distal pole. Two mutants, *bud8* and *bni1*, disrupt the ability of daughters to bud from this pole; *bud8* mutants are still able to bud from the proximal pole (Figure 3-7). *bni1* mutant daughters cannot utilize the distal pole and bud instead in a completely random fashion. *bud9* mutants cannot use the proximal pole, and bud only from the distal pole. *bud6* mutant daughters can direct their first bud to the distal pole but then these cells bud randomly in subsequent cell cycles (Zahner et al., 1996). I transformed this battery of bipolar budding mutants (*bud6* Δ , *bud8* Δ , *bud9* Δ , and *bni1* Δ) and an isogenic wild-type strain with a centromere-based plasmid carrying a tagged allele of *ASH1*. The wild-type parent strain, the *bud6* Δ strain, and the *bud9* Δ strain displayed normal asymmetric staining of Ash1p (Figure 3-8). In contrast, *bud8* Δ mutants showed a significant loss of asymmetry: only 26% of large-budded cells showed completely asymmetric staining compared with 72% of wild-type cells. The phenotype of *bni1* mutants was even more dramatic: only 17% of *bni1* Δ cells showed asymmetric staining. The Spa2 protein, which accumulates at the neck of large-budded cells (Snyder, 1989; Gehrung and Snyder, 1990; Snyder et al., 1991), was also localized in all of the samples to insure that large-budded cells rather than two adjacent unbudded cells were being monitored. An example of the symmetric staining observed in *bud8* Δ mutants is shown in Figure 3-9.

Discussion

Ash1p is a cell-fate determinant that localizes asymmetrically to the incipient daughter nucleus in large budded-cells. I have determined that the *ASH1*

Figure 3-7. The Budding Pattern of Mutants Defective in the Bipolar Pattern.

This figure is adapted from data presented in Zahner et al., 1996. The wild-type bipolar budding pattern originally depicted in Figure 3-2 is shown at the very top of the diagram. The leftmost cell in the lower part of the diagram represents a daughter cell. A purple spot marks the distal pole of this daughter cell whereas a turquoise spot marks the proximal pole (the pole adjacent to the prior site of cell division). This daughter cell buds three times (indicated by the three arrows) to give rise to a variety of patterns in 5 different strains (WT [wild-type], *bud8* Δ , *bud9* Δ , *bud6* Δ , and *bni1* Δ). The same cell is shown after it has budded three times; dark blue circles represent bud scars, which are deposited at the sites of cell division. Wild-type daughter cells place their first bud at the proximal pole 95% of the time (Chant and Pringle, 1995). These cells go on to bud at the proximal pole and the distal pole. *bud8* cells cannot utilize the distal pole, and bud only at the proximal pole. *bud9* cells cannot use the proximal pole, and bud only from the distal pole. *bud6* mutant daughters can place their first bud at the distal pole, but subsequent buds are positioned randomly. *bni1* mutants place all buds randomly. *bud8* and *bni1* strains are indicated in red because each of these mutants are defective in utilization of the distal pole.

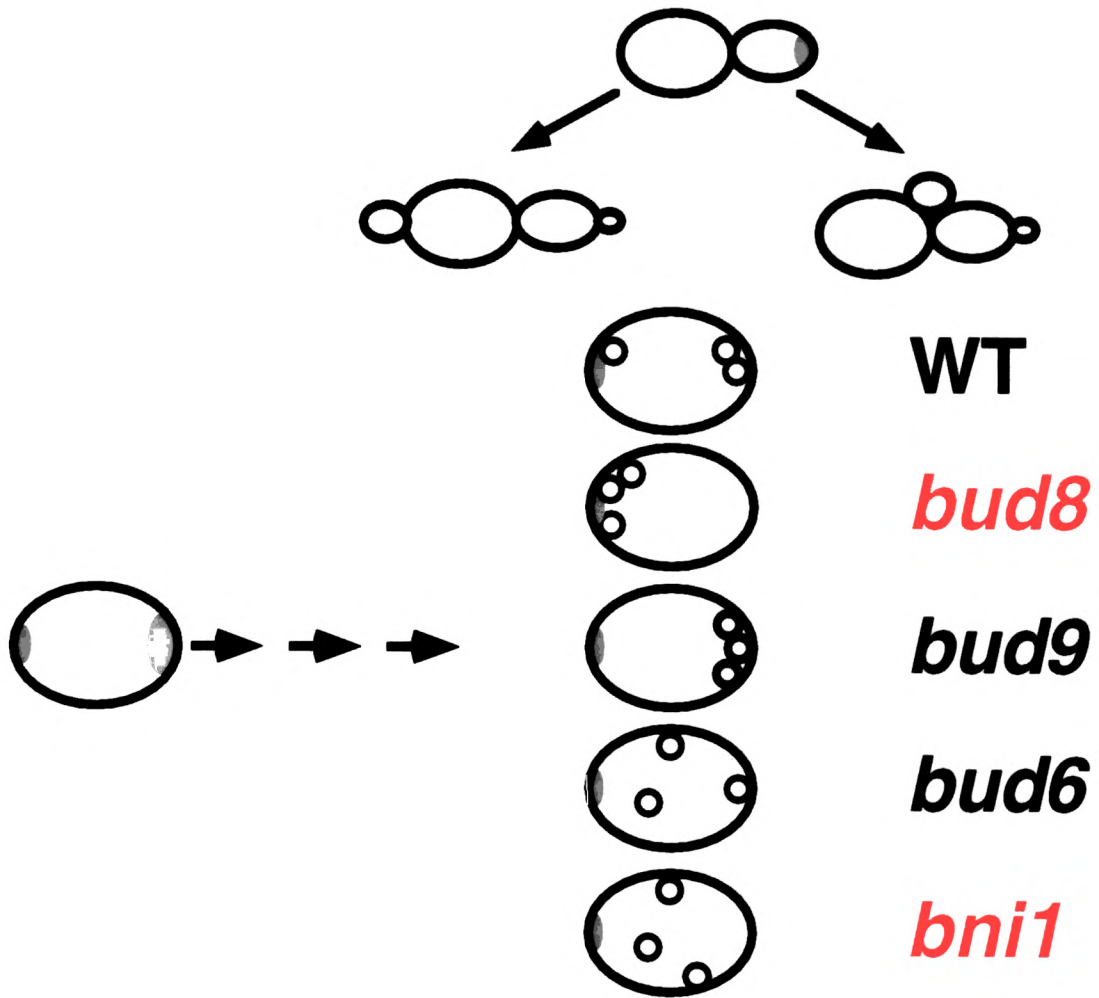
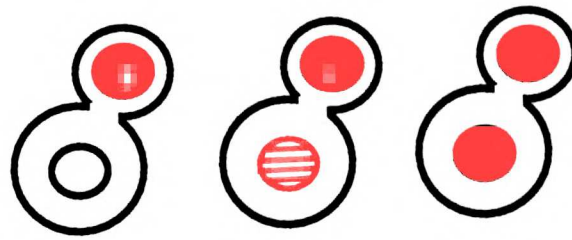


Figure 3-8. The Effect of Mutants Defective in the Bipolar Pattern on Ash1p Localization. Isogenic wild-type (YAS212), *bud6* Δ (YAS213), *bud8* Δ (YAS214), *bud9* Δ (YAS215), and *bni1* Δ (YAS216) cells carrying a CEN-ARS *ASH1-myc* plasmid (pAS175) were grown to early log phase under selection for the plasmid. Cells were harvested and subjected to DAPI staining and indirect immunofluorescence staining with 9E10 antibodies. Three categories of large-budded post-anaphase cells were counted. Ash1 staining was either completely asymmetric (1st column), partially symmetric (second column), or completely symmetric (3rd column). n=200 for each sample; percentages of cells in each category are shown.








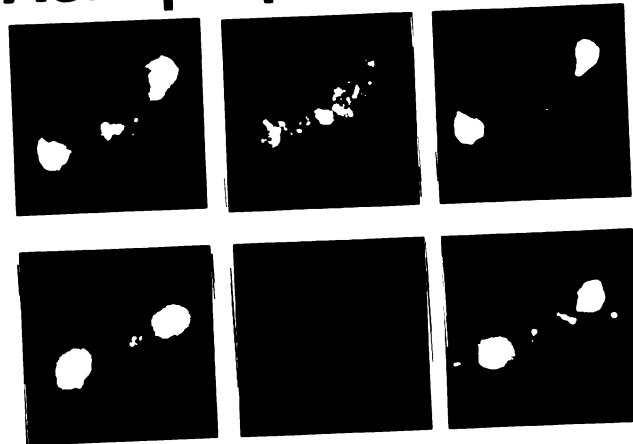
	WT	72	16	12
	<i>bud6</i>Δ	74	16	10
	<i>bud9</i>Δ	76	12	12
	<i>bud8</i>Δ	26	10	64
	<i>bni1</i>Δ	17	7	76

Figure 3-9. *bud8Δ* Cells Display Symmetric Staining of Ash1p.

Immunofluorescence images of two *bud8Δ* cells from the experiment described in Figure 3-8 are shown. Cells are stained with 9E10 antibodies and with anti-Spa2 antibodies. Spa2p stains the neck of large-budded post-anaphase cells. DAPI staining is also shown.

Ash1p Spa2p DAPI



promoter and 5'UTR are not required for the ultimate asymmetry of Ash1 protein. The 3'UTR, however, is clearly necessary for confining Ash1p to the daughter nucleus: 3'UTR Δ strains display a striking loss of asymmetric Ash1p staining. In addition to defining regions of the *ASH1* gene that are required for Ash1p asymmetry, I have determined that Bud8p, a protein that marks the distal pole of the daughter cell, is required to localize Ash1p correctly. These observations will serve as key guideposts in further investigations of the mechanism of Ash1p asymmetry.

Perturbation in levels of *ASH1* Result in Symmetric Distribution

Perturbations that disrupt the asymmetry of Ash1p can do so by interfering with the localization machinery or by causing inappropriate inheritance (perdurance) of Ash1p in mother cells. Treatment of cells with α -factor, which causes all residual Ash1p to be degraded, can be used to distinguish between these possibilities. After release from α -factor, *ASH1* is synthesized in post-anaphase cells. All of the Ash1p in these cells is synthesized *de novo*; thus these cells provide a measure of the cells that mislocalize Ash1p as opposed to those cells that show symmetric Ash1p staining due to perdurance of the protein. First, wild-type cells exhibit a high fidelity of localization; only 3% of large-budded wild-type cells show fully symmetric staining after release from pheromone arrest. In the Discussion of Chapter Two, I raise the possibility that perdurance of Ash1p in mother cells might affect the switching pattern. Since 12% of wild-type cells show symmetric staining in an asynchronous population versus 3% after release from α -factor, these data indicate that the majority of this symmetric staining is a result of perdurance of Ash1p

Overexpression of *ASH1* causes a loss of asymmetry of Ash1p. Since only 31% of large-budded cells carrying a 2-micron *ASH1* plasmid show completely asymmetric Ash1p staining after release from pheromone arrest compared with 80% of wild-type cells, a significant percentage of cells with the 2 micron plasmid subvert the localization machinery that normally limits Ash1p to the daughter nucleus. The excess of Ash1 produced in these cells may titrate out factors required for localization. Indeed, localization of Ash1p is very sensitive to the amount of Ash1 present. Integrating a tagged allele of *ASH1* at the *URA3* locus rather than at its own locus, for example, results in an increased level of *ASH1* expression and symmetric localization of the protein (A.S., unpublished observations).

Localization of Ash1 is Mediated by the 3'UTR of the RNA

Deletion of the *ASH1* 3'UTR eliminates the asymmetric localization of Ash1p. Multiple mRNAs have been localized in *Drosophila* and *Xenopus* oocytes; the signal for localization of the majority of these molecules lies in the 3'UTR (St Johnston, 1995). Since regulation of Ash1p asymmetry requires the 3'UTR of the gene, localization is likely to be mediated through the RNA in some fashion. For example, the RNA could be localized to the bud; preferential accumulation of the protein in the incipient daughter nucleus could then be achieved simply via proximity of the daughter nucleus to the site of translation. This model predicts that a landmark, such as a protein that binds to the RNA, is localized to the bud. Alternatively, Ash1 RNA could be present everywhere, but a translational activator could be localized specifically to the daughter, or an inhibitor of Ash1 translation could be localized to the mother cell. However, given the fact that overexpression of *ASH1* causes symmetric localization of Ash1p, regulation of asymmetry

seems unlikely to be caused by a daughter-specific translation factor. Rather, if the Ash1 RNA is normally localized to a discrete location in the daughter cell, increasing amounts of Ash1 transcript could saturate the localization landmark resulting in symmetric accumulation first of the RNA and then of the protein.

A complete analysis of the 3'UTRΔ phenotype begs several experiments. First, to determine whether deletion of the 3'UTR is the only lesion in the deletion construct, it is imperative to add back the *ASH1* 3'UTR to the construct and ascertain whether the asymmetry of Ash1p is restored. Furthermore, much like the 2-micron *ASH1* experiments, it is important to distinguish whether symmetry results from bypass of the localization machinery or inappropriate perdurance of Ash1 RNA or protein. It is crucial to arrest the 3'UTRΔ cells with pheromone and determine the percentage of large-budded cells with symmetric staining in the first cell cycle after release from arrest. If all of the cells show asymmetric staining in the first cell cycle after release, for example, symmetric localization of the protein in asynchronous cells is likely to be due to increased RNA stability of the 3'UTRΔ construct rather than bypass of the localization machinery. Finally, a key question is whether the 3'UTR will be sufficient to direct the localization of a heterologous molecule.

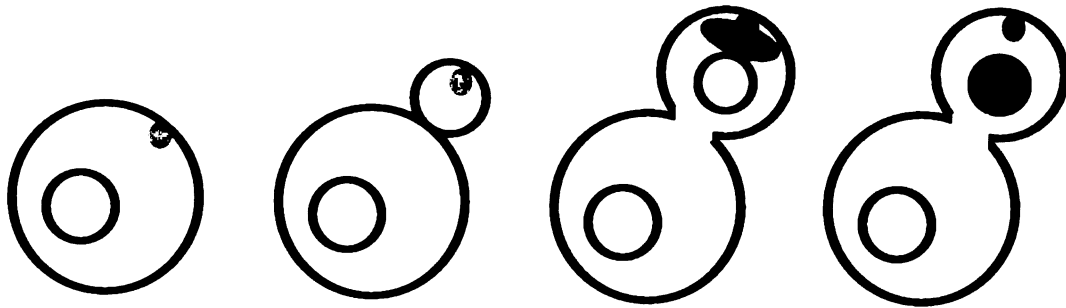
A Distal-Pole Landmark is Required for Ash1p Localization

Perhaps the most provocative finding about Ash1p localization is that it is dependent on a landmark required for the proper budding pattern. Although several bipolar budding mutants were tested for defects in Ash1p localization, a predominance of symmetric staining was seen only in *bud8* and *bni1* mutants, both of which are defective in budding from the distal

pole. The effect of *bni1* on Ash1p staining has been observed independently (Bobola et al., 1996). Loss of *BNI1* results in a number of pleiotropic phenotypes such as defects in the bipolar budding pattern, cytokinesis, cell shape, and pseudohyphal growth (John Pringle, personal communication). *bni1* mutants may be defective in the localization of a distal-pole landmark. Bni1p itself is not likely to be the landmark, however, since it relocalizes from the distal pole to the neck of large-budded cells (John Pringle, personal communication) probably before Ash1 localization occurs. Furthermore, *bni1* mutants are defective in use of the proximal bud-site in addition to the distal site.

Unlike *bni1* cells, the phenotype of cells lacking *BUD8* is very specific. *bud8* mutants are able to bud only from the proximal pole; daughter cells no longer choose to bud at the distal pole. Since Bud8p localizes to the distal pole for the duration of the cell cycle (Heidi Harkins and John Pringle, personal communication), it is an excellent candidate for the distal pole landmark for bud-site selection. Does Bud8p directly bind and localize Ash1 RNA at the distal pole of the daughter cell? I think not, for two reasons. First, the loss of asymmetry observed in *bud8* mutants is not complete; 64% of *bud8* cells vs 76% of *bni1* cells have completely symmetric staining. Second, Bud8p is clearly a transmembrane protein but has no RNA binding domains. I propose that Bud8p is a component of a complex of proteins at the distal pole; in this model, at least one of these proteins binds Ash1 RNA directly (Figure 3-10). In the absence of Bud8p, the complex is less stable. Some cells maintain the Ash1 RNA-binding protein at the distal pole but many do not. Thus the majority of large-budded cells show symmetric Ash1p staining. In this model, Bud8 is the landmark for bud-site selection, but a different molecule is

Figure 3-10. A Distal Pole Landmark that Binds Ash1 RNA is Localized as a Consequence of Bud Growth. This figure represents a model for how the localization of Ash1p is achieved. A yeast cell is shown progressing through the cell cycle. As the bud grows, a landmark (pink dot) is deposited at the distal pole. One component of this landmark is Bud8p. Late in the cell cycle, *ASH1* is transcribed, and Ash1 RNA (or an activator of Ash1 RNA translation) is localized to the landmark at the distal pole. This localization confines translation of Ash1 RNA to the bud; for reasons of proximity, Ash1p is imported mainly into the incipient daughter nucleus.



Distal landmark (Bud8p)

Ash1 RNA or Translational Activator



the landmark for Ash1 localization. It may be significant to note that *ash1* mutants do not have a bipolar budding defect (A.S. unpublished observations); thus localization of Ash1 is dependent on a protein required for bipolar budding but localization of the budding landmark is not dependent on Ash1.

Interestingly, the distal pole of the cell is an ideal place to localize a daughter-specific determinant such as Ash1. First, it is as far away as possible from the mother cell; thus localization of a determinant to the distal pole makes it easier to confine such a molecule to the daughter. Second, since the secretory apparatus is directed at the distal pole during bud emergence, the cell can utilize its pre-existing polarized growth machinery to position the requisite landmark. Finally, the beauty of this particular link between polarity and asymmetry is that it does not depend on the budding *pattern* but on budding *per se*. A cell needs only the capability to synthesize the landmark; any such cell that grows a bud will deposit the landmark (and localize Ash1) at the distal pole simply as a consequence of growth. Whether or not that cell has the capability to *recognize* the budding landmark in the next cell cycle and place the next bud in the correct location is irrelevant for Ash1 localization. Thus strains that bud randomly because they cannot recognize the landmark (e.g. *bud1Δ* strains; see Appendix Four) rather than being defective in the landmark itself (e.g. *bud8* strains) will still localize Ash1 properly. To emphasize this point, it is worth noting that all of the "wild-type" strains used for Ash1 localization in Chapter 2 are in the W303 background; these strains bud randomly but show no defects in Ash1 localization.

Table 3-1. Chapter Three Strain List

<u>Strain name</u>	<u>Relevant Genotype</u>	<u>Source</u>
YAS140	a <i>ho</i> <i>ASH1</i>	K. Nasmyth (K699)
YAS141	a <i>ho</i> <i>ASH1-myc</i>	This study
YAS209	a <i>ho</i> <i>ASH1::GAL-ASH1-myc URA3</i>	This study
YAS211	a <i>ho</i> <i>ASH1::ASH1-myc 3'UTRΔ URA3</i>	This study
YAS212	a <i>BUD+</i> <i>ura3</i>	J. Pringle
YAS213	a <i>bud6Δ</i> <i>ura3</i>	J. Pringle
YAS214	a <i>bud8Δ</i> <i>ura3</i>	J. Pringle
YAS215	a <i>bud9Δ</i> <i>ura3</i>	J. Pringle
YAS216	a <i>bni1Δ</i> <i>ura3</i>	J. Pringle

YAS140, 141, 209, 211 are isogenic (W303 background)

YAS212-216 are isogenic

CHAPTER FOUR

CONCLUSION

The study of asymmetric cell fate in *S. cerevisiae* has been a rewarding process. Although it was not clear at the start of this analysis whether an asymmetrically localized determinant would govern expression of *HO*, it is now evident that regulation of *HO* activity is very much like asymmetric divisions in more complex organisms. The Ash1 protein of budding yeast is both necessary and sufficient for cell-fate determination. Furthermore, the pre-divisional cell exploits its innate mechanism of polarized cell growth to establish localization of Ash1. Finally, the strength of molecular genetics and biochemistry in yeast should allow a thorough dissection of the link between cellular polarity and asymmetry.

Ash1p Asymmetry

Now that we have *ASH1* in hand, the next goal is to understand what controls the asymmetric localization of Ash1p. Several key advances have been made toward this end. First, I have shown that the *ASH1* 3'UTR is necessary for asymmetry. Second, I have shown that Bud8p, a protein that localizes to the distal pole of the daughter cell, is also required for Ash1 asymmetry. These data suggest a model in which Ash1 RNA is localized to the distal pole of the daughter cell via its 3'UTR. In this model, Bud8p marks the distal pole for the bud-site selection machinery, but it may not be the landmark that binds Ash1 directly. Instead, Bud8p may form a complex with a putative RNA-binding protein that targets Ash1 RNA to the distal pole. In the absence of Bud8p, the ability of this putative protein to stably localize to the distal pole is decreased, and Ash1 asymmetry is lost.

Data from the Nasmyth lab also suggest that a landmark required to position Ash1 may be localized to the daughter cell as the bud grows. Jansen

et al. (1996) identified five genes (*SHE1-5*) that are required for the asymmetric localization of Ash1p to the daughter cell; in the *she* mutants, Ash1p is localized to both mother and daughter nuclei. *SHE5* is identical to *BNI1*, which like *BUD8*, plays a role in utilization of the distal pole for budding. *SHE1* is identical to *MYO4*; *SHE 2, 3, and 4* encode novel proteins. Interestingly, She1p and She3p localize to the growing bud for much of the cell cycle and then redistribute evenly between the mother and bud before the mitotic spindle breaks down. Given the homology between *SHE1/MYO4* and myosin, Bobola et al. (1996) propose that the She proteins may be required to transport a molecule required for Ash1 asymmetry to the bud. Ash1 itself is not thought to be the target of the She proteins because by the time Ash1 RNA is synthesized at anaphase, the She proteins are already symmetrically localized. It is possible, however, that the She proteins are involved in positioning a landmark that binds Ash1 at the distal pole.

It may be possible to identify such a landmark genetically. Presumably, expression and localization of the landmark are required for Ash1 asymmetry. Conversely, overexpression of the landmark might cause its mislocalization; inappropriate localization of the landmark could result in symmetric localization of Ash1p. This scheme is reminiscent of the observation that overexpression of *BUD8* is sufficient to randomize the budding pattern, presumably due to mislocalization of Bud8p (Heidi Harkins, personal communication). I propose to use *HO* reporters to monitor the localization of Ash1p; when Ash1p is symmetric, *HO* transcription is greatly diminished in mother cells (Jansen et al., 1996; also see Chapter 2). Thus it is possible to screen or select for high copy plasmids that cause Ash1 to be symmetrically localized. It is simple to determine if decrease in *HO*

expression is dependent on the *ASH1* gene and to check whether Ash1p is symmetric in the presence of the high-copy plasmid. Along these lines, it will be interesting to determine if overexpression of *BUD8* is sufficient to disrupt asymmetric localization of Ash1p.

I have shown that the 3'UTR is necessary for Ash1 localization. Mutagenesis of this region of the *ASH1* gene could be used to identify alleles of *ASH1* that confer symmetric localization of the protein. A biochemical analysis of proteins that bind the wild-type 3'UTR but not a mutant 3'UTR could identify a protein that binds to the Ash1 RNA and localizes it. Furthermore, *in situ* localization (Long et al., 1995) of Ash1 RNA should be performed to determine if the RNA is actually localized to the daughter cell.

The possibility that localization of Ash1 RNA effectively titrates out a ubiquitous translational inhibitor has not been sufficiently addressed. If an inhibitor prevents translation of Ash1 in the mother cell, however, one might expect that when Ash1 RNA is delocalized (which may be occurring in a *bud8* mutant), titration of the inhibitor would not occur, and Ash1p would not be synthesized. Instead, at least in the case of *bud8* and the *she* mutants, Ash1p is symmetric.

Finally, in order for the asymmetry of Ash1p to be maintained once it is established, it is essential for the protein to be degraded in daughter cells after they pass through G1 and are no longer in danger of inappropriately transcribing *HO*. The examination of synchronous populations reveals that Ash1p disappears after cells transit late G1 (as marked by bud emergence). A series of other proteins, including G1 cyclins, are degraded at this point in the cell cycle (reviewed in Deshaies, 1995a, 1995b). Whether Ash1p degradation depends on the same factors that control the stability of these other proteins is

unknown. The regulation of Ash1p degradation is being investigated by Mary Maxon.

The Mechanism of Ash1p Function

The means by which Ash1p controls the expression of *HO* is another intriguing mystery. It is quite likely that Swi5p activity is limiting in daughter cells (see Chapter 1) and that Ash1p holds the reins that stifle Swi5p function. For example, Ash1p could affect the ability of Swi5p to bind its target sequence in the *HO* promoter by masking the DNA site or by sequestering Swi5p in an inactive complex. Alternatively, Ash1p could squelch Swi5p activity after Swi5p has bound to the *HO* promoter. Mary Maxon is pursuing these aspects of Ash1p function.

The timing of transcription of the *HO* promoter is likely to be crucial for the inhibition of *HO* activity in daughter cells. Most *SWI5*-dependent genes are transcribed at anaphase when Swi5p enters the nucleus. *HO* transcription, however, does not occur until late G1. This temporal constraint on *HO* transcription is governed by the URS2 regulatory region; Ramon Tabtiang is elucidating the mechanism of how URS2 restricts activation of *HO* to late G1. Since *ASH1* transcription is dependent on *SWI5*, Swi5p is by definition present in the nucleus before Ash1p. If *HO* were transcribed at anaphase like other *SWI5*-dependent genes, Ash1p would never have the opportunity to inhibit Swi5p function in daughter cells with regards to *HO* transcription. The temporal delay between anaphase and late G1 provides Ash1p with a window of opportunity in which to function.

Other Roles of Ash1p

Is Ash1p function limited to inhibition of *HO* transcription? Recent work has revealed a role for *ASH1* in pseudohyphal growth (Judy Shih and A.S., unpublished observations). *a/α* diploid cells exhibit pseudohyphal growth when they are starved for nitrogen. Pseudohyphal cells have an altered morphology and budding pattern, and grow in a filamentous fashion (Gimeno et al., 1992;). Unlike vegetative cells, pseudohyphal mother and daughter cells exhibit a G1 phase of the same length (Kron et al., 1994). We have shown that *ash1Δ* strains are unable to form pseudohyphae. Interestingly, a strain carrying a 2 micron *ASH1* plasmid produces enhanced pseudohyphae when compared to a strain carrying a vector control. Since Ash1p is a transcriptional regulator, it may be involved either in the repression of genes that inhibit pseudohyphal growth, or in the activation of genes that stimulate pseudohyphal growth. Whether or not Ash1p is asymmetrically localized in cells forming pseudohyphae remains to be determined.

The Purpose of Mother/Daughter Regulation

Finally, what purpose does mother/daughter regulation serve? The asymmetric regulation of *HO* may facilitate diploidization; diploid cells are thought to have a selective advantage in the wild due to an increased growth rate and ploidy. When wild-type spore cells germinate, they exhibit either the *a* or *α* mating type. An *a* cell, for example, will divide once to yield a mother *a* cell and a daughter *a* cell. In the next division, the mother cell will switch and divide to give rise to two *α* cells. The daughter, however, will give rise to two *a* cells. Because wild-type cells haploid cells place their buds adjacent to the previous site of cell division (the axial pattern), cells of opposite mating-

type will be juxtaposed at the four-cell stage. Thus, expression of *HO* coupled with the axial budding pattern enhances the probability that haploid cells will mate with each other.

Although *ASH1* itself is not an essential gene, it is possible that the landmark that serves to localize Ash1p might have an essential role in polarized cell growth. If so, the yeast cell may have coupled the ability to localize Ash1 to an vital function, thereby insuring that mothers and daughters maintain their differences indefinitely.

APPENDIX ONE

A HIGH COPY SCREEN FOR GENES THAT ACTIVATE *HO* IN DAUGHTER CELLS

Abstract

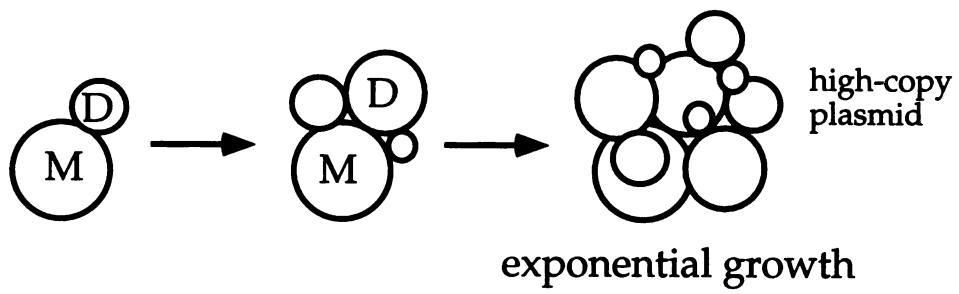
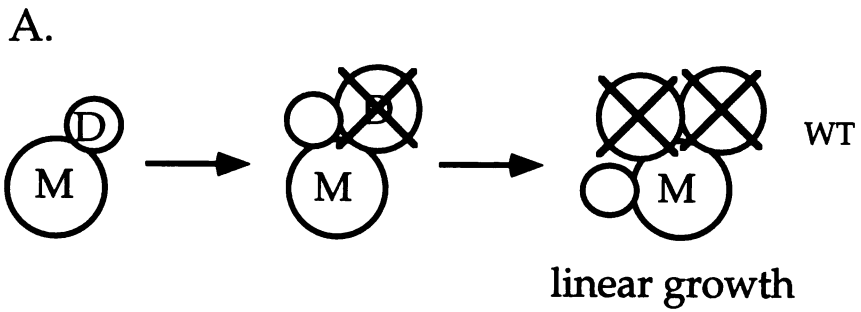
In order to identify genes that, when overexpressed, activate the *HO* gene in daughter cells, I constructed a strain in which such activation causes a significant increase in growth rate. I used this strain to select for genes that confer a distinct growth advantage when expressed at high copy. Candidate plasmids were screened further to determine if they affected regulation of mating-type switching. Plasmids of the desired class were not obtained.

Introduction

The *HO* gene is transcriptionally active only in mother cells but not in daughter cells. We proposed that an asymmetrically-distributed transcriptional regulator governs the lineage specificity of *HO* activation (see Introduction). Possibilities for such a regulator include an activator of *HO* transcription that localizes preferentially to the mother cell or an inhibitor of *HO* expression that localizes preferentially to the daughter cell. I reasoned that overexpression of a gene encoding a putative mother-specific activator might allow such a protein to seep into the daughter cell, thus allowing activation of *HO* in both mother and daughter cells. To search for such an activator, I constructed a special strain that utilizes growth rate rather than mating-type switching as an assay for *HO* promoter regulation. This strain contains an essential gene under the control of the *HO* promoter; much like *HO*, this gene is transcribed only in mother cells. Since daughter cells are unable to transcribe the essential gene, these cells do not divide; thus growth rate is significantly reduced in such a strain (see Figure A1-1). I used this strain to screen for high copy plasmids that increased growth rate. A

Figure A1-1. A Special Strain Couples Activation of *HO* to Growth Rate. (A)

The growth pattern of a strain that contains an essential gene under the control of the *HO* promoter is shown. In a wild-type strain (top panel), mother cells can activate the *HO* promoter and transcribe the essential gene but daughter cells cannot. Thus, only mother cells are capable of division, resulting in a strain that grows linearly rather than exponentially. The inability of cells to divide is indicated by an X over the cell. In contrast, a strain carrying a high-copy plasmid that activates the *HO* promoter in daughter cells (bottom panel) can grow exponentially since daughter cells can now survive and divide. (B) The ability of mothers and daughters to divide on galactose vs. glucose is shown. The strain contains the essential gene under the control of the *GAL1-10* promoter. In galactose, both mothers and daughters can transcribe the essential gene and divide. In glucose, however, the only source of the essential gene is from the *HO* promoter. Mother cells, but not daughter cells, are able to transcribe the essential gene.



B.

	M	D
GAL	+	+
GLU	+	-

candidate group of plasmids were isolated and tested further to identify those that affected the regulation of mating-type switching.

Materials and Methods

Genetic and Molecular Biological Methods

DNA manipulations were as described in Sambrook et al., 1989. Yeast genetic methods were as described in Rose et al., 1990.

Strains and Plasmids

Strains are described in Table A1-4, at the end of this appendix.

Plasmids The 2 μ *URA3* Carlson library was a gift of Joachim Li (UCSF). The 2 μ *GAL-lacZ LEU2* plasmid was a gift from the laboratory of Alexander Johnson (UCSF).

Pedigree of Death Analysis Cells were grown to early log phase in galactose, washed twice with water, sonicated, and plated on 4% YEPD agar slabs. The ability of individual cells to bud and divide was monitored microscopically. Once a cell divided it was separated from its bud with a dissecting needle. Mothers and daughters could be distinguished on the basis of size.

Four-shmoo Microcolony Assay Transformants were grown to early log phase in SD-ura, sonicated, and transferred to 4% agar YEPD slabs containing 25 μ g/ml α -factor. These slabs were incubated at 30°C for 10-14 hours and the resultant microcolonies were examined under 250X magnification. The number of four-shmoo microcolonies per 1000 microcolonies was counted for each sample. Multiple transformants were scored for each high-copy plasmid.

B-galactosidase filter assays Cells were replica-plated to Whatman 50 filters placed on SD-ura plates and grown at 30°C overnight. The filters were frozen in liquid nitrogen and then thawed to permeabilize the cells. The filters were then perfused in 3 ml of X-gal solution for 5-8 hours at 37°C. X-gal solution consists of 3 ml Z buffer (8.53g/L Na₂HPO₄ (anhydrous), 5.5g/L NaH₂PO₄, 0.75g/L KCl, 0.246g/L MgSO₄ 7H₂O), 8.1μl B-mercaptoethanol, 36μ 3% X-gal in DMF.

Results

A Strain whose Growth Rate Reflects *HO* Promoter Activity

I constructed a strain whose growth rate was dependent on *HO* promoter activity. *CLN2*, which encodes a G1 cyclin essential for viability in the absence of G1 cyclins *CLN1* and *CLN3*, (Richardson et al., 1989; Cross, 1990) is present in this strain both under the control of the conditional *GAL1-10* promoter and under control of the *HO* promoter. When the conditional promoter is activated by growth on galactose, both mother and daughter cells transcribe *CLN2*, and both are viable. When the *GAL* promoter is repressed by growth on glucose, however, the only source of *CLN2* is from the *HO* promoter (Figure A1-1B). In the latter situation, only mother cells, but not daughter cells, are able to accumulate G1 cyclins and transit the cell cycle. Since daughter cells cannot grow and divide, these strains grow linearly rather than exponentially. It is worth noting that *CLN2* was chosen for this scheme because Cln2p is degraded after the G1 to S transition of each cell cycle (reviewed in Deshaies, 1995a, 1995b); thus daughter cells should not be able to inherit Cln2p from their counterpart mother cells.

The genotype of the starting strain for the high copy screen was *cln1Δ cln2Δ cln3Δ leu2::LEU2 pGAL-CLN2 ho::pHO-CLN2 ura3-52*. To ensure that the viability of mother and daughter cells was as expected, single cells were followed over multiple divisions on glucose slabs, where the GAL promoter is repressed. Rather than pedigrees of mating-type switching, these experiments were "pedigrees of death" (Table A1-1). As predicted, mother cells were largely viable (96 to 100% of mother cells could divide in the absence of galactose), indicating that the *HO* promoter produced sufficient levels of CLN2. Daughter cells, in contrast, were largely incapable of progression through the cell cycle (6-24% of daughter cells were able to divide). Many of the daughter cells that divided did so after languishing on glucose for several hours, suggesting that these cells might be slowly accumulating sufficient levels of Cln2 from non-specific gene activation. Interestingly, daughter cells that ultimately were able to divide on glucose did not give rise to daughter cells with the same properties, suggesting that no heritable change had occurred in these cells.

Preliminary Screening for High Copy Plasmids that Stimulate Growth Rate of the *HO-CLN2* Strain

Strains YAS76-5A and YAS76-6B (see Table A1-1) were transformed with a 2 micron *URA3*-based library (data summarized in Figure A1-2). A total of 19,000 transformants (representing approximately 12 genome equivalents) were selected on synthetic galactose medium lacking uracil (SGal-ura; permissive conditions for growth). The resultant colonies were replica-plated on glucose medium lacking uracil (SD-ura; restrictive conditions where the only source of *CLN2* is from the *HO* promoter). 407 colonies grew more rapidly on glucose medium than those containing a 2

Table A1-1. The Pedigree of Death.

Frequency of Divisions		
Strain	%M	%D
YAS76-5A	98 (49/50)	6 (3/50)
YAS76-5B	96 (52/54)	11 (6/53)
YAS76-6A	97 (56/58)	24.5 (14/57)
YAS76-6B	100 (46/46)	8 (3/36)

M= mother, D= daughter

These strains represent four isolates of strains of identical genotype.

Figure A1-2. Statistics from the High Copy Screen. 19,000 high-copy plasmid transformants were obtained on galactose medium (SGal-ura). Of these, 407 conferred growth on glucose (SD-ura). A flow-chart of various secondary screens is depicted in the figure.

19,000 transformants on SGal - ura
↓
407 grow on SD - ura
↓
319 passed initial rescreening
↓
302 did not grow on glucose-5FOA
↓ (plasmid-dependent)
295 did not rescue a/α $cln1\Delta$ $cln2\Delta$ $cln3\Delta$
↓
215 plasmids were recovered from yeast
↓
≤66 different plasmids by
restriction mapping

micron vector control; these colonies were patched onto SGal-ura and replica-plated again to SD-ura (Figure A1-3). Growth on SD-ura was compared to the same strain transformed with either a 2 micron vector control or with 2 micron *CLN2*, which completely reverses the reduced growth of the strain on glucose. 319 transformants improved growth of the strain on SD-ura when compared to the vector control; only 20 of these plasmids restored growth as well as the 2 micron *CLN2* control.

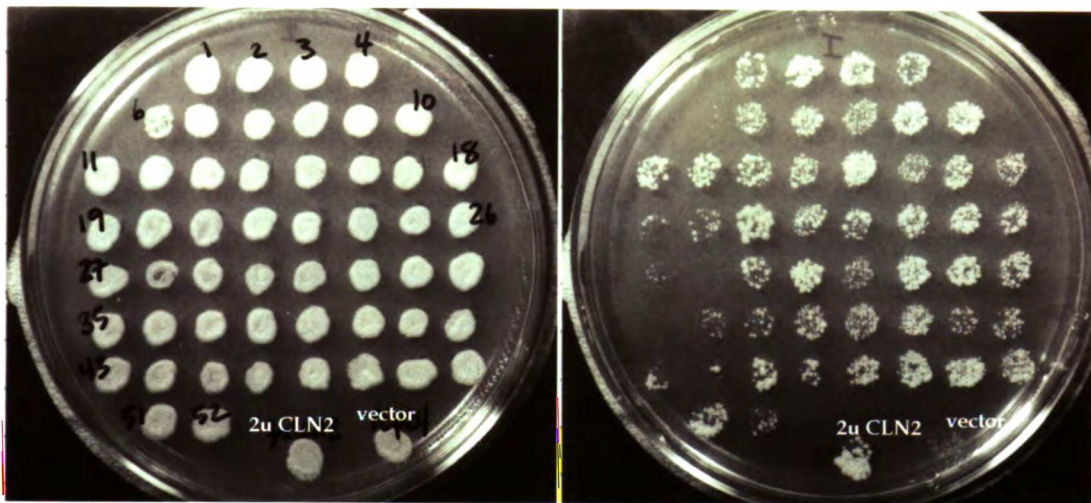
In order to test which of the 319 transformants had a growth phenotype dependent on the library plasmid they were carrying, I selected for cells that had lost the *URA3*-marked plasmid with 5-fluoro-orotic acid (5-FOA). If growth on glucose is dependent on the library plasmid, such a strain will not be able to grow on glucose medium containing 5-FOA. 302 transformants could not grow on 5-FOA and thus were plasmid-dependent.

Since I was interested in plasmids that conferred an increased growth rate on glucose because they allowed the *HO* promoter to be active in daughter cells, I wanted to discard plasmids that conferred growth on glucose because they encoded G1 cyclins. To eliminate such plasmids, we devised a quick test to determine if the plasmid-dependent growth phenotype was dependent on the activity of the *HO* promoter (the desired result) or independent of the activity of the *HO* promoter (a property, for example, of a plasmid encoding a G1 cyclin). Since the *HO* promoter is repressed in *a/α* diploids, evaluation of the ability of the appropriate *a/α* diploids to grow on glucose is an assay for dependence of the growth phenotype on activity of the *HO* promoter. Hence, the *a cln1Δ cln2Δ cln3Δ ho::pHO-CLN2 leu2::LEU2 pGAL-CLN2* library transformants were mated with an *α cln1Δ cln2Δ cln3Δ pGAL-CLN2* strain. The resultant *a/α* diploids were assayed for the ability to

Figure A1-3. Growth of Strains Carrying High Copy Plasmids on Glucose vs. Galactose. An example of the initial screening of the high-copy plasmid transformants is shown. Transformants were patched on SGal-ura (the plate on the left). These plates were then replica-plated to SD-ura (glucose) plates (on the right). Different transformants varied in their ability to grow on glucose. A 2μ CLN2 plasmid, which confers robust growth on glucose, and a vector control, which does not confer growth on glucose, are labelled.

GAL

GLU



grow well on glucose. If the growth phenotype conferred by the plasmid was independent of activation of the *HO* promoter, then the *a/α* diploids were still able to grow on glucose. If, however, the ability to grow on glucose was dependent on activation of the *HO* promoter, the *a/α* diploids were not able to grow on glucose due to repression of the *HO* promoter in *a/α* cells. 295 transformants fell into the latter category.

Of these 295 transformants, I recovered the library plasmid from 215 isolates. Each plasmid was subjected to rudimentary restriction mapping. These experiments revealed that at most 66 different plasmids had survived the secondary screens thus far. Some of the 66 plasmids may have contained overlapping inserts, and as such might have defined the same gene.

Secondary screens

The 66 plasmids obtained from the preliminary screening were put through a battery of secondary screens (Table A1-2) in an attempt to eliminate plasmids that stimulated growth on glucose for reasons that did not pertain to mother/daughter regulation of the *HO* promoter. I reasoned that plasmids that bypassed the requirement for *SWI5*, *SWI4*, or *SWI6* (known activators of *HO*; see Chapter 1) might allow inappropriate expression of the *HO* promoter in daughter cells. To test this hypothesis, each of the 66 plasmids were transformed into *swi5Δ HO-lacZ*, *swi4Δ HO-lacZ*, or *swi6Δ HO-lacZ* strains. In each of these strains, activation of the *HO* promoter was followed by measuring B-galactosidase activity by a filter assay. None of the 66 plasmids conferred appreciable amounts of B-galactosidase activity when compared to a vector control. Hence, none of the plasmids bypassed *SWI5*, *SWI4*, or *SWI6*.

Although failure to allow growth of *a/α cln1Δ/cln1Δ cln2Δ/cln2Δ cln3Δ/cln3Δ ho::pHO-CLN2/ho GAL-CLN2/GAL-CLN2* cells on glucose was

Table A1-2. Secondary Screens.

Secondary Screens	# high copy plasmids eliminated
<i>swi5</i> Δ <i>H</i> <i>O</i> <i>lacZ</i>	0
<i>swi4</i> Δ <i>H</i> <i>O</i> <i>lacZ</i>	0
<i>swi6</i> Δ <i>H</i> <i>O</i> <i>lacZ</i>	0
<i>cln1</i> Δ <i>cln2</i> Δ <i>cln3</i> Δ <i>GAL-CLN2</i>	2
2 μ <i>pGAL-lacZ</i>	0

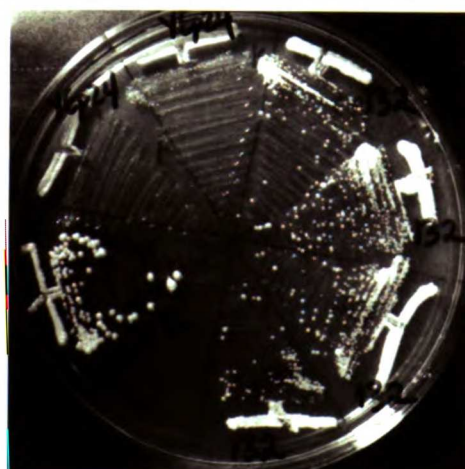
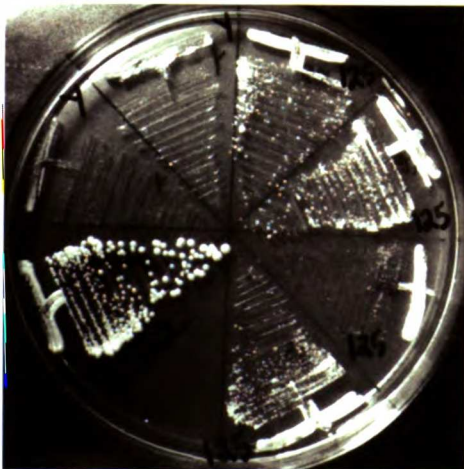
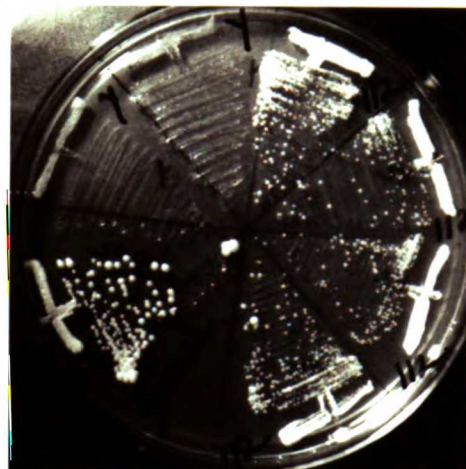
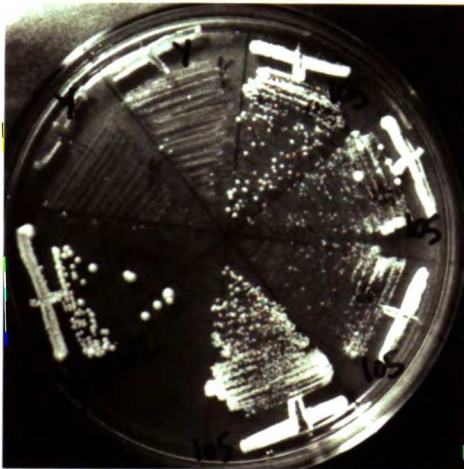
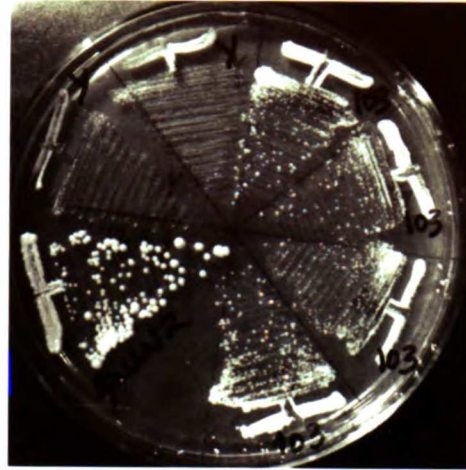
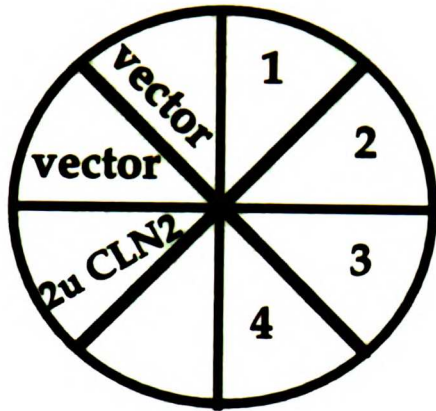
2 μ *pGAL-lacZ* screening was done in strain JO14

used to eliminate plasmids encoding G1 cyclins (described above), restriction mapping of the 66 plasmids revealed a single plasmid encoding the *CLN2* gene. In order to eliminate other G1 cyclin plasmids that might have escaped the α/α test, an *a cln1 Δ cln2 Δ cln3 Δ GAL-CLN2* strain was transformed with all 66 plasmids. Two plasmids were able to stimulate growth of this strain on glucose (data not shown) and were duly eliminated. Restriction mapping revealed that one of these plasmids encoded *CLN2* whereas the other encoded *CLN3*.

High copy plasmids that allowed the strain to bypass catabolite repression of the *GAL* promoter would also allow growth on glucose. Even though the phenotype of such plasmids should be independent of activation of the *HO* promoter, and as such should have been eliminated by the α/α test, I decided to test for these plasmids specifically. A strain containing a 2 micron *GAL-lacZ* plasmid was transformed with all 66 plasmids. If any of the 66 plasmids bypassed catabolite repression, these plasmids should stimulate β -galactosidase activity in glucose medium. None of the 66 plasmids fell into this category (data not shown).

Finally, the 66 plasmids were re-transformed into the starting *cln1 Δ cln2 Δ cln3 Δ leu2::LEU2 pGAL-CLN2 ho::pHO-CLN2* strain. Of the 66 plasmids, 34 conferred a stronger ability to grow on glucose (Figure A1-4) than the remaining 32 plasmids. The effect of these 34 plasmids on the regulation of mating-type switching was determined by transforming them into a *ste3 Δ HO* strain. The resultant transformants were subjected to the four-shmoo microcolony assay described in detail in Chapter 2. In brief, when the *ste3 Δ HO* strain is grown in the presence of α -factor, the number of microcolonies composed of four shmooing cells correlates with the frequency of daughter-

Figure A1-4. Comparison of the Ability of Different Plasmids to Confer Growth on Glucose. Sixty-six plasmids were re-transformed into the starting *clnΔ* strain. Four transformants from each of the plasmids were streaked for single colonies on SD-ura (glucose) plates. An example of 5 of the 66 plasmids is shown in the figure. Each plate corresponds to one of the plasmids. A key for each plate is shown in the top left corner. Each plate contains two sectors that correspond to a vector control, which does not confer the ability to form single colonies on glucose medium. Each plate also contains a sector that contains a 2 μ *CLN2* transformant, which confers robust growth on glucose. Sectors 1, 2, 3, and 4 correspond to four different transformants for each of the plasmids.



cell switching. None of the 34 plasmids conferred a significant increase of four-shmoo microcolonies when compared to a vector control (Table A1-3).

Discussion

I performed a screen to search for high-copy plasmids that allowed activation of the *HO* promoter in daughter cells. This screen utilized a strain whose *HO* promoter activity was monitored by following growth rate rather than mating-type switching. Although the ease of the assay facilitated a large scale screen, no plasmids that affected mating-type switching in daughter cells were obtained.

High copy plasmids encoding G1 cyclins were obtained from the screen, indicating that I was able to recover plasmids that increased the growth rate on glucose. The fact that many different plasmids of unknown function displayed the desired phenotype, however, may indicate that the selection criteria were not adequately specific. Furthermore, although the ability of mother and daughter cells to grow on glucose was largely asymmetric, this asymmetry was less stringent than mother/daughter regulation of mating-type switching: in general, no daughter cells in *HO* strains are observed to switch, whereas 6-24% of daughter cells in the *HO-CLN2* strain were able eventually to progress through the cell cycle. This difference was evidenced by the fact that the starting strain would, given enough time, grow on glucose. The phenotype of the strain was complicated by the fact that daughter cells could remain in G1 for many hours, as observed during the pedigree of death analysis, before accumulating the minimum level of Cln2p required to transit the cell cycle. Since these daughter cells were probably on a hair trigger for progression through the cell cycle, many plasmids that influenced progression in a non-specific manner could have been obtained.

Table A1-3. The Effect of the High-Copy Plasmids in the Four-Shmoo Microcolony Assay

Plasmid	# times screened	average # four-shmoo microcolonies/1000 microcolonies
YEp24	28	2.6
6*	5	1.8
43*	4	2.8
45*	4	2.3
6	8	5.3
8	6	2.5
24	4	4.3
29	5	2.4
30	3	2.7
33	2	3
47	4	4
84-1	4	4.2
103	4	2.5
112	6	4.2
143	10	5.3
174	6	2.8
184	3	2.6
210	7	4.3
212	7	5.1
256	3	3
262	4	5.5
263	4	3.5
307	4	3.7
38*	3	3.5
53*	2	2
12	1	4
25	1	1
50	3	7.3
128	2	3
132	2	4.5
136	3	2.3
141	2	3
170	3	2.3
180	2	5.5
185	3	2.3
2 μ SWI4	8	6.1
2 μ SWI5	3	2.7

In retrospect, it is tempting to hypothesize that the plasmid-*independent* isolates obtained during the screen should have been analyzed further. These isolates could have accumulated mutations in genes required to maintain proper regulation of the *HO* promoter. Mutations in genes such as *ASH1* (see Chapter 2) would allow the *HO* promoter to be active in daughter cells as well as mothers; thus *CLN2* would have been transcribed in both mother and daughter cells in a plasmid-independent fashion.

Finally, this screen illustrates the danger of following a phenotype only indirectly related to mating-type switching. Perhaps addition of a second *HO*-dependent reporter would have increased the stringency of the selection criteria. At any rate, the results of this screen prompted me to use a direct mating-type switching assay to isolate mutants whose daughter cells have gained the ability to switch mating-type (Chapter 2).

Table A1-4. Appendix One Strain List

<u>Strain name</u>	<u>Relevant Genotype</u>	<u>Source</u>
YAS76-5A	a <i>cln1Δ cln2Δ cln3Δ leu2::pGAL-CLN2 ho::pHO-CLN2</i>	This study
YAS76-5B	a <i>cln1Δ cln2Δ cln3Δ leu2::pGAL-CLN2 ho::pHO-CLN2</i>	This study
YAS76-6A	a <i>cln1Δ cln2Δ cln3Δ leu2::pGAL-CLN2 ho::pHO-CLN2</i>	This study
YAS76-6B	a <i>cln1Δ cln2Δ cln3Δ leu2::pGAL-CLN2 ho::pHO-CLN2</i>	This study
YAS72-4B	a <i>swi5Δ HO-lacZ ura3-52</i>	This study
JO51-2D	a <i>swi4Δ HO-lacZ ura3-52</i>	Joe Ogas
JO52-4A	a <i>swi6Δ HO-lacZ ura3-52</i>	Joe Ogas
JO271	a <i>cln1Δcln2Δcln3Δ leu2::pGAL-CLN2</i>	Joe Ogas
YAS115	a and α <i>HO ste3Δ ura3</i>	This study
JO14	a <i>ura3-52 leu2-Δ1</i> (S288c wild-type)	Joe Ogas

YAS76-5A, 5B, 6A, 6B, and JO271 are isogenic

JO14, JO51-2D, JO52-4A, YAS72-4B are isogenic (S288c background)

YAS115 is in the W303 background

APPENDIX TWO

THE EFFECT OF VEGETATIVE GROWTH ON THE SWITCHING PATTERN

Vegetative growth of wild-type *HO* cells yields both **a** and α cells, which then mate to form an **a**/ α diploid that no longer expresses *HO*. Hence, classic lineage studies of mating-type switching must begin with spore cells that are produced meiotically from such an **a**/ α diploid. After germination, mating-type switching of mother and daughter cells that arise from these spores is monitored. I constructed a special strain that allowed such pedigree analysis to be performed with vegetatively-growing mitotic cells (see Chapter 2). This *HO* strain is defective in the *STE3* gene, which encodes the **a**-factor pheromone receptor (Nakayama et al., 1985; Hagen et al., 1986). In theory, *HO ste3Δ* cells can switch back and forth between **a** *HO ste3Δ* and α *HO ste3Δ*. Since the α *ste3Δ* cells cannot sense the presence of **a**-factor produced by **a** cells in their environment, they do not induce the signal transduction pathway required for mating. Thus, **a**/ α diploids are not formed. The surprising result was that in three of four strain backgrounds tested, *HO ste3Δ* cells that are grown vegetatively for many generations ("long-term vegetative cells") lose their ability to switch mating type efficiently. (Disruption of *STE3* in one *HO* strain background resulted in long-term vegetative cells with a normal level of mating-type switching; see Chapter 2.)

α mother cells derived from *HO ste3Δ* spores (Table A2-1) are able to switch to **a** at a normal frequency: 59% of these cells vs. 70% of *STE3* mothers are able to switch mating type. This typical level of switching continues for the duration of the pedigree (five or six generations). In contrast, if *HO ste3Δ* spores are grown overnight in liquid culture, and the resultant cells are plated on a slab and followed microscopically in lineage studies, the mating-type switching of mother cells decreases sharply to about 2% (Table A2-1). The *ste3Δ* cells that are grown vegetatively prior to pedigree analysis did not

Table A2-1. The Switching Frequency of Various Strains

Strain	Starting Cells	Switching Frequency %M
<i>α HO STE3 STE6</i> (YAS81)	spores	70 (32/46)
<i>α HO ste3Δ</i> (YAS97)	spores	59 (39/66)
<i>α HO ste3Δ</i> (YAS93)	vegetative cells	2 (3/131)
<i>a HO ste3Δ</i> (YAS93)	vegetative cells	5 (10/200)
<i>α HO ste6Δ</i> (YAS96)	spores	57 (17/30)
<i>α HO ste6Δ</i> (YAS91)	vegetative cells	2 (2/129)

M = mother

regain the ability to switch efficiently during the 10 generations that were monitored microscopically. However, such cells always gave rise to cells of the opposite mating type, if only at a low frequency. I do not know if mating of these long-term vegetative cells followed by sporulation resulted in spore cells that gave rise to lineages with normal switching frequencies.

Pedigree analysis is most easily performed by monitoring switching of α cells to **a**. To determine whether the ability of a *ste3* Δ cells to switch to α was affected, I allowed lineages of a *ste3* Δ cells to divide for at least six generations and then moved cells into the presence of α -factor; α cells are resistant to α -factor, whereas **a** cells are not. The pattern of mating-type switching throughout the lineage could be derived from monitoring the mating-type of cells at the end of the lineage (Strathern and Herskowitz, 1979). These studies revealed that the switching frequency of a *ste3* Δ cells to α was only 5% (Table A2-1).

To test whether or not this phenomenon was specific to disruption of the *STE3* gene, I constructed an isogenic *HO ste6* Δ strain. *STE6* encodes a pump necessary for efflux of **a**-factor from **a** cells (Kuchler, et al., 1989); in its absence, **a** cells are sterile because they are unable to signal to their counterpart α cells. The *HO ste6* Δ strain behaved identically to the *ste3* Δ strain (Table A2-1): lineages of cells derived directly from spores showed 57% switching, while lineages derived from cells grown overnight showed only 2% switching. Thus inhibition of mating-type switching in vegetative cells was not specific to strains that lacked *STE3*, but, in certain strain backgrounds, might occur generally in vegetatively-grown haploid *HO* cells. A second set of experiments supports this hypothesis: I constructed a *swi4* Δ *HO URS2* Δ strain; such a strain cannot form viable **a**/ α diploids since *SWI4*, in this strain

background, is essential in diploid cells. Haploid α and α *swi4* Δ cells can, despite the lack of SWI4, transcribe a special *HO* allele (the *HO URS2* Δ allele) that lacks the region of the *HO* promoter normally activated by SWI4. Single cells from such a strain always gave rise to colonies that contained cells of both mating-type, indicating that some level of switching was occurring. When the frequency of switching was measured by pedigree, however, I found that only 2% (5/294) of the cells switched. Again, these results may indicate a general inhibition of mating-type switching in "long-term" vegetative cells.

To determine if ectopic expression of *HO* could restore normal ability to switch mating type in the *HO ste3* Δ strain, I transformed these cells with a *GAL-HO* plasmid and assayed the switching frequency. Cells were grown under selection for the plasmid in either glucose (where *GAL-HO* is repressed) or galactose (where *GAL-HO* is induced) for 19.5 hours, and then followed by pedigree analysis on either YEPD or YEPGal (Table A2-2). When *GAL-HO* is expressed, 16% of the mothers and 3% of the daughters were observed to switch mating type; no mothers and no daughters were observed to switch in glucose medium. Hence ectopic expression of *HO* can increase the level of switching but not to wild-type levels. I did not monitor any *GAL-HO* lineages that began as spore cells, so I do not know the maximum level of switching inducible by this construct in this strain background; however, in other strain backgrounds, *GAL-HO* causes 52% of mother cells and 39% of daughter cells to switch (Nasmyth, 1987).

Is the reduced mating-type switching of the vegetative lineages explained by a block upstream or downstream of *HO* transcription? Several lines of evidence make it likely that the *HO* promoter is still active in these

Table A2-2 Switching Frequency of *HO ste3Δ* Strain Transformed with a *GAL-HO* Plasmid

		GAL	DEX
Switching Frequency	%M	16 (10/61)	< 1 (0/40)
	%D	3 (2/59)	< 1 (0/39)

M = mother, D = daughter

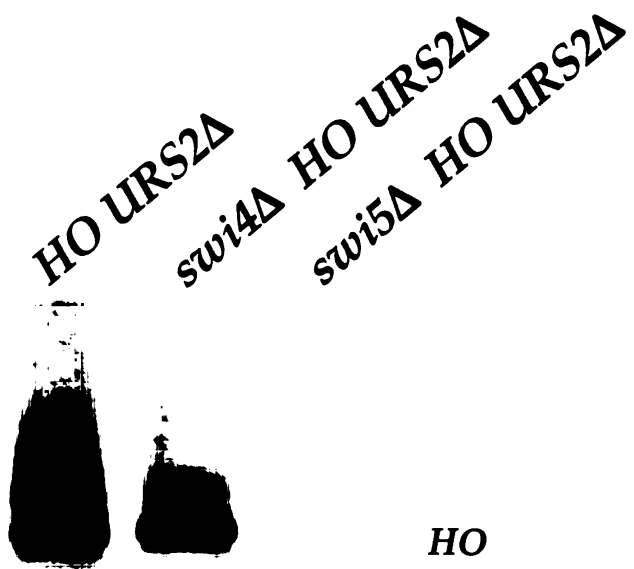
GAL = growth on galactose, DEX = growth on glucose

strains. First, ectopic expression of *HO* from the *GAL* promoter, as mentioned above, does not fully restore wild-type switching frequency to these strains. Second, reporters such as *HO-lacZ*, *HO-ADE2*, and *HO-CAN1* are still active in isogenic strains grown vegetatively for long periods of time. Finally, *HO* RNA levels in the *swi4Δ HO URS2Δ* strain mentioned above were completely normal when measured by primer extension (Figure A2-1). However, measurement of *HO* RNA levels in the *HO ste3Δ* strains should be performed to rule out the possibility that transcription of *HO* is affected in these cells.

What are some of the possible explanations for the reduced switching phenomenon? In cells that switch at a wild-type frequency, *HO* expression and mating-type switching do not occur in daughter cells due to the action of *ASH1* (see Chapter 2), and in *a/α* cells, due to the repressor *a1-α2*. It might be interesting to know if the decrease in switching frequency in "long-term" vegetative cells is *ASH1*-dependent. If so, this would imply that although Ash1p is normally confined to daughter cells, it is symmetrically localized to mothers and daughters under conditions of "long-term" vegetative growth in certain strain backgrounds. Alternatively, it is possible that the "long-term" vegetative cells form *a/α* diploids at some frequency: though the strains are sterile, a failure to segregate both nuclei properly at mitosis can result in an *a/a* or *α/α* diploid cell; switching of one of the two mating-type loci will then yield an *a/α* diploid. *a/α* diploid cells would no longer switch mating type. However, such cells would display an altered (*a/α*-specific) budding pattern, which was never observed.

It is possible that if the haploid cell density is high, a signalling event might occur between cells that, by an unknown mechanism, reduces the

Figure A2-1. Transcription of *HO* Occurs at Normal Levels in *swi4Δ* *HOURS2Δ* Strains. Primer extension was used to detect *HO* and *URA3* transcripts in RNA made from *HO URS2Δ*(IH1997), *swi4Δ HO URS2Δ*(YAS46-17B), and *swi5Δ HO URS2Δ* (YAS62-2C) strains.



levels of mating-type switching. It should be noted, however, that "long-term" vegetative cells never recovered their ability to switch efficiently during the duration of the pedigree (as long as 10-12 generations). Thus, any reduction in mating-type switching was not reversed by isolating single cells (as is done in a pedigree) and separating them from their progeny as they divide. If a cell signalling event *does* occur, it is unlikely to depend on mating pheromone, since pheromone signalling is attenuated in both *ste3Δ* and *ste6Δ* strains.

Finally, why cells would want to inhibit mating-type switching under conditions of increased cell density is unclear. Perhaps nutrient limitation triggers a change in cell physiology that limits the function of a component of the switching machinery. For the moment, this mystery remains unsolved.

Materials and Methods

Genetic and Molecular Biological Methods

DNA manipulations were as described in Sambrook et al., 1989. Yeast genetic methods were as described in Rose et al., 1990.

Strains and Plasmids

Strains are described in Table A2-3, at the end of this appendix.

The *GAL-HO* plasmid was constructed by Rob Jensen.

Pedigree Analysis: The starting cells for lineage studies were either spore cells or vegetative cells. In the former case, a/ α diploids were sporulated and the resultant tetrads were dissected on 4% YEPD agar slabs using conventional protocols. Each tetrad was dissected in close proximity to a wall of α cells that produced α -factor for the duration of the experiment. Mothers and daughters

could be distinguished on the basis of size. A switch from α to **a** was scored as the acquired ability to respond morphologically to α -factor. When the starting diploids were heterozygous for *ste3 Δ* or *ste6 Δ* , the deletion lineages were identified by the auxotrophic marker associated with the deletion. If the starting cells for pedigrees were vegetative cells, these cells were grown to early log phase in YEPD, sonicated, and placed proximal to a wall of α cells. In the case of the *GAL-HO* experiments, the cells were grown under selection for the plasmid, sonicated, and then assayed on YEPD slabs.

Table A2-3. Appendix Two Strain List

<u>Strain name</u>	<u>Relevant Genotype</u>	<u>Source</u>
YAS81	<i>a/α HO/HO STE3 STE6</i>	This study
YAS97	<i>a/α HO/HO ste3Δ::LEU2/STE3</i>	"
YAS93	<i>a and α HO ste3Δ::LEU2</i>	"
YAS96	<i>a/α HO/HO ste6Δ::HIS3/STE6</i>	"
YAS91	<i>a and α HO ste6Δ::HIS3</i>	"

All strains are isogenic to S288c background.

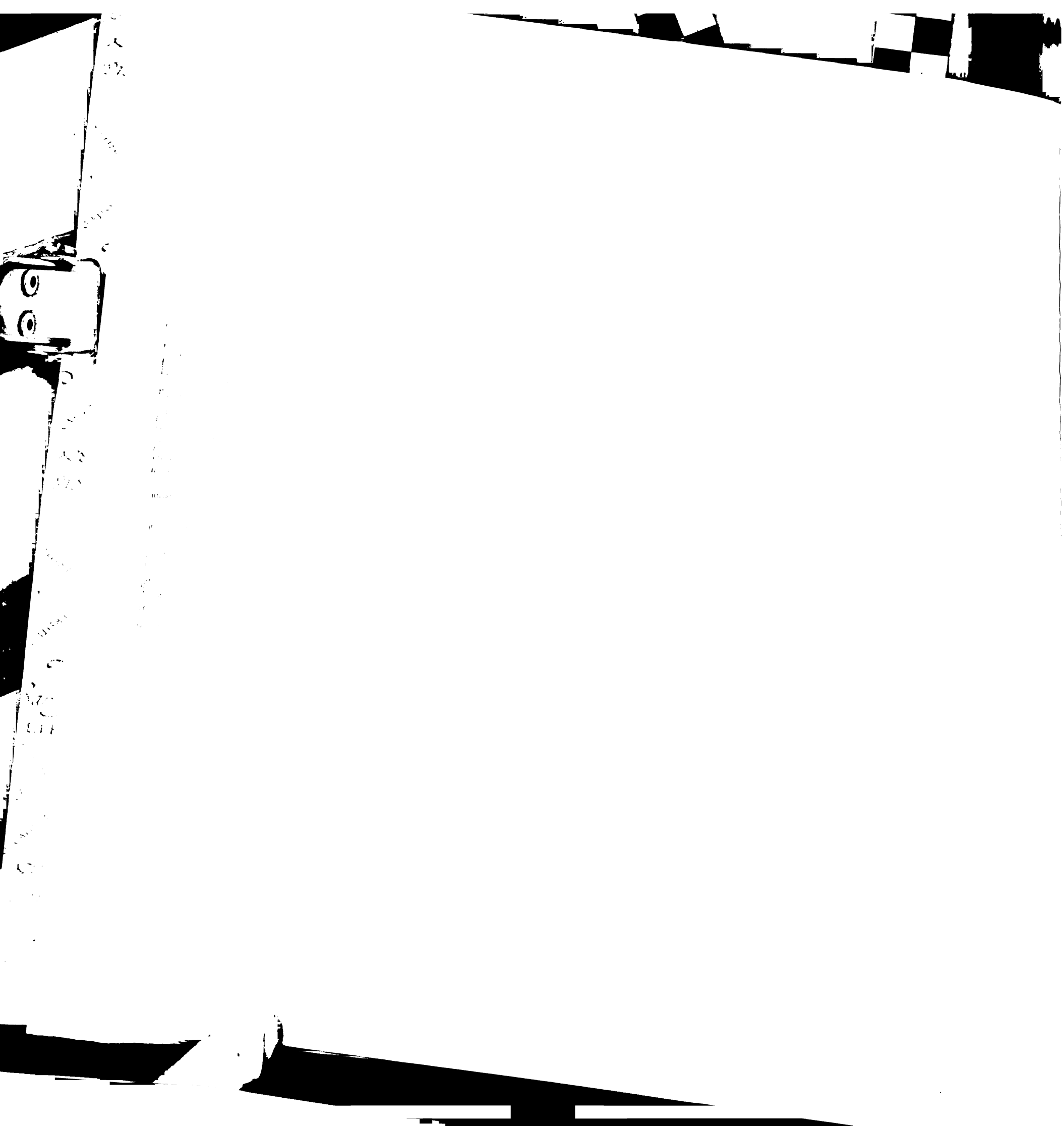
APPENDIX THREE

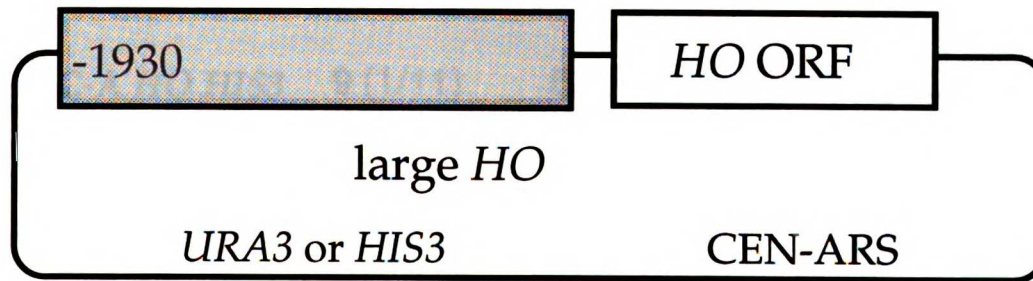
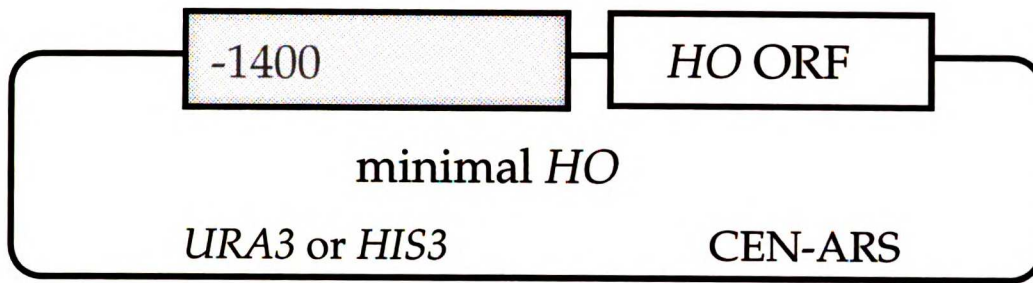
REGIONS OF THE *HO* PROMOTER REQUIRED FOR MOTHER/DAUGHTER REGULATION

To determine the minimal region of the *HO* promoter that is sufficient to confer mother/daughter regulation, I constructed a CEN-ARS plasmid (marked with either *HIS3* or *URA3*) containing approximately 1400 nucleotides of *HO* promoter region driving the *HO* open reading frame (Figure A3-1). An *ho* S288c strain was transformed with these plasmids. The transformants switched mating type and formed **a**/ α diploids which were then sporulated for lineage studies. Pedigree analysis was performed on spores that contained the *HO* plasmid (presence of the *URA3* or *HIS3* marker was confirmed for cells from each lineage). Although an isogenic genomic *HO* strain displayed wild-type mother/daughter regulation (69% of mothers switched whereas no daughters or spores switched), neither the *URA3*-marked or *HIS3*-marked plasmids conferred proper regulation (Table A3-1). Approximately 10% of spores were observed to switch in both transformants. Mothers switched at 57% in the *HIS3* transformants and at 33% in the *URA3* transformants. Remarkably, daughter cells switched at 33% in the former case and at 12% in the latter case. (The decreased levels of switching in the *URA3* transformants as compared to the *HIS3* transformants may be due to a lower mitotic stability for the *URA3* vector [pRS316] in general [A.S. and others, unpublished observations].)

I reasoned that the *HO* plasmid constructs might bypass mother/daughter regulation because they bypass the need for an activator of *HO* that is normally limiting in spore cells and in daughters. To check this hypothesis, I transformed the plasmids into an isogenic set of *ho* S288c strains that were deficient in various *SWI* genes, all of which are required for *HO* transcription. When the plasmids were transformed into an **a** strain that is wild-type for all the *SWI* genes, transformants were able to switch mating-

Figure A3-1. CEN-ARS Plasmids Containing Different Amounts of *HO* Promoter DNA. The top panel of the diagram depicts a CEN-ARS *HO* plasmid with 1400 nucleotides of upstream sequence. This plasmid is designated "minimal *HO*" in the text and tables. Two versions of this plasmid, one marked with *URA3* (pAS110, in the pRS316 vector) and one marked with *HIS3* (pAS111, in the pRS313 vector), were made. The bottom panel depicts a CEN-ARS *HO* plasmid with 1930 nucleotides of upstream sequence. This plasmid is designated "large *HO*" in the text and tables. Three versions of this plasmid, two marked with *URA3* (one in YCp50 [pAS122] and one in pRS316 [pAS123]) and one marked with *HIS3* (pAS124, in pRS313), were made.





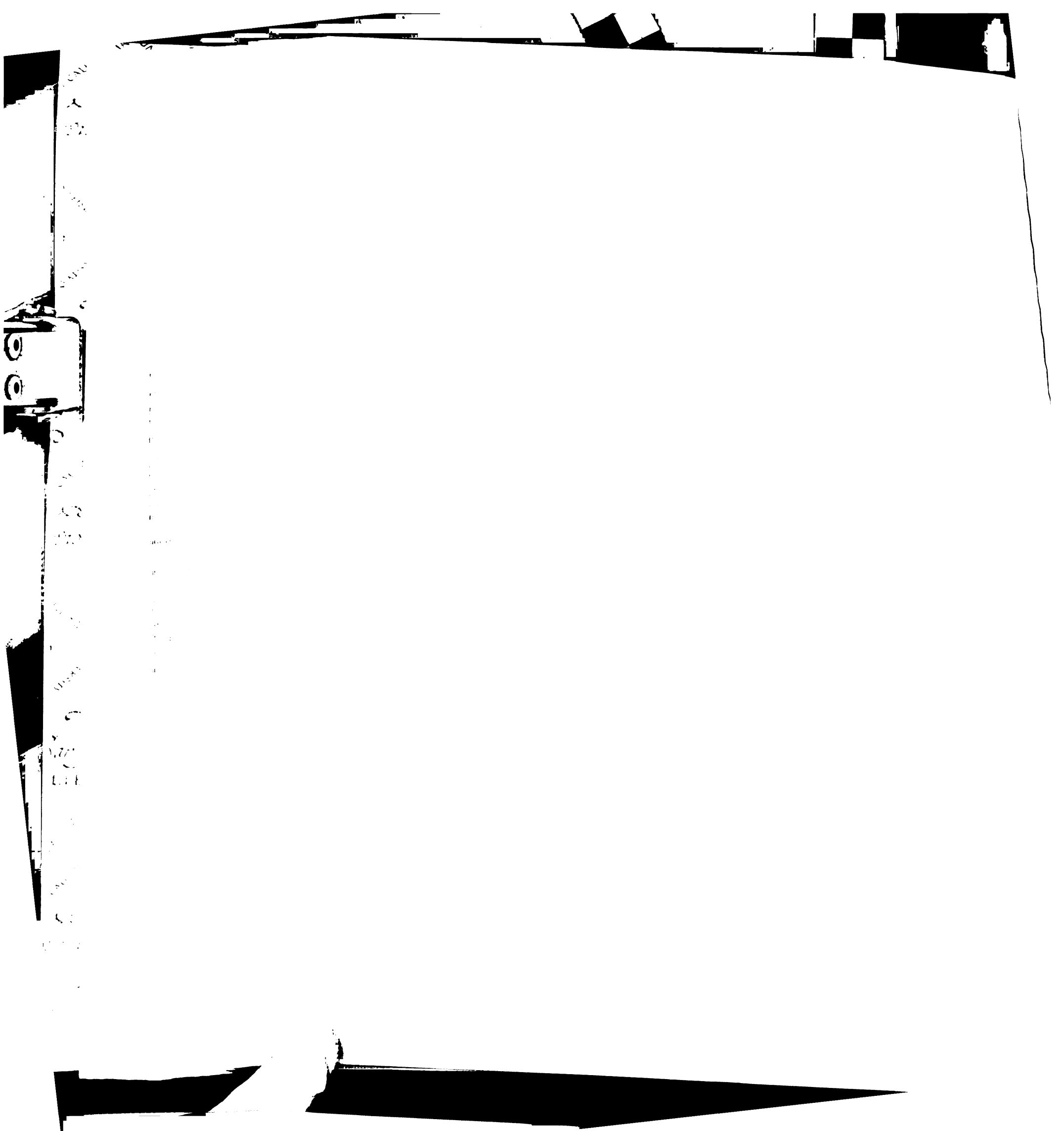


Table A3-1. CEN-ARS *HO* Plasmids Bypass Mother/Daughter Regulation

Strain	Switching Frequency		
	%S	%M	%D
<i>HO</i>	<3 (0/30)	69 (138/200)	<1 (0/190)
<i>ho C-A HO HIS3</i>	9 (1/11)	57 (20/35)	33 (10/30)
<i>ho C-A HO URA3</i>	12 (1/8)	33 (18/54)	12 (6/48)

C-A = CEN-ARS

S = spore, M = mother, D = daughter

type to α (Table A3-2). Non-maters (a/α cells that result from the mating of switched cells) and bi-maters (colonies that contain cells of both mating-types because switching is occurring) were also observed. In contrast, α *swi1 Δ* and *swi4 Δ* strains transformed with the *HO* plasmids were not able to switch mating-type; 40/40 transformants for each strain remained stably α . These results indicate that transcription of the *HO* gene on the plasmids was dependent on both *SWI1* and *SWI4*. Interestingly, *swi5 Δ* strains, much like wild-type strains, were able to switch mating-type despite the absence of the Swi5p activator (Table A3-2): 40 transformants of an α strain yielded 11 a colonies and 29 non-mating (a/α) colonies. Thus transcription of the plasmid-borne *HO* gene is *SWI5*-independent. (Mating-type switching of the endogenous *HO* allele at its own chromosomal locus did not occur in the presence of the identical *swi5 Δ* allele.)

Bypass of *SWI5*-dependence could occur for several reasons. First, the physical location of the gene--on a plasmid versus on a chromosome--could obviate the need for the activator Swi5p. To test this possibility, I made a -1400 base pair *HO* construct (identical to the original CEN-ARS version) in a *URA3*-marked integrating vector and targeted integration of the plasmid to the *ura3* locus. Interestingly, proper mother/daughter regulation was not restored when this construct is integrated (Table A3-3, line 1): 70% of mothers, 24% of daughters, and 22% of spores switched mating type. I also tested whether the integrated construct bypassed the need for *SWI5* by integrating either the *HO* plasmid or an empty vector at *ura3* in a *swi5 Δ* strain (Table A3-4). 32 of 32 α *swi5 Δ* transformants carrying the control vector remained stably α , whereas 32 α *swi5 Δ* transformants carrying the integrated

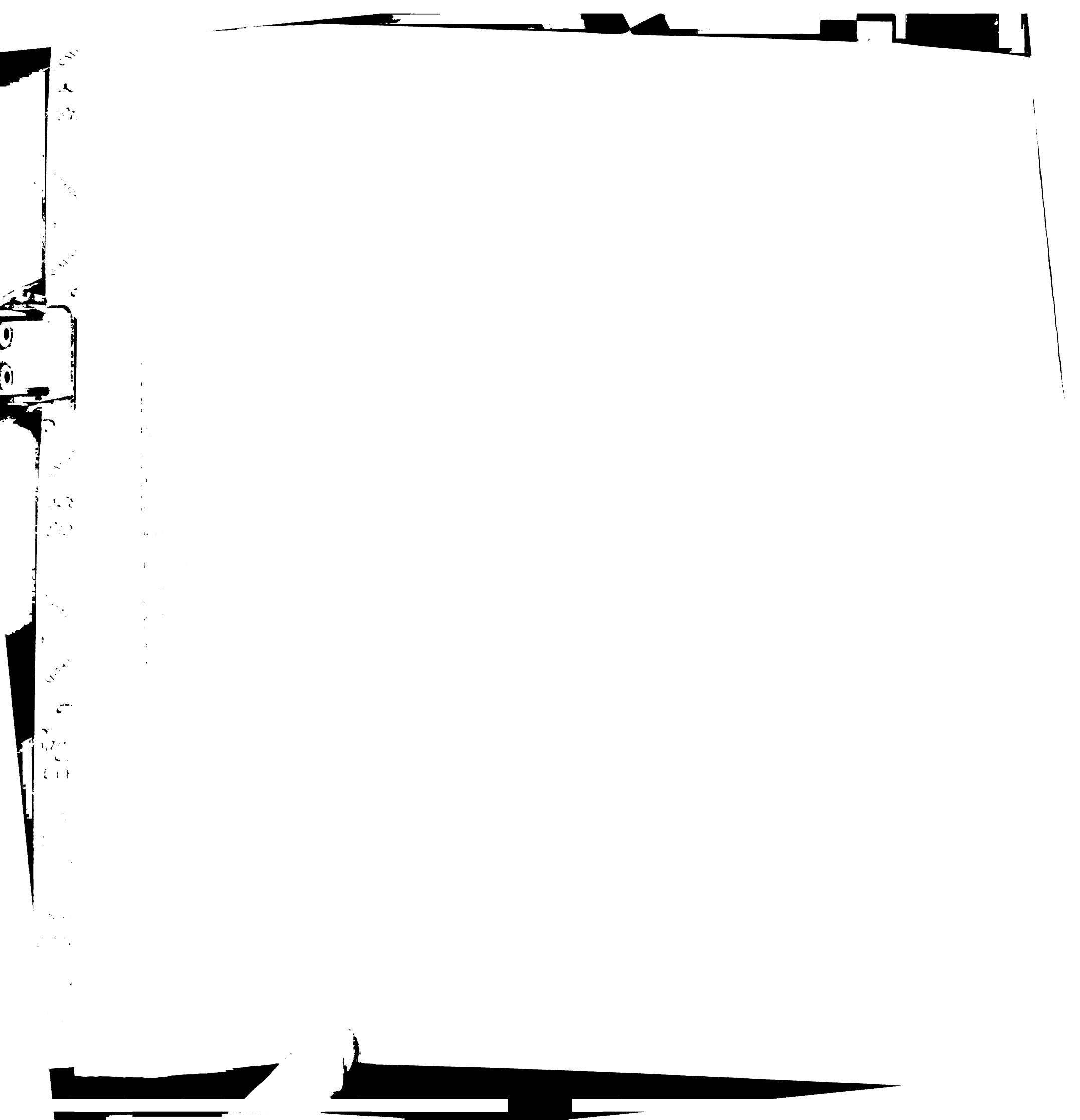


Table A3-2. CEN-ARS HO Plasmids Bypass the SWI5 Requirement

<i>MAT</i>	Swi	HO plasmid	total # analyzed	# a	# α	#NM	#BM
a	SWI+	URA3	40	33		7	
a	SWI+	HIS3	32	3		11	18
α	<i>swi1</i> Δ	URA3	20		20		
α	<i>swi1</i> Δ	HIS3	20		20		
α	<i>swi4</i> Δ	URA3	40		40		
α	<i>swi5</i> Δ	URA3	20	7		13	
α	<i>swi5</i> Δ	HIS3	20	4		16	

#a = number of colonies that mated as a cells

α = number of colonies that mated as α cells

#NM = number of colonies that did not mate (non-maters)

#BM = number of colonies that mated as both a and α (bi-maters)

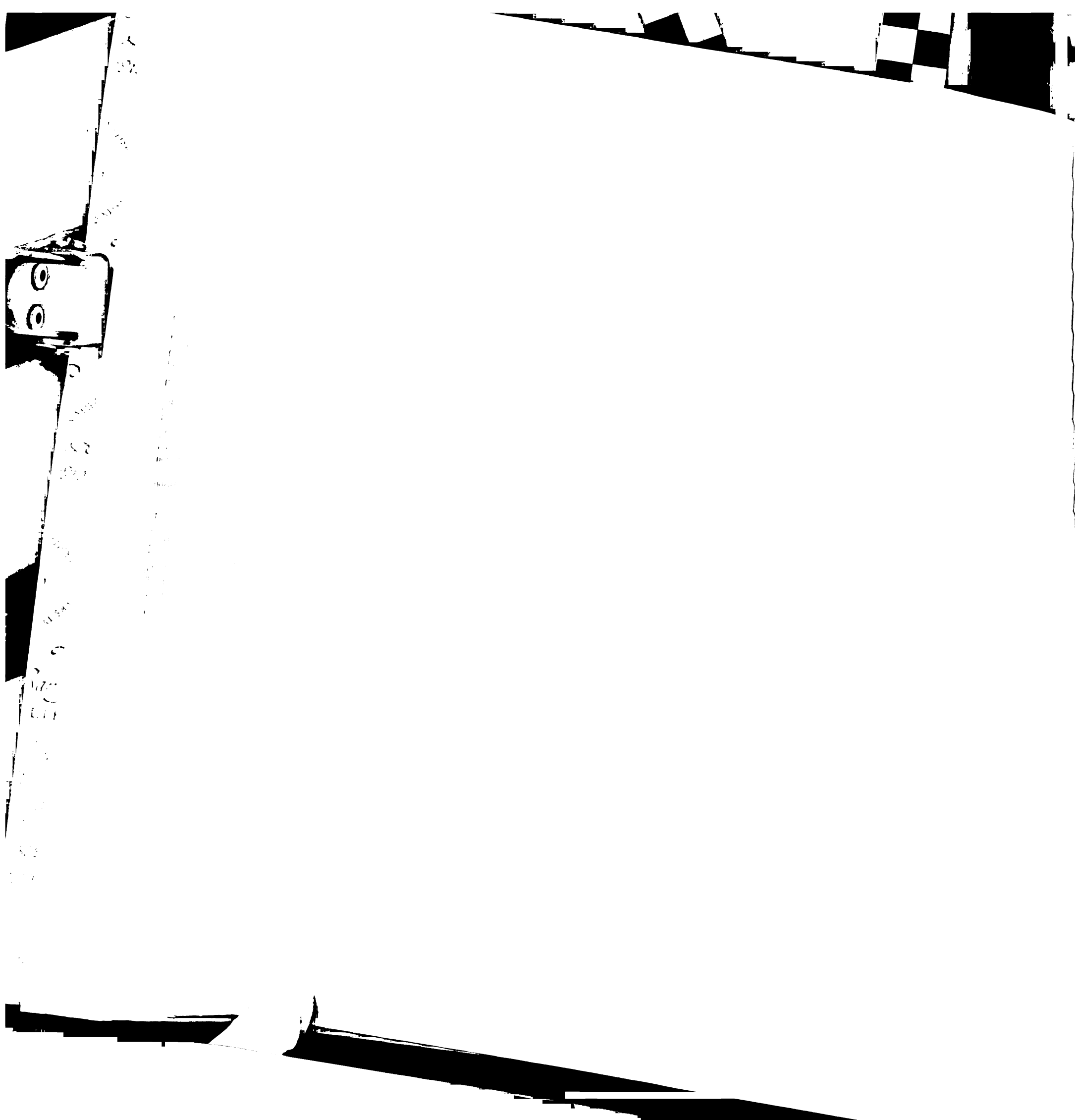


Table A3-3. Bypass of Mother/Daughter Regulation by Various HO Constructs

Strain	Switching Frequency		
	%S	%M	%D
<i>ho ura3::URA3-HO</i>	22 (4/18)	70 (37/53)	24 (11/45)
<i>ho C-A large HO HIS3</i>	<6 (0/16)	52 (41/78)	2 (1/60)

C-A = CEN-ARS

S = spore, M = mother, D = daughter

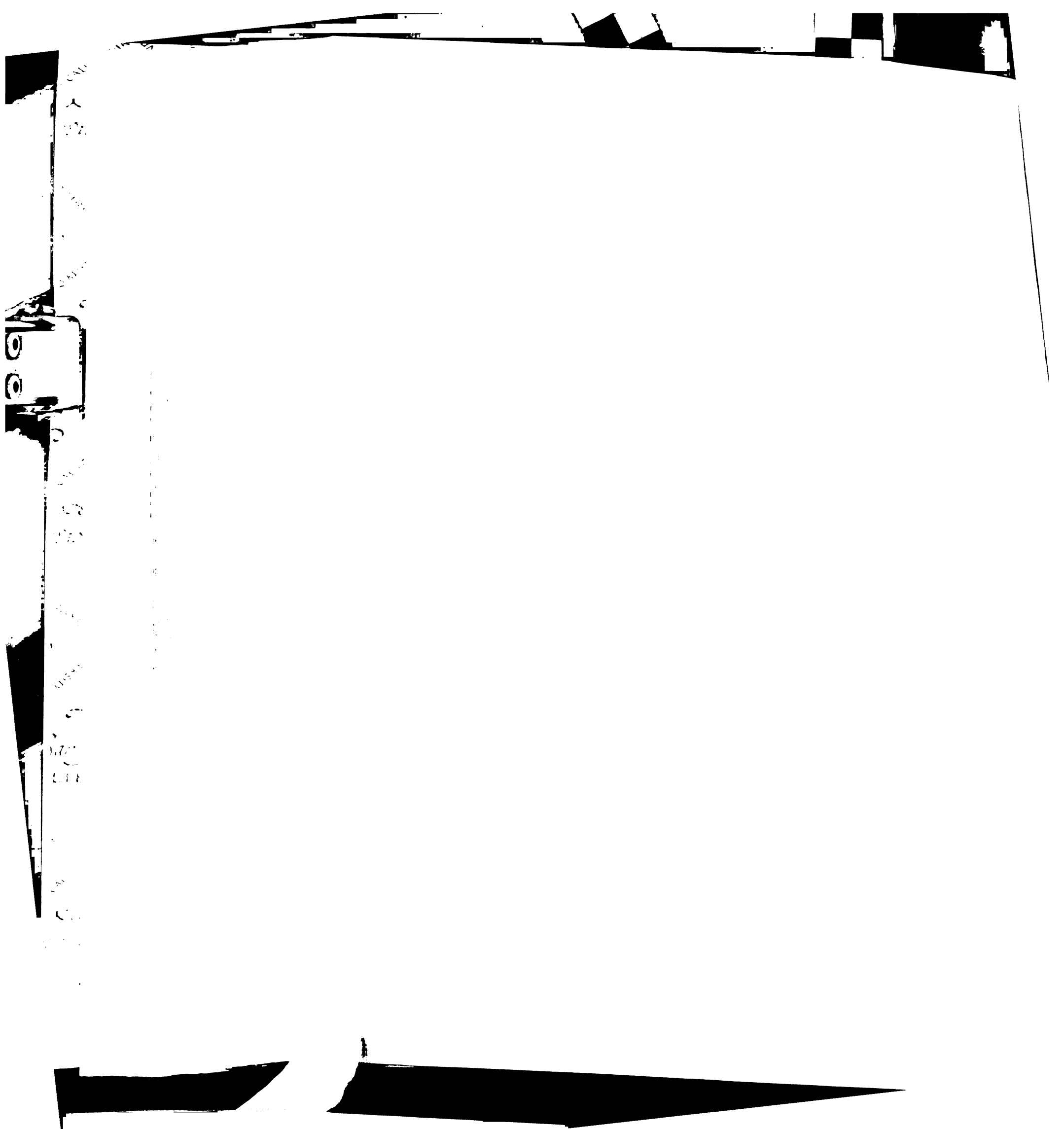


Table A3-4. Bypass of SWI5 by Minimal HO Promoter Construct Integrated at URA3

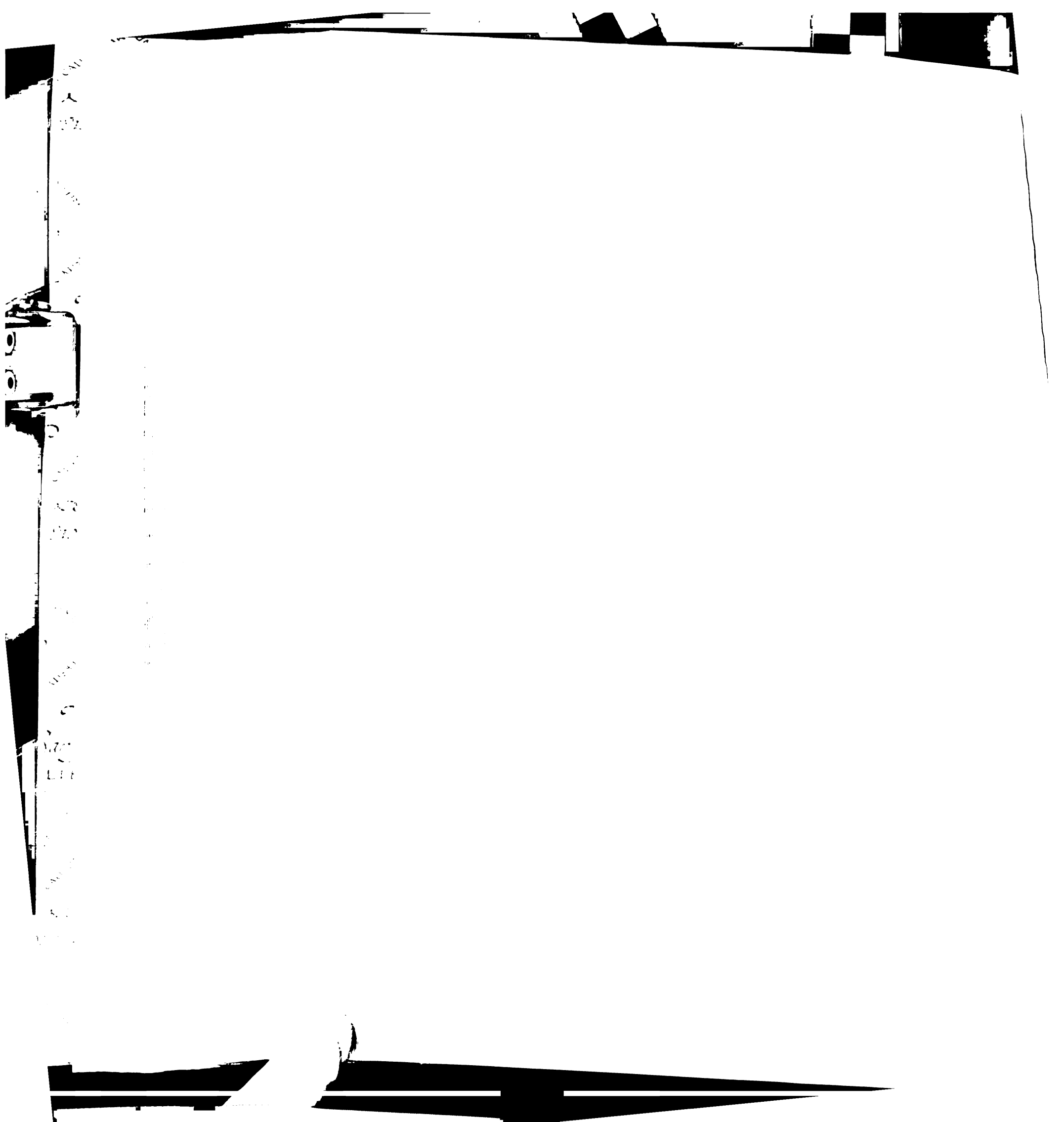
Starting Strain	total # analyzed	# a	# α	# NM	#BM
α <i>swi5</i> Δ <i>ura3::URA3</i> vector	32		32		
α <i>swi5</i> Δ <i>ura3::URA3-HO</i>	32	29		2	1

a = number of colonies that mated as a cells

α = number of colonies that mated as α cells

#NM = number of colonies that did not mate (non-maters)

#BM = number of colonies that mated as both a and α (bi-maters)



HO allele gave rise to 29 α , 2 non-maters, and 1 bi-mater. Thus bypass of *SWI5* occurs not only on a plasmid, but also on the chromosome.

A second explanation for the bypass of *SWI5* is the absence of sufficient regulatory sequences on the 1400 base pair promoter fragment. Amar Klar (1987) states that the identical *HO* fragment, when integrated at *LEU2*, allows mother cells to switch at 37%, "confirming that the mother-daughter asymmetry is indeed determined by sequences contained within the *SacI-EcoRI HO* fragment." No data are shown, however, regarding the switching frequency of spores and daughters. The *HO* promoter is known to contain two binding-sites for Swi5p, one at approximately -1300 and one approximately -1800 from the start site of translation (Tebb et al., 1993). To determine if the addition of a second Swi5p-binding site would restore mother/daughter regulation, three CEN-ARS plasmids, each with a large segment (1930 base pairs) of *HO* promoter DNA (named "large *HO*;" see Figure A3-1), were constructed. Two of the three plasmids were identical to the *HIS3* and *URA3* (pRS316) CEN-ARS vectors used before; a third plasmid was constructed in the *URA3*-marked YCp50 vector, which has a very different backbone sequence from pRS316. Pedigree analysis was performed with an *ho* strain transformed with the large *HO HIS3* plasmid (Table A3-3, line 2): 52% of mothers, 2% of daughters, and no spores were observed to switch. Although this degree of mother/daughter regulation is significantly closer to wild-type, transformation of the three CEN-ARS plasmids into a *swi5 Δ* strain revealed that they still bypassed the normal requirement for Swi5p (Table A3-5): 8 of 8 α *swi5 Δ* colonies transformed with the *HIS3* vector remained stably α , whereas 32 α *swi5 Δ* colonies transformed with the *HIS3* large *HO* construct gave rise to 11 α , 1 α , 12 non-maters, and 8 bi-maters. A

Table A3-5. Bypass of SWI5 by Minimal and Large HO Promoter Constructs

<i>MAT</i>	<i>Swi</i>	plasmid	total # analyzed	# a	# α	# NM	#BM
α	<i>swi5</i> Δ	pRS313 <i>HIS3</i> vector	8		8		
α	<i>swi5</i> Δ	pRS313 <i>HIS3</i> minimal <i>HO</i>	32			18	14
α	<i>swi5</i> Δ	pRS313 <i>HIS3</i> large <i>HO</i>	32	11	1	12	8
α	<i>swi5</i> Δ	pRS316 <i>URA3</i> large <i>HO</i>	32	1		22	9
α	<i>swi5</i> Δ	YCp50 <i>URA3</i> large <i>HO</i>	32	9		6	17
α	<i>swi4</i> Δ	pRS316 <i>URA3</i> large <i>HO</i>	32		32		
α	<i>swi4</i> Δ	YCp50 <i>URA3</i> large <i>HO</i>	32		32		

#a = number of colonies that mated as a cells

α = number of colonies that mated as α cells

#NM = number of colonies that did not mate (non-maters)

#BM = number of colonies that mated as both a and α (bi-maters)

100

100

100

100

100

100

100

100

100

100

100

100

100

100

100

100

100

100

100

100

100

100

100

100

100

100

100

100

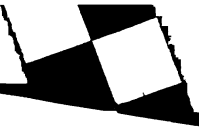
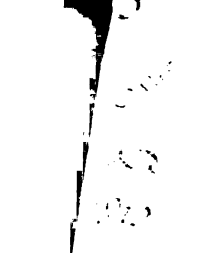
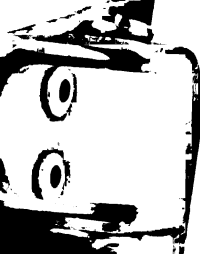
100

100

100

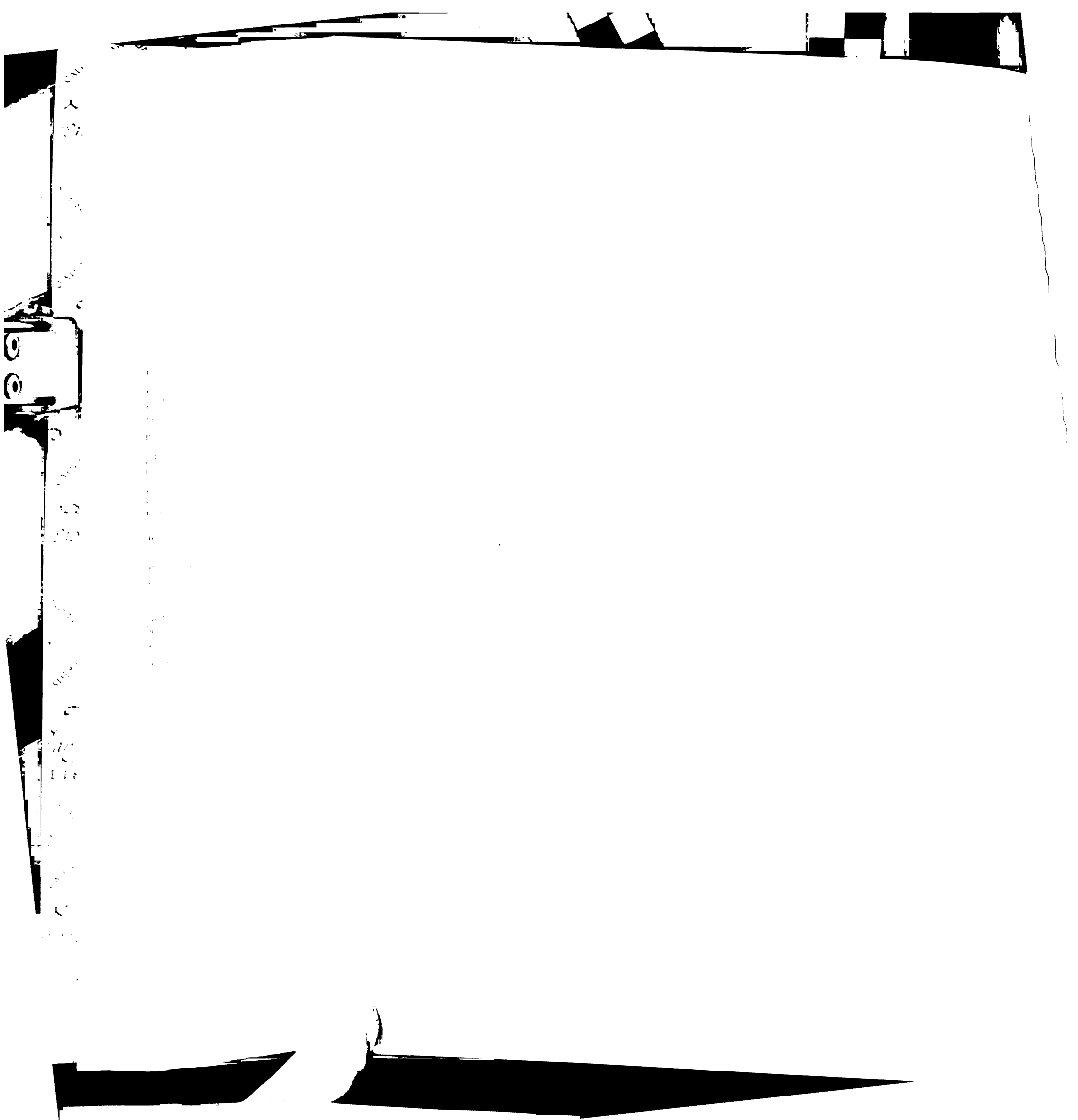
100

100



HIS3 minimal *HO* construct was assayed in parallel for comparison: 32 such transformants gave rise to 18 non-maters and 14 bi-maters. I conclude that addition of a large region of the *HO* promoter does not restore proper regulation of *HO* expression with regards to *SWI5*-dependence. It should be noted that although transcription of *HO* from this construct is *SWI5*-independent, a large degree of asymmetry is still maintained. Since we think asymmetry is normally due to the inhibition of Swi5p activity in daughter cells by Ash1p, it is difficult to understand the mechanism of asymmetry in these cells and worthy of further investigation. Large *HO* constructs in pRS316 and YCp50 also bypassed the need for *SWI5* (Table A3-5). Thus, even though the YCp50 vector has a very different plasmid backbone than pRS316, the expression of *HO* from either vector is deregulated with respect to *SWI5*. The effect of these constructs on the switching asymmetry was not determined.

These data suggest that the -1800 region may not contain sufficient mother/daughter regulatory sequences. Interestingly, there is approximately 3 kb of DNA between the gene 5' of *HO* and the *HO* ATG. This spacing is rather generous for the yeast genome, since the average yeast gene has a promoter size of approximately 300 base pairs (Dujon, 1996). This large region 5' of the *HO* gene may contain elements that insulate the *HO* promoter from inappropriate transcriptional activation due to upstream genes; such regulation is known to be important for proper stripe formation in *Drosophila* (Cal and Levine, 1995). Thus it may be possible to find specific-sequence elements in this putative insulator region that restore proper *HO* regulation when added to the constructs described in this chapter. Alternatively, the distance itself between *HO* and the next upstream



transcription unit may serve to shield the promoter from unsavory influences. In any case, the key experiment is to see if placement of the entire 3 kb region described above on a plasmid confers proper regulation of *HO*.

Materials and Methods

Genetic and Molecular Biological Methods

DNA manipulations were as described in Sambrook et al., 1989. Yeast genetic methods were as described in Rose et al., 1990.

Strains and Plasmids

Strains are described in Table A3-6, at the end of this appendix.

Plasmids *Minimal HO*: The *URA3*-marked plasmid was pAS110; the *HIS3*-marked plasmid was pAS111. pAS110 was constructed by inserting a *SacI* to *EcoRI HO* fragment from pAS106 into pRS316. pAS111 was constructed by inserting a *SacI* to *EcoRI HO* fragment from pAS106 into pRS313. *Large HO*. pAS122 was constructed by inserting a *Sall* to *EcoRI* fragment from M419 (kind gift of David Stillman, University of Utah) into YCp50. pAS123 was constructed by inserting a *Sall* to *EcoRI* fragment from M419 into pRS316. pAS124 was constructed by inserting a *Sall* to *EcoRI* fragment from M419 into pRS313.

Pedigree Analysis: *a*/ α diploids were sporulated and the resultant tetrads were dissected using conventional protocols. Each tetrad was dissected in close proximity to a wall of α cells that produced α -factor for the duration of the experiment. Mothers and daughters could be distinguished on the basis of size. A switch from α to *a* was scored as the acquired ability to respond morphologically to α -factor.

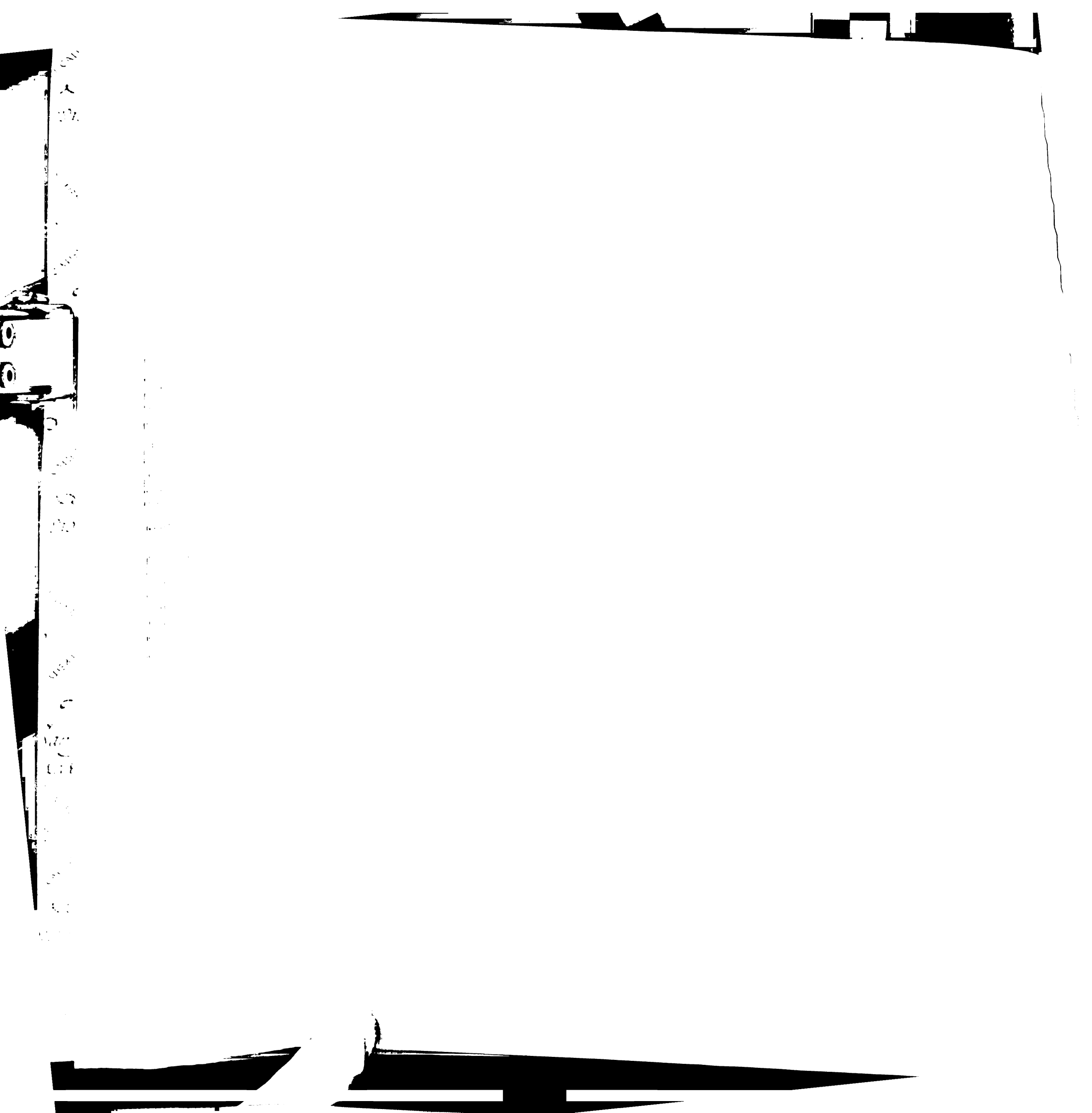
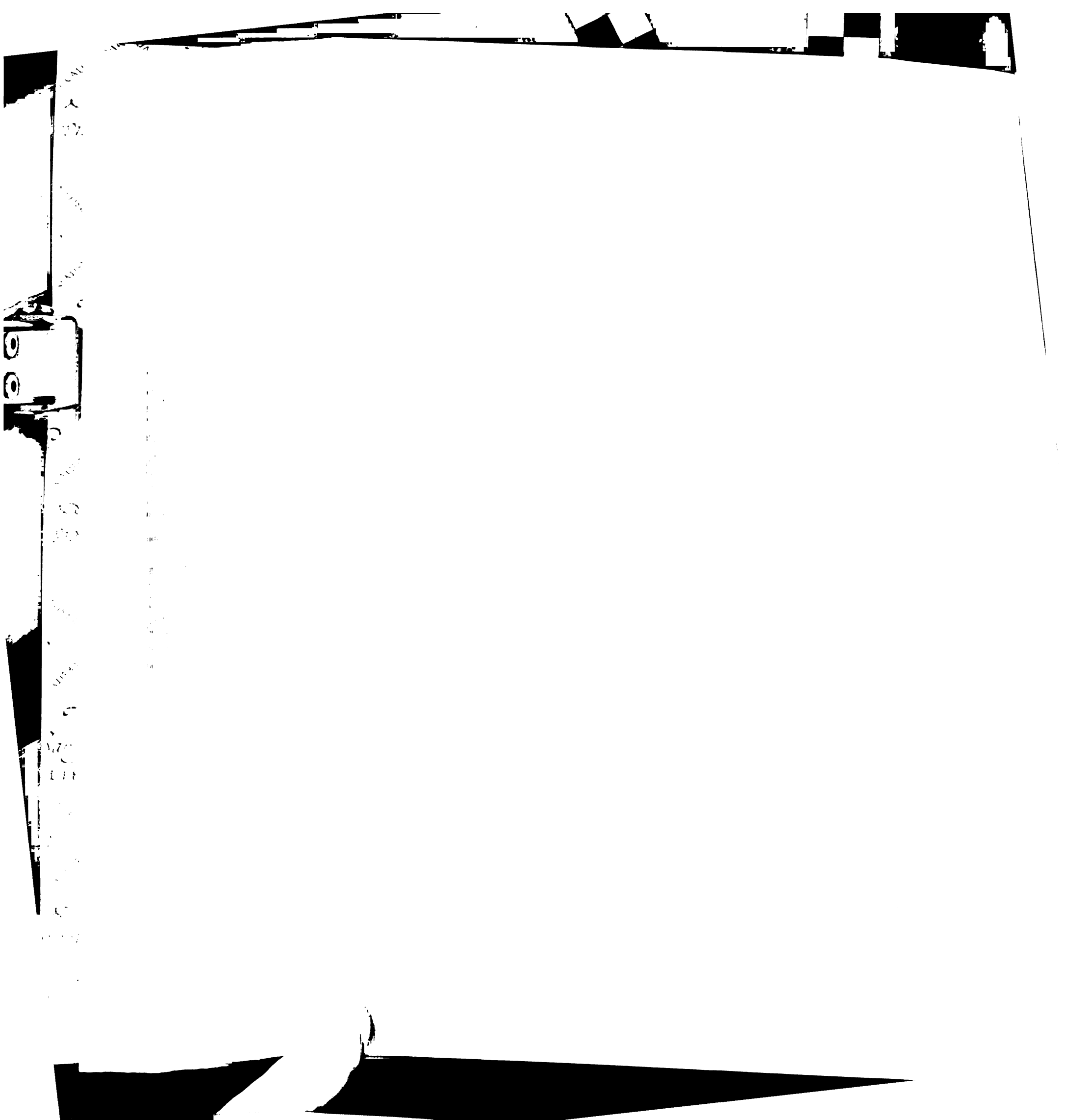


Table A3-6. Appendix Three Strain List

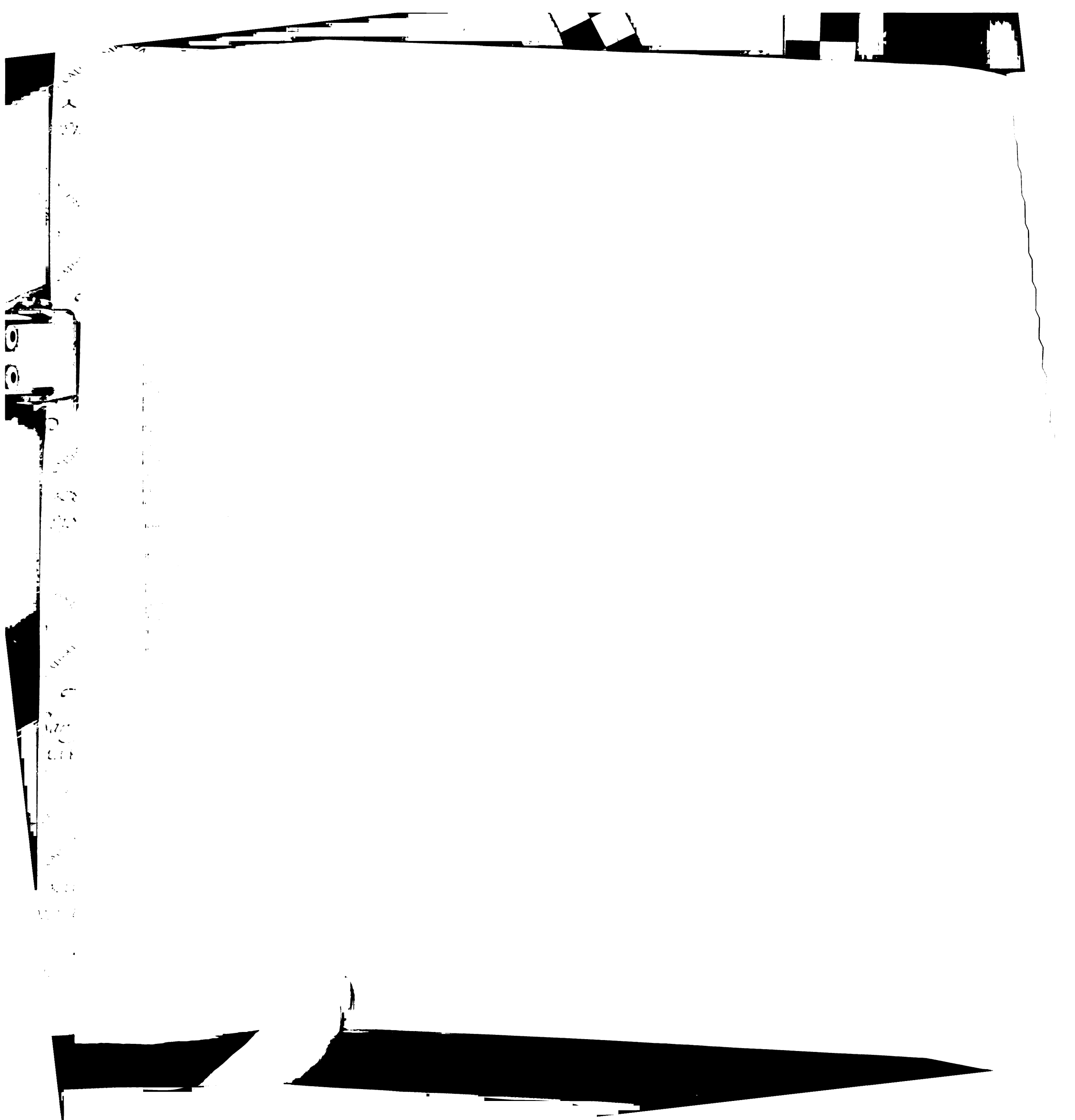
<u>Strain name</u>	<u>Relevant Genotype</u>	<u>Source</u>
YAS81	<i>a/α HO/HO</i>	This study
JO20	<i>a ho SWI+ ura3-52 his3Δ200</i>	J. Ogas
Cy297	<i>α ho swi1Δ ura3-52 his3Δ200</i>	C. Peterson
JO39-2C	<i>α ho swi4Δ ura3-52 his3Δ200</i>	J. Ogas
Cy24	<i>α ho swi5Δ ura3-52 his3Δ200</i>	C. Peterson

All strains are isogenic to the S288c background.



APPENDIX FOUR

MISCELLANEOUS PEDIGREES



This appendix describes three pedigrees whose results are shown in Table A4-1. (1) Deletion of *BUD1* does not affect *HO* regulation. *S. cerevisiae* budding pattern is thought to be guided by a landmark that directs the bud emergence machinery to a specific site in the cell. Such a landmark could also serve as a means of localizing Ash1p appropriately to the presumptive daughter cell. *bud1Δ* cells are thought to choose a bud site at random either because they do not position a landmark appropriately or because they are defective in recognition of the spatial landmark that normally recruits the bud-site selection machinery. I tested whether *bud1Δ HO* cells maintain mother/daughter regulation (Table A4-1). *bud1Δ HO* mothers switched at a frequency of 45% whereas *bud1Δ HO* daughters were not observed to switch. Therefore, disruption of *BUD1* does not allow mating-type switching in daughter cells. However, since *bud1Δ* cells may be deficient in interfacing between the landmark and the bud-site selection machinery rather than in establishing the landmark itself, one might not expect Ash1p localization to be affected. Whether the decrease in switching frequency observed in *bud1Δ* mother cells (45%) compared to wild-type mother cells (70%) is significant is unknown.

(2) Deletion of *CLN3* does not affect *HO* regulation. *HO* is normally expressed in late G1 mother cells. To determine if perturbing the normal kinetics of transit through G1 would affect the pattern of *HO* expression, I constructed a strain lacking *CLN3*, one of the G1 cyclins, and analyzed its switching pattern (Table A4-1). It was essentially indistinguishable from wild-type: 62% of *cln3Δ* mothers and no *cln3Δ* daughters were observed to switch.

(3) High copy number expression of an *HO* promoter fragment does not affect the switching pattern. I hypothesized that a negative regulator

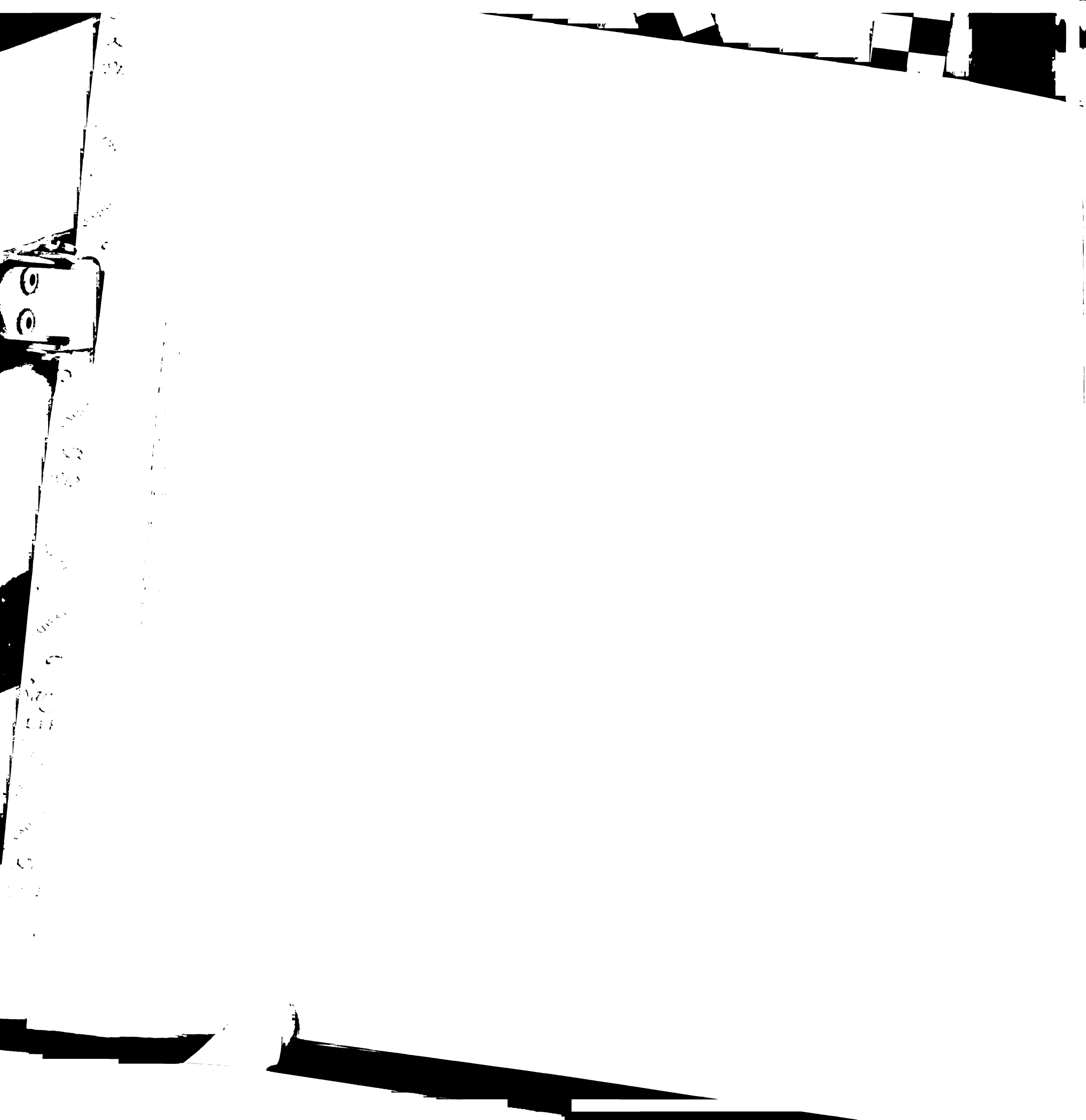
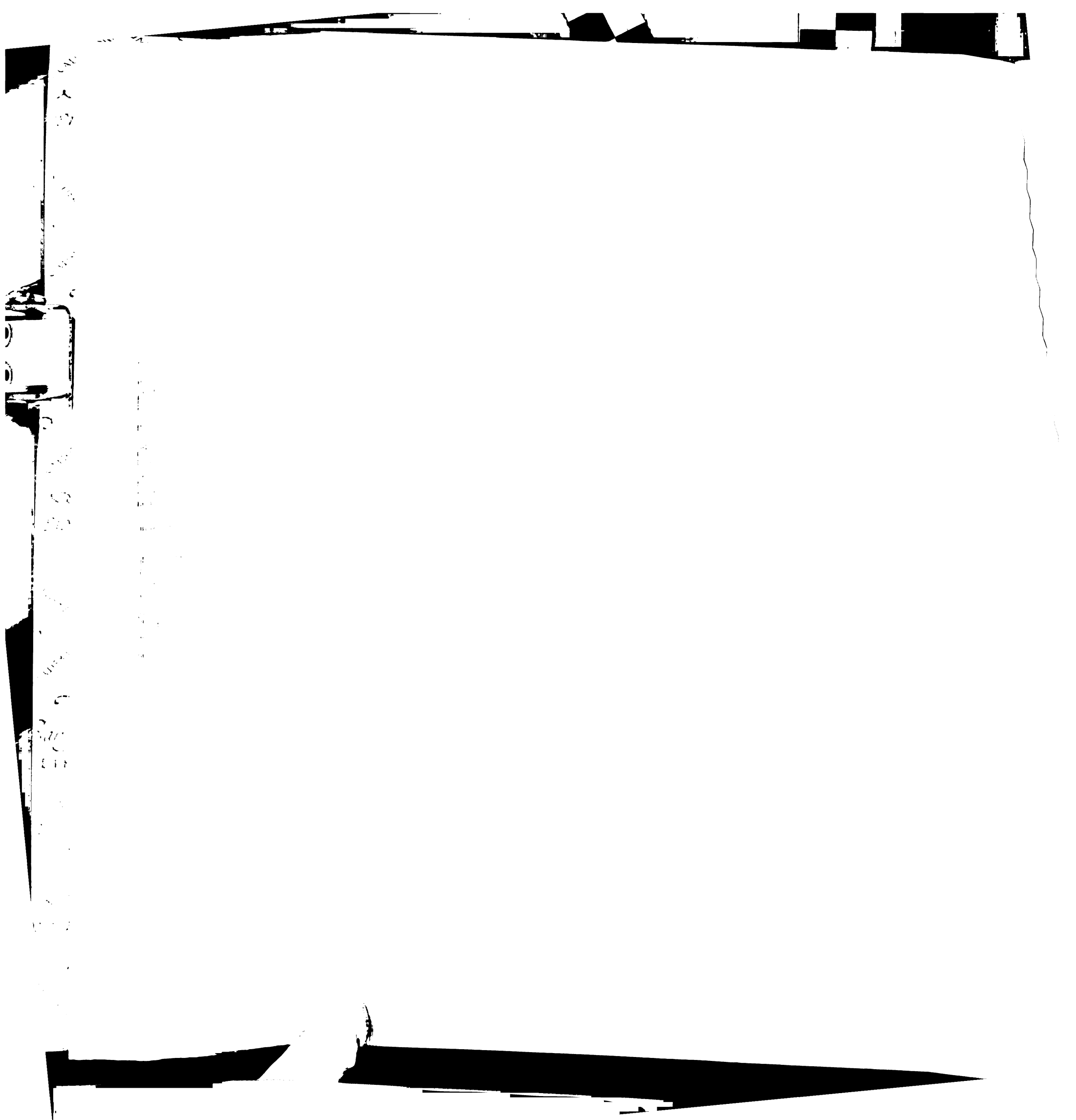


Table A4-1. Switching Frequency of Various *HO* Strains

Strain	Switching Frequency	
	%M	%D
<i>HO</i>	70 (70/98)	<1 (0/88)
<i>HO bud1Δ</i>	45 (24/53)	<3 (0/37)
<i>HO cln3Δ</i>	62 (51/82)	<1 (0/70)
<i>HO 2μ URS1</i>	72 (54/75)	<1 (0/81)

M = mother, D = daughter



(such as Ash1p) might bind the upstream region of the *HO* promoter in daughter cells. If so, it might be possible to titrate out such a negative regulator by providing multiple copies of the target site. I constructed a high copy plasmid carrying a 400 base pair fragment of the URS1 region of the *HO* promoter. An *HO* strain was transformed with this plasmid and the resultant switching pattern was determined (Table A4-1). The plasmid did not perturb the wild-type switching pattern: 72% of mothers and no daughter cells switched. Whether a larger region of the *HO* promoter would affect the switching pattern is unknown.

Materials and Methods

Genetic and Molecular Biological Methods

DNA manipulations were as described in Sambrook et al., 1989. Yeast genetic methods were as described in Rose et al., 1990.

Strains and Plasmids

Strains are described in Table A4-2, at the end of this appendix.

Plasmids 2μ *URS1* (pAS113) consists of the SphI to BamHI fragment of the *HO* promoter in pRS426.

Pedigree Analysis: *a*/ α diploids were sporulated and the resultant tetrads were dissected using conventional protocols. Each tetrad was dissected in close proximity to a wall of α cells that produced α -factor for the duration of the experiment. Mothers and daughters could be distinguished on the basis of size. A switch from α to *a* was scored as the acquired ability to respond morphologically to α -factor.

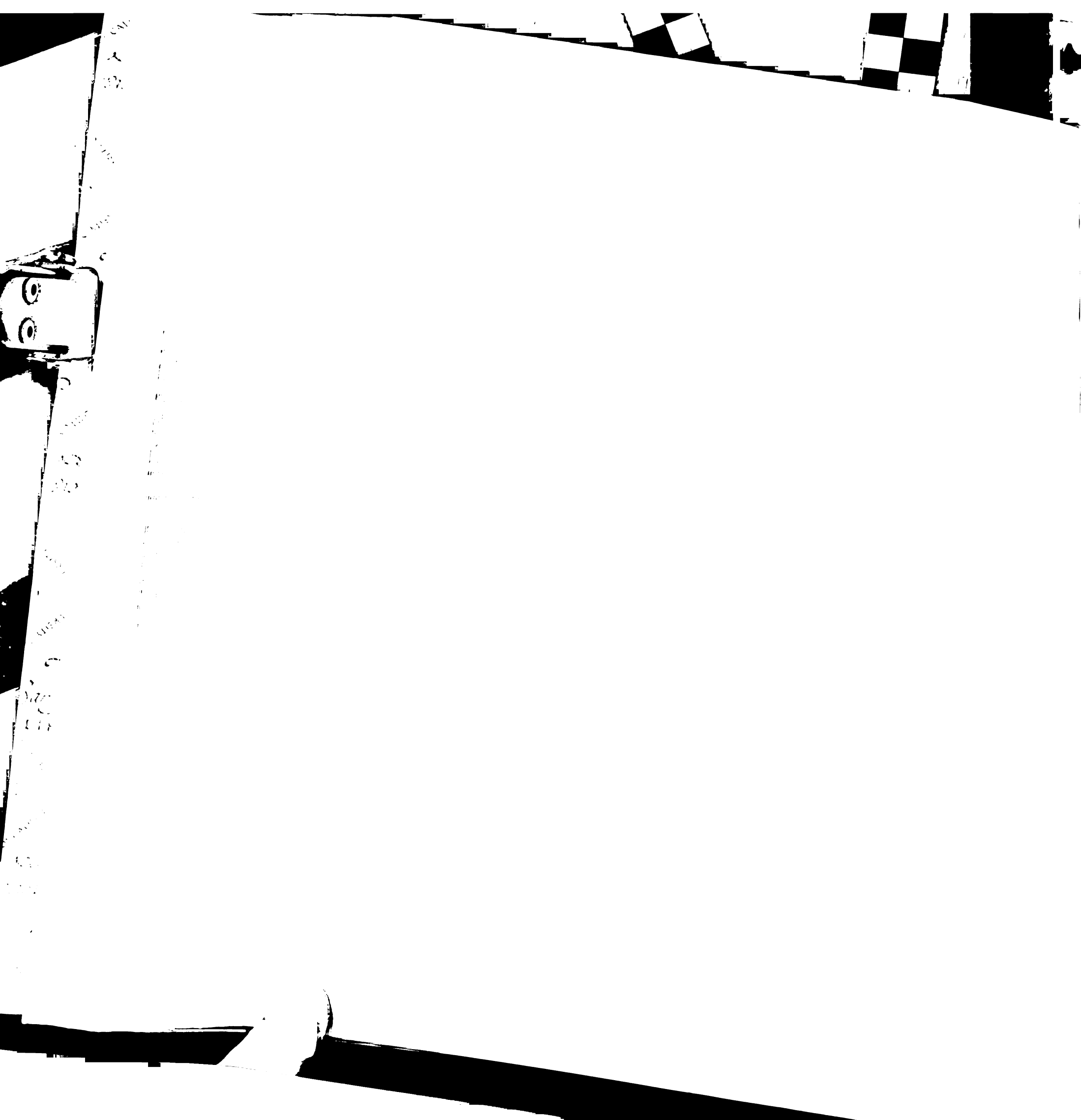
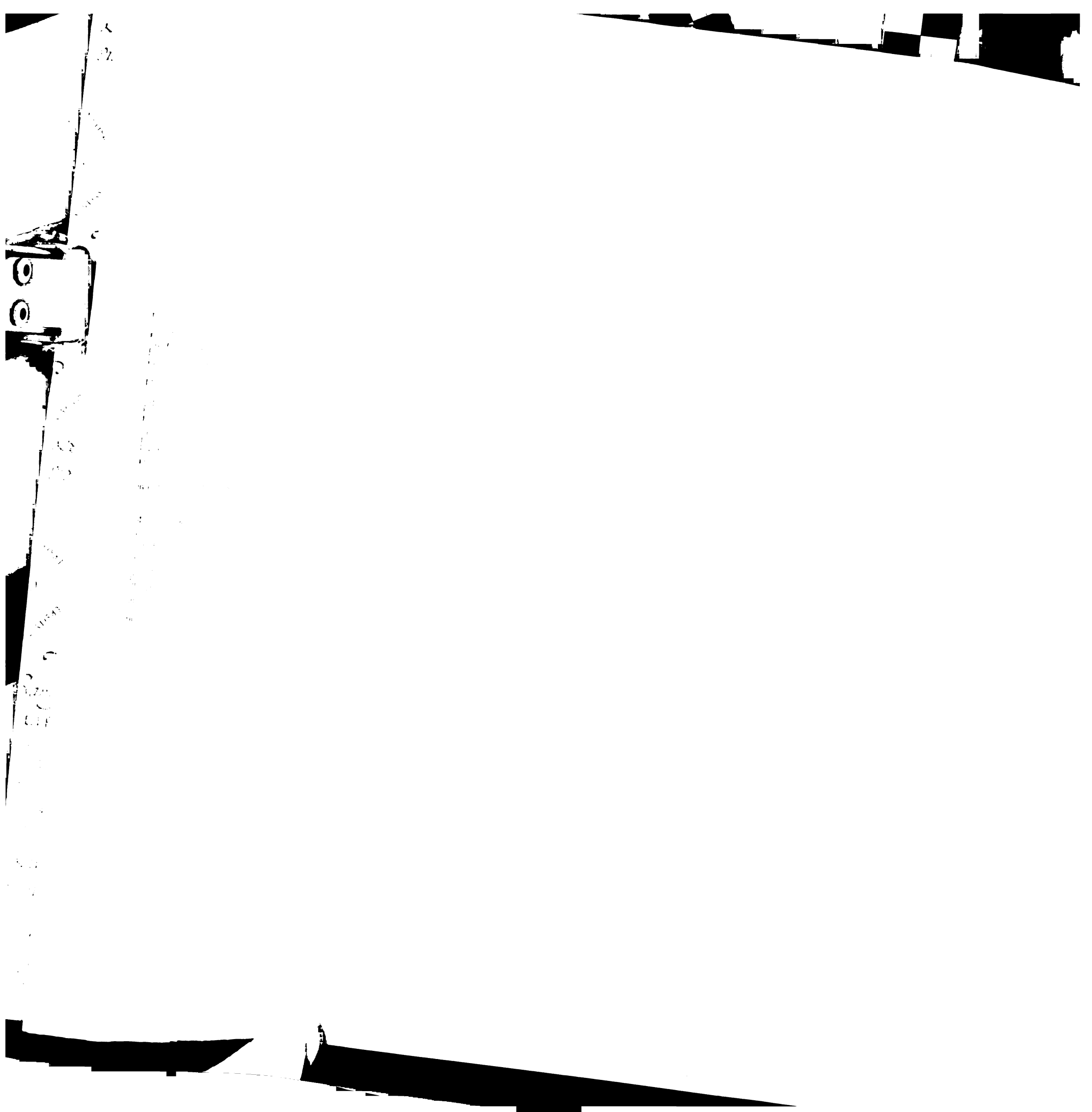
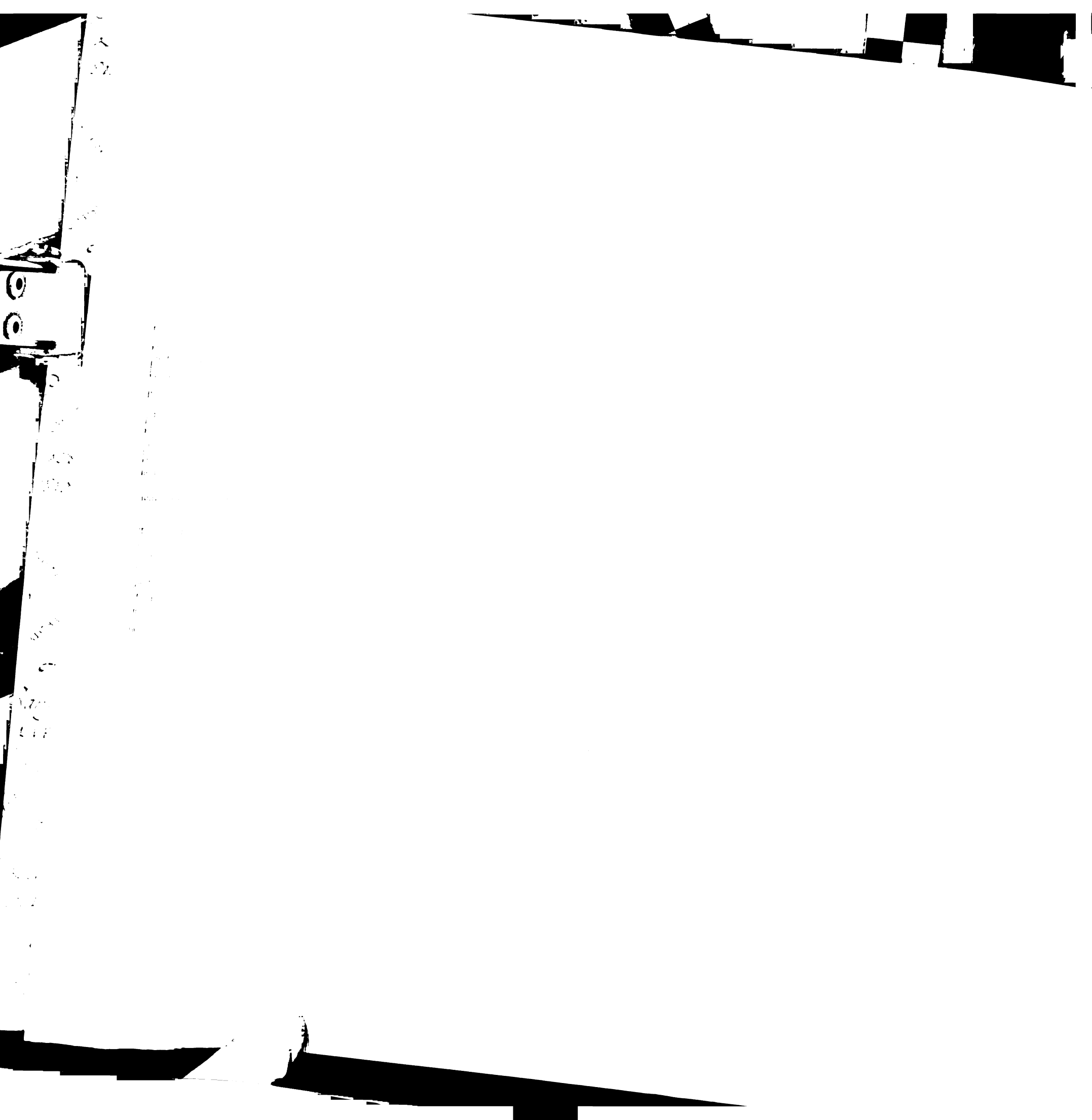


Table A4-2. Appendix Four Strain List

<u>Strain name</u>	<u>Relevant Genotype</u>	<u>Source</u>
YAS81	<i>a/α HO/HO</i>	This study
YAS43-1B	<i>a/α HO/HO bud1Δ/bud1Δ</i>	"
YAS44-2D	<i>a/α HO/HO cln3Δ/cln3Δ</i>	"



REFERENCES



Adler, H.I., Fisher, W.D., Cohen, A., and Hardigree, A.H. (1967). Miniature *Escherichia coli* cells deficient in DNA. *Proc. Nat. Acad. Sci.* 57, 321-326.

Alper, S., Duncan, L., and Losick, R. (1994). An adenosine nucleotide switch controlling the activity of a cell type-specific transcription factor in *B. subtilis*. *Cell* 77, 195-205.

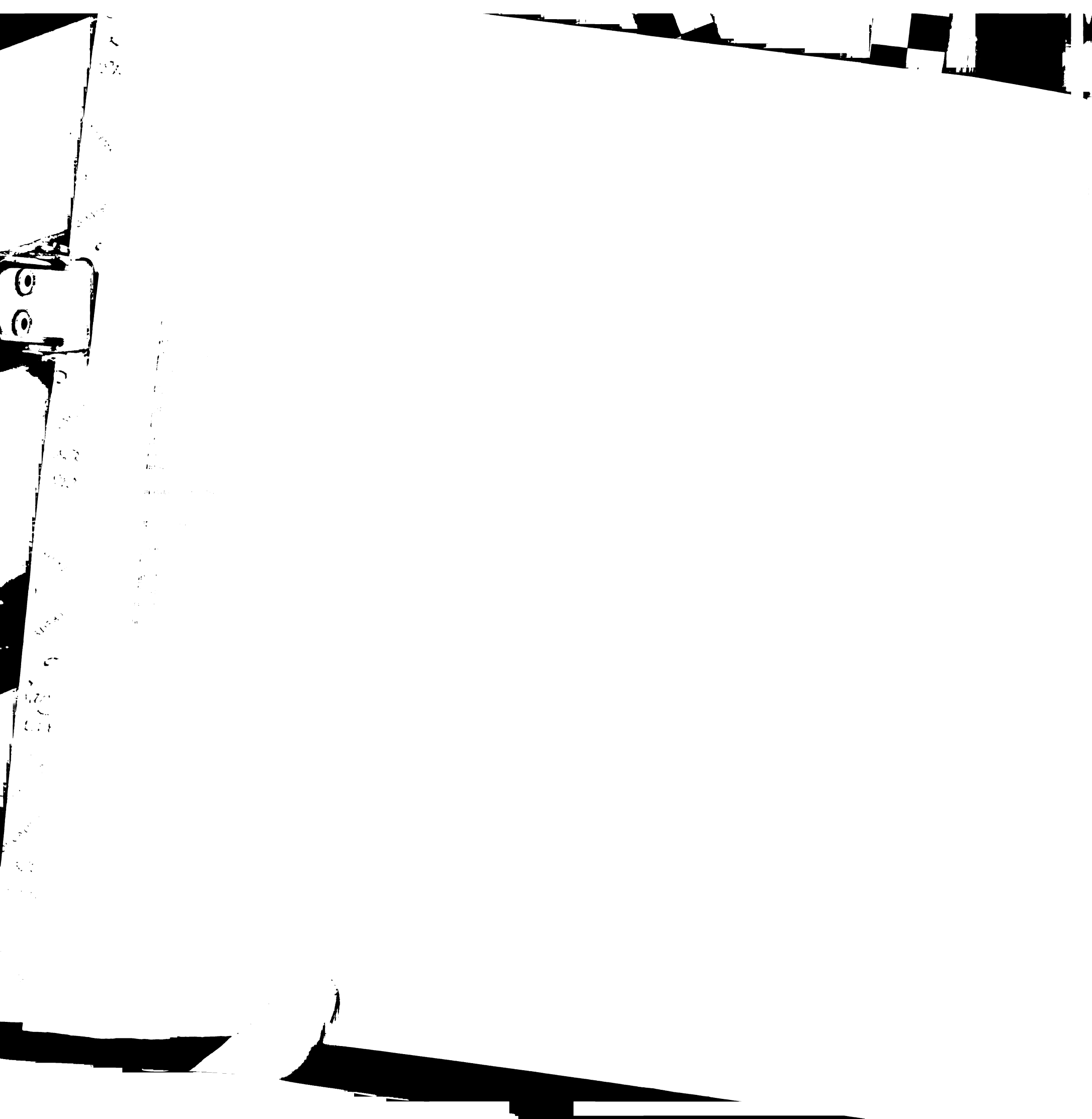
Andrews, B.J., and Herskowitz, I. (1989a). Identification of a DNA binding factor involved in cell-cycle control of the yeast *HO* gene. *Cell* 57, 21-29.

Andrews, B.J. and Herskowitz, I. (1989b). The yeast SW14 protein contains a motif present in developmental regulators and is part of a complex involved in cell-cycle-dependent transcription. *Nature* 342, 830-833.

Arigoni, F., Pogliano, K., Webb, C.D., Stragier, P., Losick, R. (1995). Localization of protein implicated in establishment of cell type to sites of asymmetric division. *Science* 270, 637-640.

Bobola, N., Jansen, R-P., Shin, T-H., and Nasmyth, K. (1996). Asymmetric accumulation of Ash1 in post-anaphase nuclei depends on a myosin and restricts yeast mating-type switching to mother cells. *Cell* 84, 699-709.

Boyd, L., Guo, S., Levitan, D., Stinchcomb, D.T., and Kemphues, K.J. PAR-2 is asymmetrically distributed and promotes association of P granules and PAR-1 with the cortex in *C. elegans* embryos. *Development*, in press.



Breeden, L. and Mikesell, G.E. (1991). Cell cycle-specific expression of the SWI4 transcription factor is required for the cell cycle regulation of HO transcription. *Genes Dev.* 5(7):1183-90.

Breeden, L., and Nasmyth, K. (1987). Cell cycle control of the yeast *HO* gene: *cis*- and *trans*-acting regulators. *Cell* 48, 389-397.

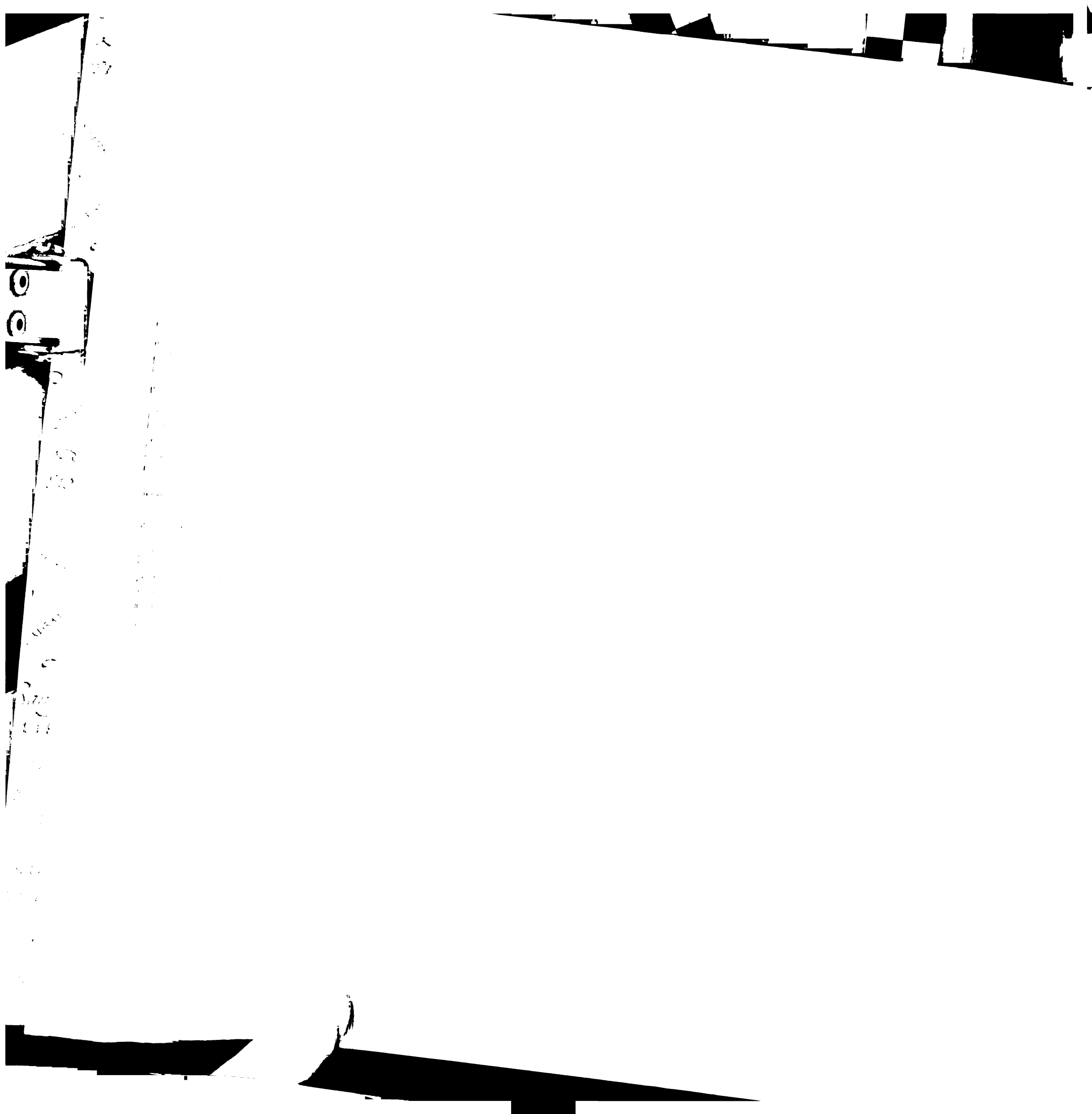
Cal H and Levine M. (1995). Modulation of enhancer-promoter interactions by insulators in the *Drosophila* embryo. *Nature* 376(6540), 533-536.

Chant, J., and Herskowitz, I. (1991). Genetic control of bud site selection in yeast by a set of gene products that constitute a morphogenetic pathway. *Cell* 65, 1203-1212.

Chant, J., and Pringle, J.R. (1995). Patterns of bud-site selection in the yeast *Saccharomyces cerevisiae*. *J. Cell Biol.* 129, 751-765.

Cheng, N.N., Kirby, C.M., and Kemphues, K.J. (1995). Control of cleavage spindle orientation in *Caenorhabditis elegans*: The role of the genes *par-2* and *par-3*. *Genetics* 139, 549-559.

Cross, F.R. (1990). Cell cycle arrest caused by *CLN* gene deficiency in *Saccharomyces cerevisiae* resembles START-I arrest and is independent of the mating pheromone signalling pathway. *Mol. Cell. Biol.* 10, 6482-6490.



Cross, F.R., and Tinkelenberg, A.H. (1991). A potential positive feedback loop controlling *CLN1* and *CLN2* gene expression at the start of the yeast cell cycle. *Cell* 65, 875-883.

Cunningham, T.S., and Cooper, T.G. (1991). Expression of the *DAL80* gene, whose product is homologous to the GATA factors and is a negative regulator of multiple nitrogen catabolic genes in *Saccharomyces cerevisiae*, is sensitive to nitrogen catabolite repression. *Mol. Cell. Biol.* 11, 6205-6215.

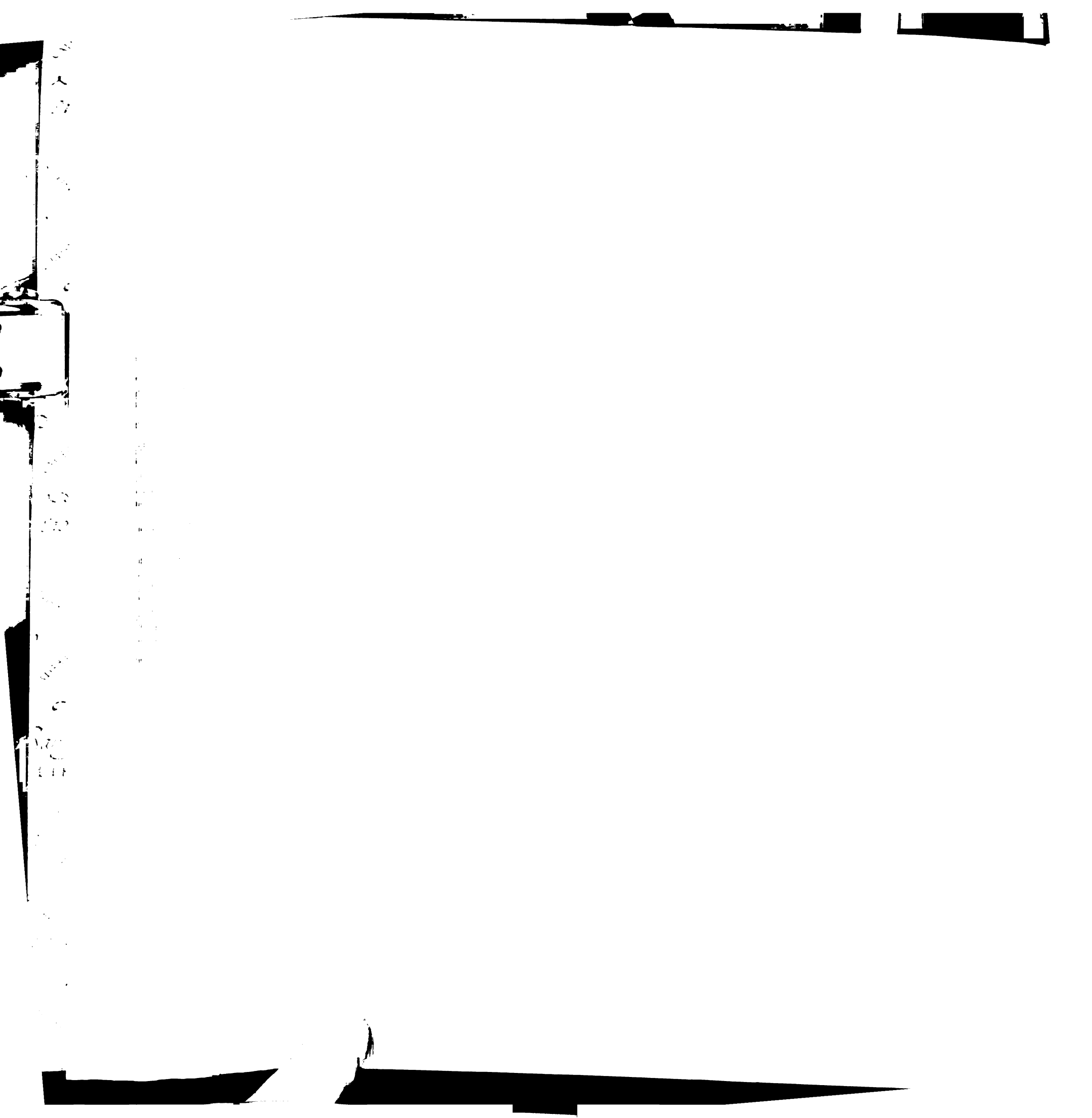
de Boer, P.A.J., Crossley, R.E., and Rothfield, L.I. (1989). A division inhibitor and a topological specificity factor coded for by the minicell locus determine proper placement of the division septum. *Cell* 56, 641-649.

de Boer, P.A.J., Crossley, R.E., and Rothfield, L.I. (1992). Roles of MinC and MinD in the site-specific septation block mediated by the MinCDE system of *Escherichia coli*. *J. Bact.* 174, 63-70.

Deshaies, R.J. (1995a). Make it or break it: the role of ubiquitin-dependent proteolysis in cellular regulation. *Trends in Cell Biology* 5(11), 428-434.

Deshaies, R.J. (1995b). The self-destructive personality of a cell cycle in transition. *Current Opin. Cell Biol.* 7, 781-789.

Diederich, B., Wilkinson, J.F., Magnin, T., Najafi, M., Errington, J., Yudkin, M.D. (1994). Role of interactions between SpoIIAA and SpoIIAB in regulating



cell-specific transcription factor sigma F of *Bacillus subtilis*. *Genes Dev* 8, 2653-2663.

Dujon, B. (1996). The yeast genome project: what did we learn? *Trends in Genetics* 12(7), 263-270.

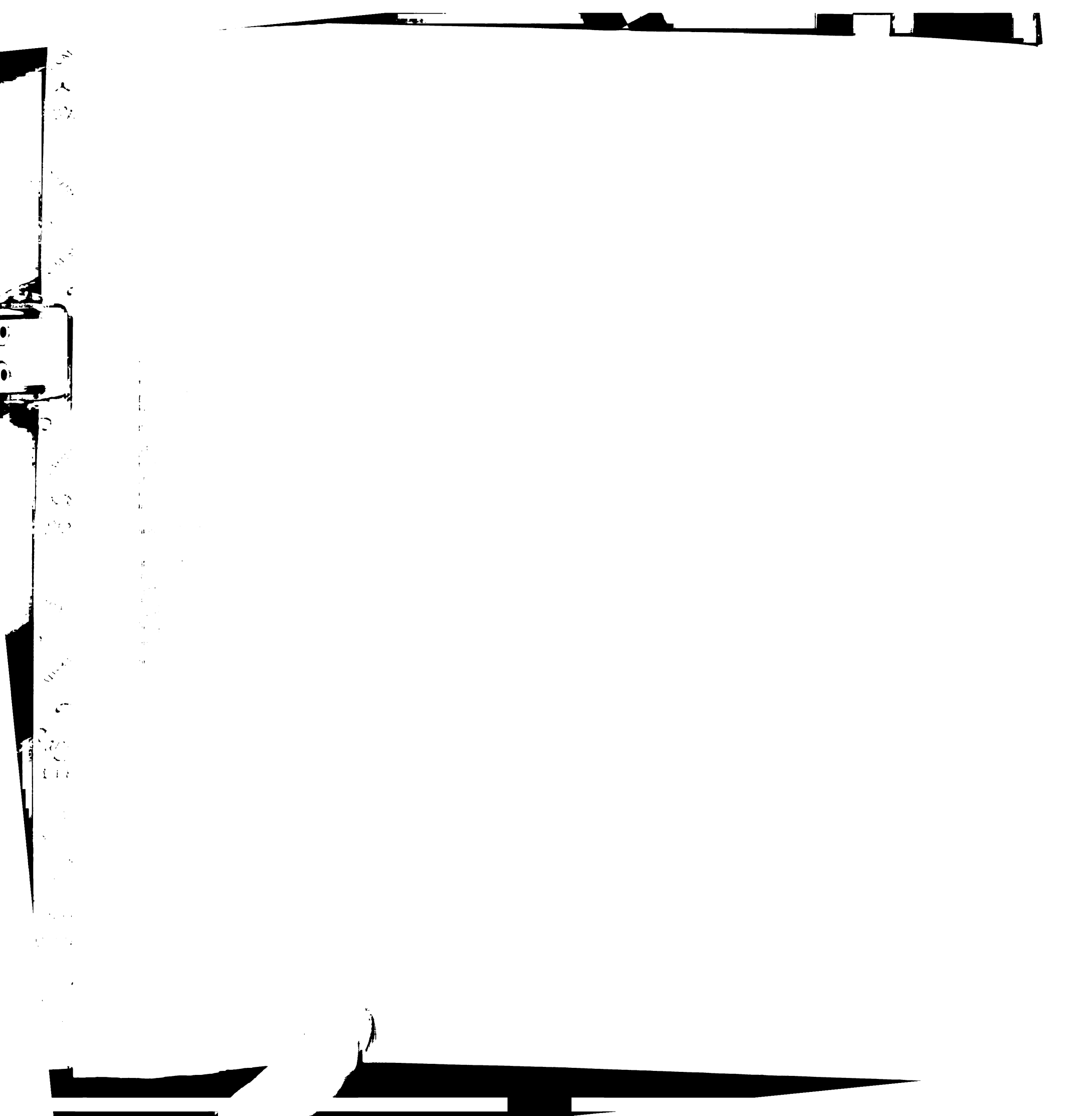
Duncan, L., Alper, S., and Losick, R. (1994). Establishment of cell-type specific gene transcription during sporulation in *Bacillus subtilis*. *Current Opinion in Genetics and Development* 4(5), 630-636.

Duncan, L., Alper, S., Arigoni, F., Losick, R., Stragier, P. (1995). Activation of cell-specific transcription by a serine phosphatase at the site of asymmetric division. *Science* 270, 641-644.

Dujon, B., Alexandraki, D., Andre, B., Ansorge, W., Baladron, V., Ballesta, J. P., Banrevi, A., Bolle, P.A., Bolotin-Fukuhara, M., Bossier, P., et al. (1994). Complete DNA sequence of yeast chromosome XI. *Nature* 369, 371-378.

Etemad-Moghadam, B., Guo, S., Kempfues, K.J. (1995). Asymmetrically distributed PAR-3 protein contributes to cell polarity and spindle alignment in early *C. elegans* embryos. *Cell* 83, 743-752.

Freifelder, D. (1960). Bud formation in *Saccharomyces cerevisiae*. *J. Bact.* 80, 567-568.



Fujita, A., Oka, C., Arikawa, Y., Katagai, T., Tonouchi, A., Kuhara, S., and Misumi, Y. (1994). A yeast gene necessary for bud-site selection encodes a protein similar to insulin-degrading enzymes. *Nature*, 372(6506), 567-570.

Gehring, S. and Snyder, M. (1990). The *SPA2* gene of *Saccharomyces cerevisiae* is important for pheromone-induced morphogenesis and efficient mating. *J. Cell Biol.* 111, 1451-1464.

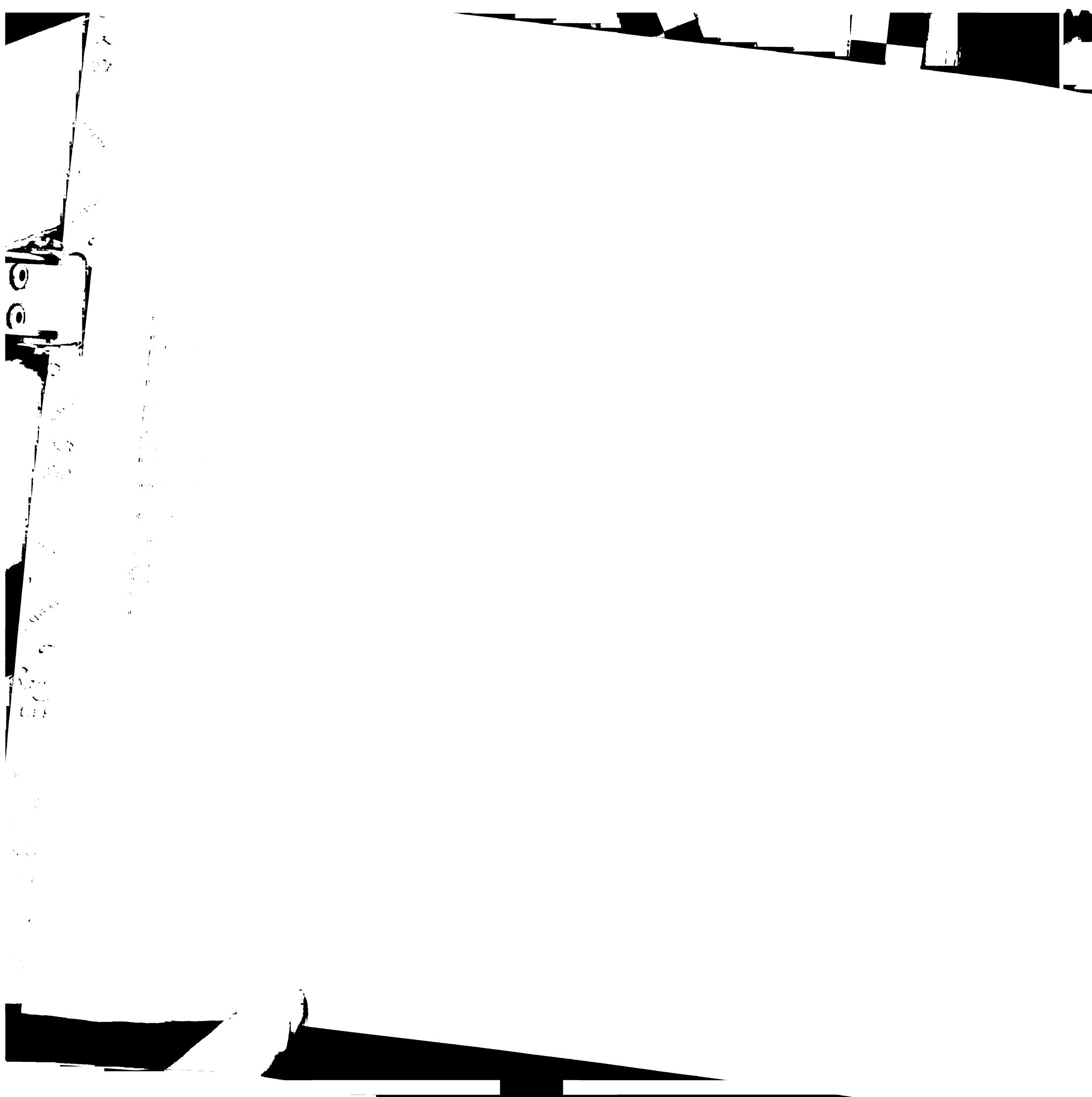
Gimeno, C.J., Ljungdahl, P.O., Styles, C.A., and Fink, G.R. (1992). Unipolar cell divisions in the yeast *S. cerevisiae* lead to filamentous growth: regulation by starvation and *RAS*. *Cell* 68, 1077-1090.

Gober, J.W., Champer, R., Reuter, S., and Shapiro, L. (1991). Expression of positional information during cell differentiation in *Caulobacter*. *Cell* 64, 381-391.

Gober, J.W. and Marques, M.V. (1995). Regulation of cellular differentiation in *Caulobacter crescentus*. *Microbiological Reviews* 59(1), 31-47.

Guo, M., Bier, E., Jan, L.Y., and Jan, Y.N. (1995). *tramtrack* acts downstream of *numb* to specify distinct daughter cell fates during asymmetric cell divisions in the *Drosophila* PNS. *Neuron* 14, 913-925.

Haber, J.E. and Garvik, B. (1977). A new gene affecting the efficiency of mating-type interconversions in homothallic strains of *Saccharomyces cerevisiae*. *Genetics* 87, 33.



Hadwiger, J.A., and Reed, S.I. (1990). Nucleotide sequence of the *Saccharomyces cerevisiae* CLN1 and CLN2 genes. *Nucleic Acids Res.* 18, 4025.

Hadwiger, J.A., Wittenberg, C., Richardson, H.E., de Barros Lopes, M., and Reed, S.I. (1989). A family of cyclin homologs that control the G1 phase in yeast. *Proc. Natl. Acad. Sci. USA* 86, 6255-6259.

Hagen, D.C., McCaffrey, G., and Sprague, G.F., Jr. (1986). Evidence the yeast STE3 gene encodes a receptor for the peptide pheromone α -factor: gene sequence and implications for the structure of the presumed receptor. *Proc. Natl. Acad. Sci. USA* 83, 1418-1422.

Halme, A., Michelitch, M., Mitchell, E.L., Chant, J. (1996). Bud10p directs axial cell polarization in budding yeast and resembles a transmembrane receptor. *Current Biology* 6(5), 570-579.

Herskowitz, I. (1988). Life cycle of the budding yeast *Saccharomyces cerevisiae*. *Microbiol. Rev.* 52, 536-553.

Herskowitz, I. (1989). A regulatory hierarchy for cell specialization in yeast. *Nature* 342(6251) 749-757.

Herskowitz, I., Andrews, B., Kruger, W., Ogas, J., Sil, A., Coburn, C., Peterson, C. (1992). Integration of multiple regulatory inputs in the control of *HO* expression in yeast. In *Transcriptional Regulation*, S. L. McKnight and K. R.



Yamamoto, eds. (Cold Spring Harbor, New York: Cold Spring Harbor Laboratory Press), pp. 949-974.

Herskowitz, I., and Oshima, Y. (1981) In *Molecular Biology of The Yeast Saccharomyces* (eds Strathern, J.N., Jones, E.W., and Broach, J.) (Cold Spring Harbor Laboratory, New York).

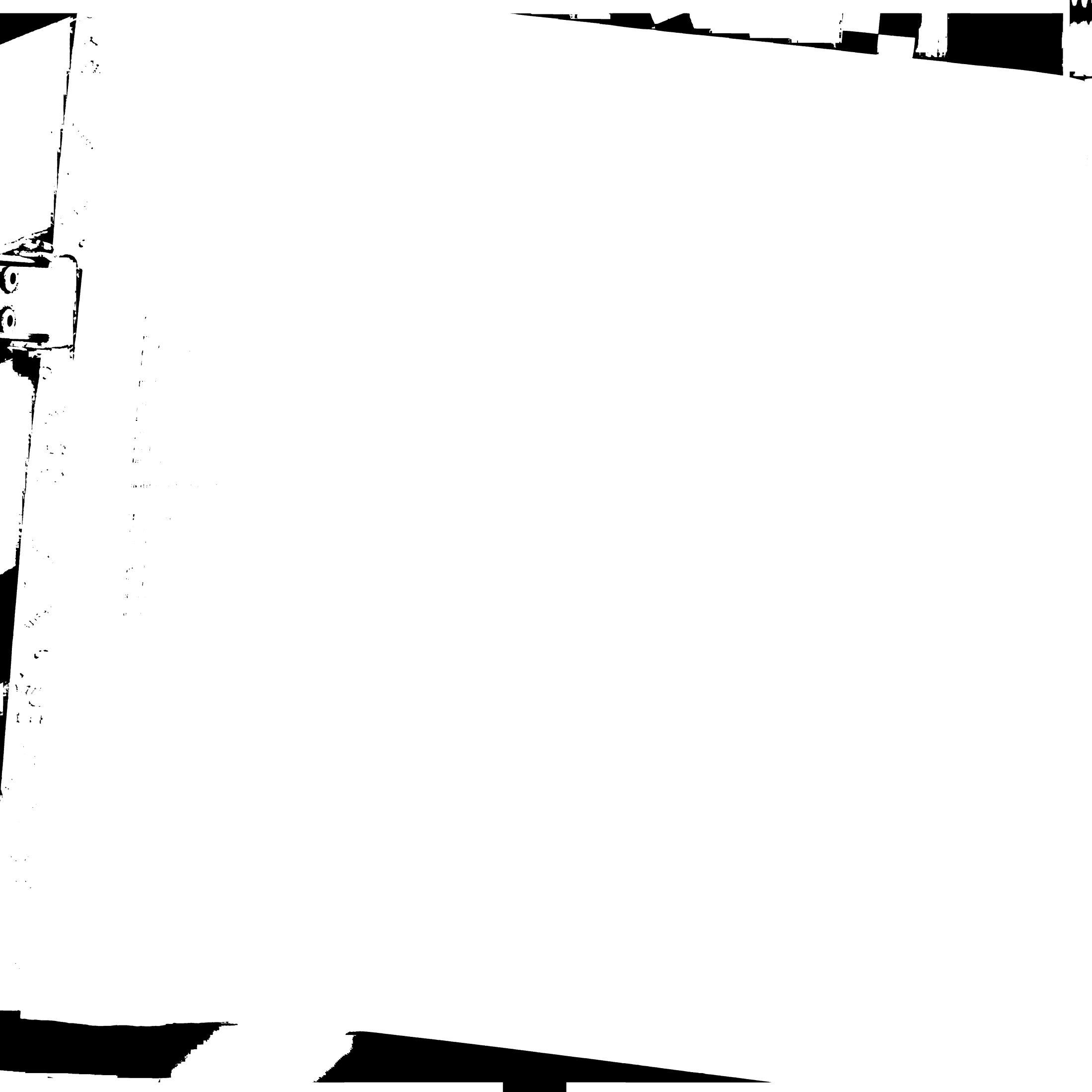
Hicks, J. B., and Herskowitz, I. (1976). Interconversion of yeast mating type. I. Direct observation of the action of the homothallism (*HO*) gene. *Genetics* 83, 245-258.

Hicks, J.B., Strathern, J.N., Herskowitz, I. (1977). Interconversion of yeast mating types. III. Action of the homothallism (*HO*) gene in cells homozygous for the mating type locus. *Genetics* 85, 395-405.

Horvitz, H. R., and Herskowitz, I. (1992). Mechanisms of asymmetric cell division: two Bs or not two Bs, that is the question. *Cell* 68, 237-255.

Hyman, A.A. (1989). Centrosome movement in the early divisions of *Caenorhabditis elegans*: a cortical site determining centrosome position. *J. Cell Biol.* 109, 1185-1194.

Hyman, A.A. and White, J.G. (1987). Determination of cell division axes in the early embryogenesis of *Caenorhabditis elegans*. *J. Cell Biol.* 105, 2123-2135.



Jansen, R.-P., Dowzer, C., Michaelis, C., Galova, M., and Nasmyth, K. (1996). Mother cell-specific *HO* expression in budding yeast depends on the unconventional myosin Myo4p and other cytoplasmic proteins. *Cell* 84, 687-697.

Jenal, U. and Stephens, C. (1996). Bacterial differentiation: Sizing up sporulation. *Current Biology* 6(2), 111-114.

Jenal, U., Stephens, C., and Shapiro, L. (1995). Regulation of asymmetry and polarity during the *Caulobacter* cell cycle. *Advances in Enzymology and Related Areas of Molecular Biology* 71, 1-39.

Jensen, R.E. and Herskowitz, I. (1984). Directionality and regulation of cassette substitution in yeast. *Cold Spring Harbor Symposia on Quantitative Biology* 49, 97-104.

Jensen, R., Sprague, G.F., Jr., and Herskowitz, I. (1983). Regulation of yeast mating-type interconversion: feedback control of *HO* gene expression by the mating-type locus. *Proc. Natl. Acad. Sci. USA* 80, 3035-3039.

Kemphues, K.J. (1989). *Caenorhabditis*. In *Frontiers in Molecular Biology: Genes and Embryos*, D.M. Glover and E.D. Hames, eds. (London: IRL Press).

Kemphues, K.J., Priess, J.R., Morton, D.G., and Cheng, N. (1988). Identification of genes required for cytoplasmic localization in early *C. elegans* embryos. *Cell* 52, 311-320.

Klar, A.J.S. (1987). The mother-daughter mating type switching asymmetry of budding yeast is not conferred by the segregation of parental *HO* gene DNA strands. *Genes Dev.* 1, 1059-1064,

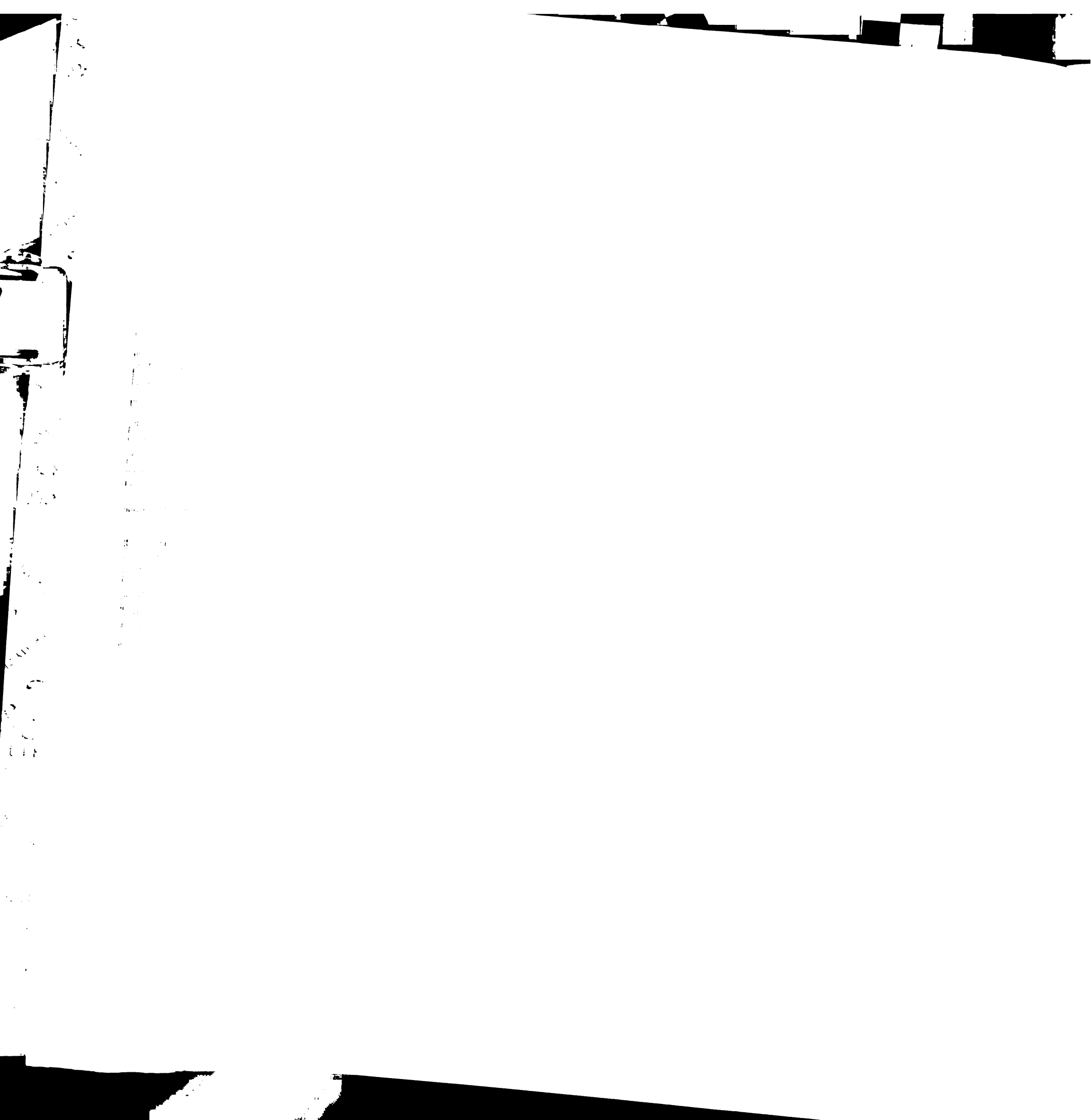
Knoblich, J.A., Jan, L.Y., and Jan, Y.N. (1995). Asymmetric segregation of Numb and Prospero during cell division. *Nature* 377, 624-627.

Kolodziej, P.A., and Young, R.A. (1991). Epitope tagging and protein surveillance. In *Methods in Enzymology: Guide to Yeast Genetics and Molecular Biology*, C. Guthrie and G. R. Fink, eds. (San Diego: Academic Press, Inc.), pp. 508-519.

Kraut, R., Chia, W., Jan, L.Y., Jan, Y.N., and Knoblich, J.A. Function of *inscutable* in orientation of asymmetric cell divisions in *Drosophila*. *Nature*, in press.

Kron, S.J., Styles, C.A., and Fink, G.R. (1994). Symmetric cell division in pseudohyphae of the yeast *Saccharomyces cerevisiae*. *Molecular Biology of the Cell* 5, 1003-1022.

Kruger, W.D. (1991). Analysis of the *SIN1* and *SIN2* gene products and their role in transcriptional regulation in *Saccharomyces cerevisiae*: University of California, San Francisco.



Kuchler, K., Sterne, R.E., and Thorner, J. (1989). *Saccharomyces cerevisiae* STE6 gene product: a novel pathway for protein export in eukaryotic cells. EMBO J. 8(13), 3978-3984.

Labie, C., Bouche, F., and Bouche, J.-P. (1990). Minicell-forming mutants of *Escherichia coli*: Suppression of both DicB- and MinD-dependent division inhibition by inactivation of the *minC* gene product. J. Bact. 172, 5852-5855.

Levin, P.A., and Losick, R. (1996). Transcription factor Spo0A switches the localization of the cell division protein FtsZ from a medial to a bipolar pattern in *Bacillus subtilis*. Genes Dev. 10, 478-488.

Long, R.M., Elliott, D.J., Stutz, F., Rosbash, M., Singer, R.H. (1995). Spatial consequences of defective processing of specific yeast mRNAs revealed by fluorescent in situ hybridization. RNA 1, 1071-1078.

Losick, R. and Stragier, P. (1992). Crisscross regulation of cell-type-specific gene expression during development in *B. subtilis*. Nature 355(6361), 601-604.

Lydall, D., Ammerer, G., and Nasmyth, K. (1991). A new role for MCM1 in yeast: cell cycle regulation of *SWI5* transcription. Genes Dev. 5, 2405-2419.

Marczynski, G.T., and Shapiro, L. (1995). The control of asymmetric gene expression during *Caulobacter* cell differentiation. Archives of Microbiology 163(5), 313-321.



Min, K.T., Hilditch, C.M, Diederich, B., Errington, J., Yudkin, M.D. (1993). Sigma F, the first compartment-specific transcription factor of *B. subtilis*, is regulated by an anti-sigma factor that is also a protein kinase. *Cell* 74, 735-742.

Morton, D.G., Roos, J.M., and Kemphues, K.J. (1992). *par-4*, a gene required for cytoplasmic localization and determination of specific cell types in *Caenorhabditis elegans* embryogenesis. *Genetics* 130, 771-790.

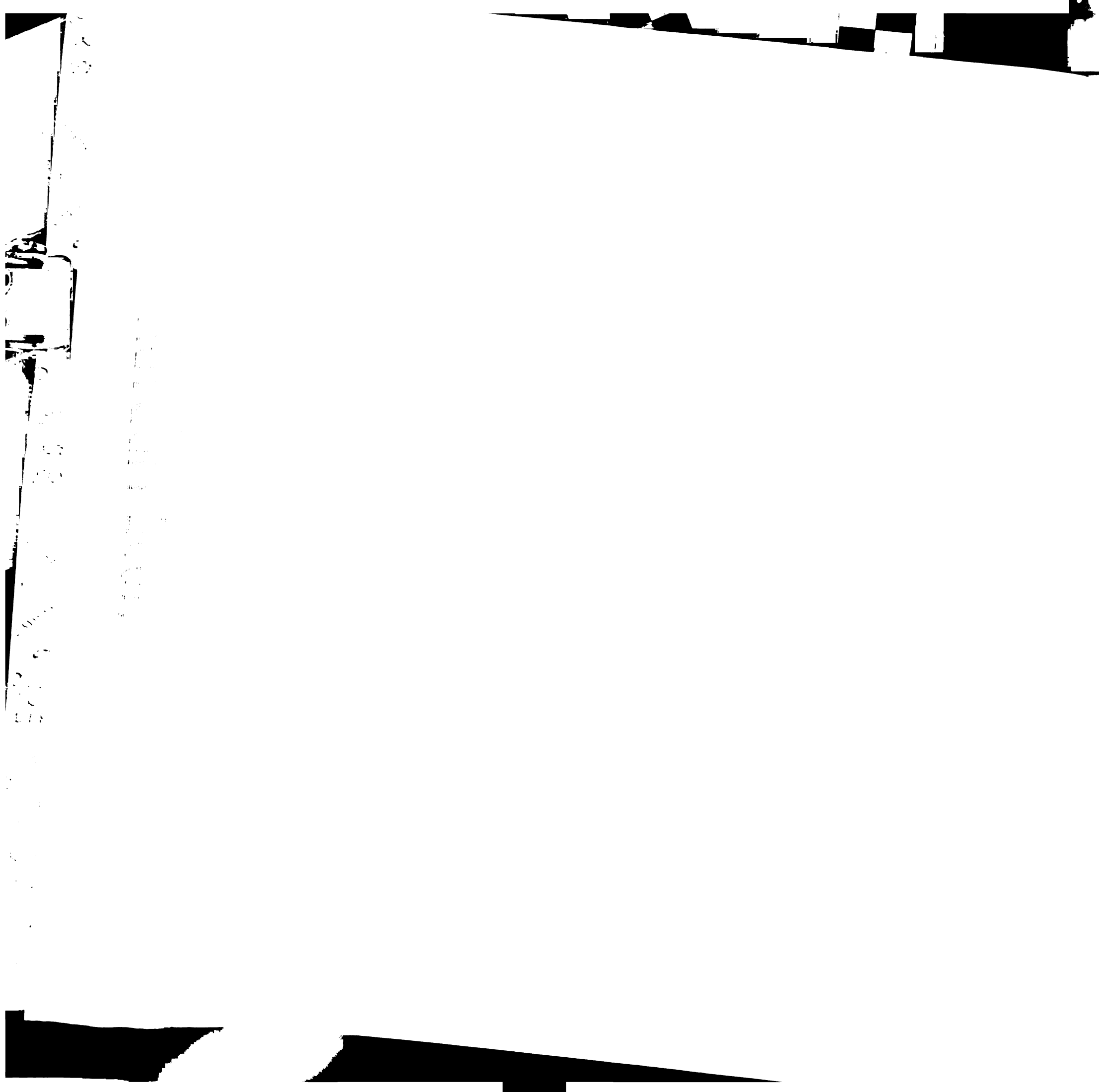
Murray, A.W., and Szostak, J.W. (1983). Pedigree analysis of plasmid segregation in yeast. *Cell* 34, 961-970.

Nakayama, N., Miyajima, A., and Arai, K. (1985). Nucleotide sequences of *STE2* and *STE3*, cell type-specific sterile genes from *Saccharomyces cerevisiae*. *EMBO J.* 4, 2643-2648.

Nasmyth, K. (1983). Molecular analysis of a cell lineage. *Nature* 302, 670-676.

Nasmyth, K. (1985a) At least 1400 base pairs of 5'-flanking DNA is required for the correct expression of the *HO* gene in yeast. *Cell* 42, 213-223

Nasmyth, K. (1985b). A repetitive DNA sequence that confers cell-cycle START (*CDC28*)-dependent transcription of the *HO* gene in yeast. *Cell* 42, 225-235.



Nasmyth, K. (1987). The determination of mother cell-specific mating type switching in yeast by a specific regulator of *HO* transcription. *EMBO J.* 6, 243-248.

Nasmyth, K. (1993). Regulating the *HO* endonuclease in yeast. *Curr. Opin. Genet. Dev.* 3, 286-294.

Nasmyth, K., and Shore, D. (1987). Transcriptional regulation of the yeast life cycle. *Science* 237, 1162-1170.

Nasmyth, K., Adolf, G., Lydall, D., and Seddon, A. (1990). The identification of a second cell cycle control on the *HO* promoter in yeast: cell cycle regulation of *SWI5* nuclear entry. *Cell* 62, 631-647.

Nasmyth, K., Seddon, A., and Ammerer, G. (1987a). Cell cycle regulation of *SWI5* is required for mother-cell-specific *HO* transcription in yeast. *Cell* 49, 549-558.

Nasmyth, K., Stillman, D., and Kipling, D. (1987b). Both positive and negative regulators of *HO* transcription are required for mother-cell-specific mating-type switching in yeast. *Cell* 48, 579-587.

Ogas, J., Andrews, B.J., and Herskowitz, I. (1991). Transcriptional activation of *CLN1*, *CLN2*, and a putative new G1 cyclin (*HCS26*) by *SWI4*, a positive regulator of G1-specific transcription. *Cell* 66, 1015-1026.



Orkin, S.H. (1992). GATA-binding transcription factors in hematopoietic cells. *Blood* 80, 575-581.

Priess, J.R. (1994). Establishment of initial asymmetry in early *Caenorhabditis elegans* embryos. *Current Opinion in Genetics and Development* 4, 563-568.

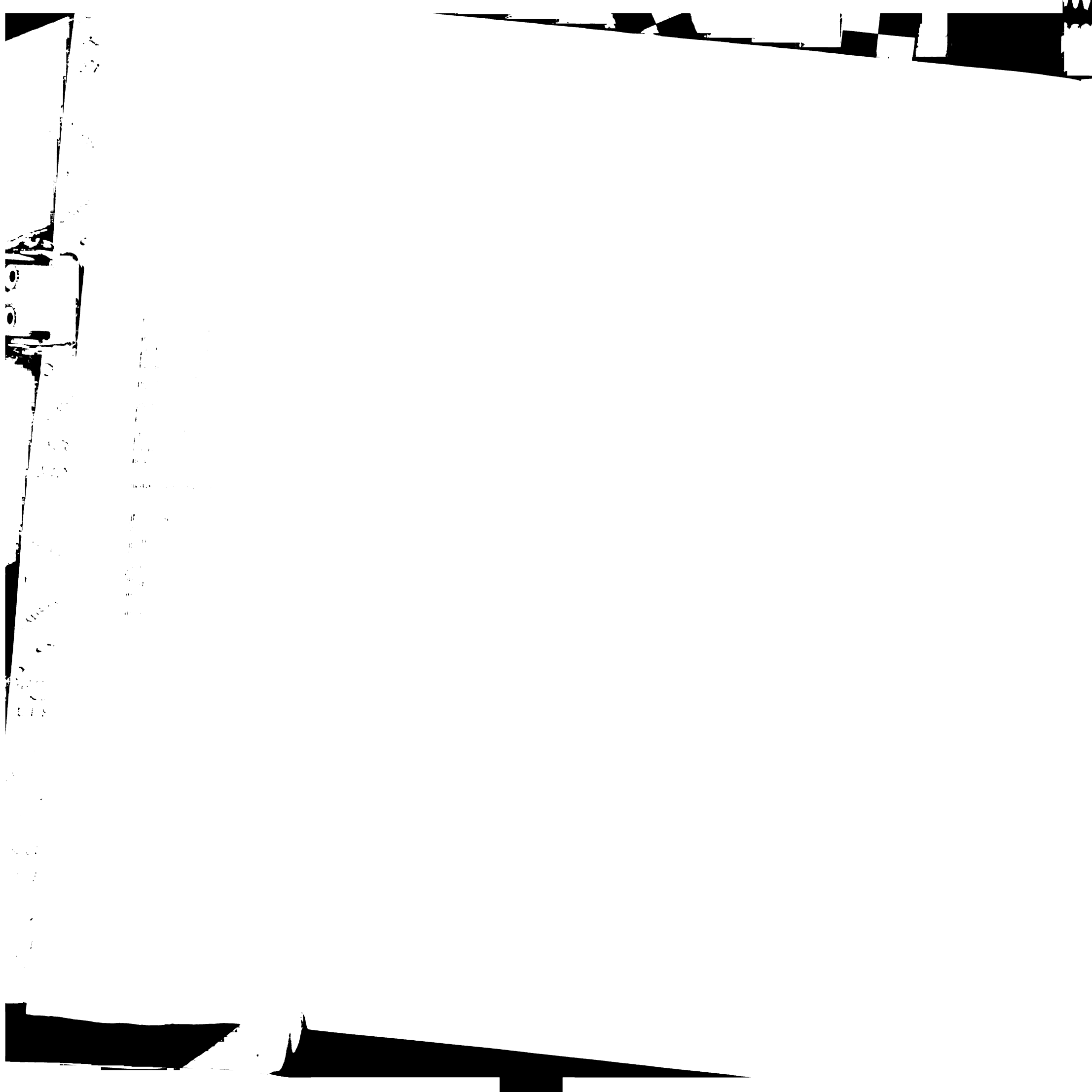
Pringle, J. R., Adams, A.E.M., Drubin, D.G., and Haarer, B.K. (1991). Immunofluorescence methods for yeast. In *Methods in Enzymology: Guide to Yeast Genetics and Molecular Biology*, C. Guthrie and G. R. Fink, eds. (San Diego: Academic Press, Inc.), pp. 565-601.

Ramain, P., Heitzler, P., Haenlin, M., and Simpson, P. (1993). *pannier*, a negative regulator of *achaete* and *scute* in *Drosophila*, encodes a zinc finger protein with homology to the vertebrate transcription factor GATA-1. *Development* 119, 1277-1291.

Rhyu, M.S., Jan, L.Y., and Jan, Y.N. (1994). Asymmetric distribution of numb protein during division of the sensory organ precursor cell confers distinct fates to daughter cells. *Cell* 76, 477-491.

Richardson, H.E., Lew, D.J., Henze, M., Sugimoto, K., and Reed, S.I. (1989). An essential G1 function for cyclin-like proteins in yeast. *Cell* 59, 1127-1133.

Roemer, T., Madden, K., Chang, J.T., and Snyder, M. (1996). Selection of axial growth sites in yeast requires Axl2p, a novel plasma membrane glycoprotein. *Genes and Dev.* 10(7), 777-793.



Rose, M. D., Winston, F., and Hieter, P. (1990). *Methods in Yeast Genetics: A Laboratory Course Manual* (Cold Spring Harbor, New York: Cold Spring Harbor Laboratory Press).

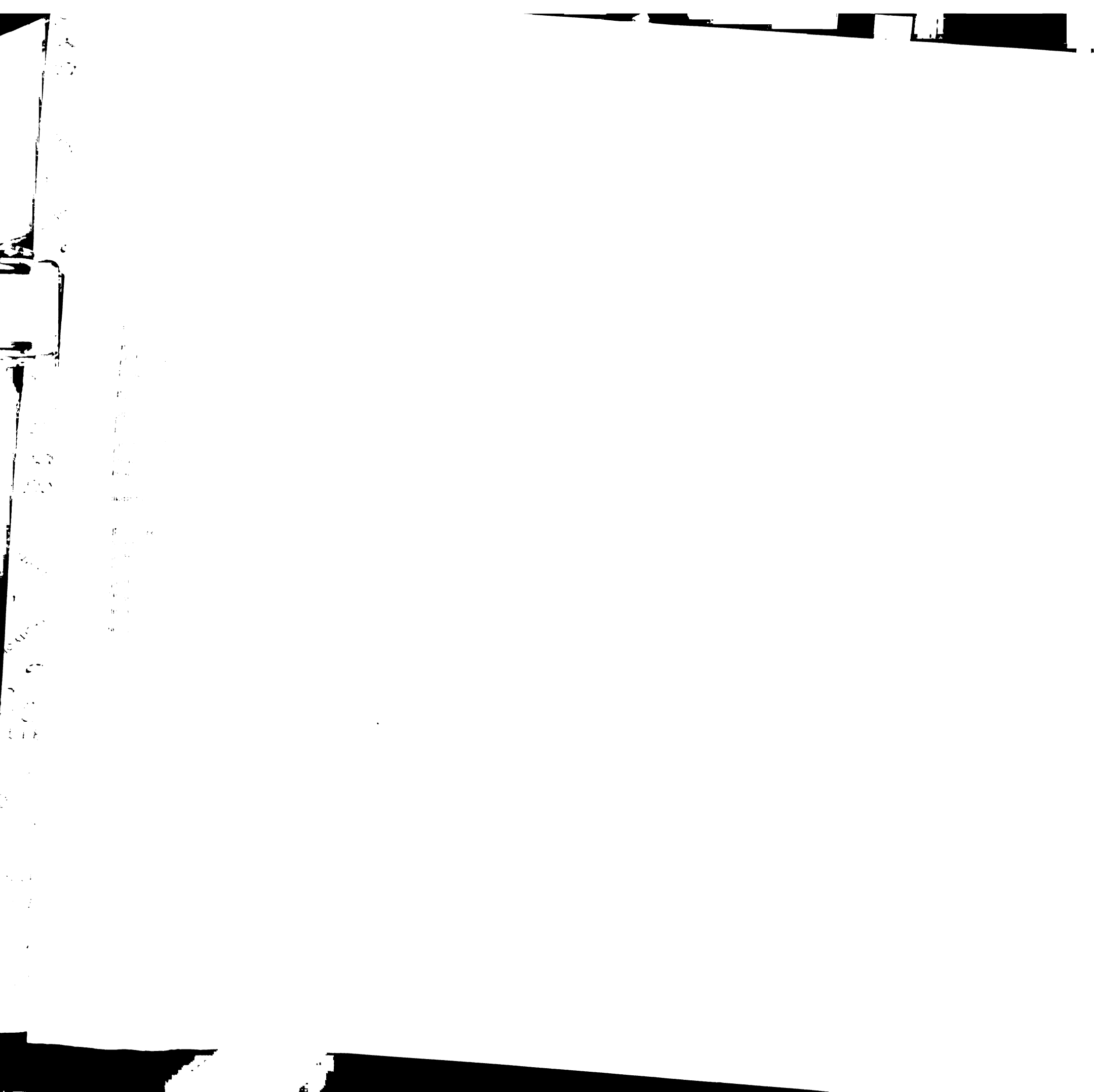
Rothstein, R. (1991). Targetting, disruption, replacement, and allele rescue: integrative DNA transformation in yeast. In *Methods in Enzymology: Guide to Yeast Genetics and Molecular Biology*, C. Guthrie and G. R. Fink, eds. (San Diego: Academic Press), pp. 281-301.

Sambrook, J., Fritsch, E.F., and Maniatis, T. (1989). *Molecular cloning: A laboratory manual*, 2nd ed. (Cold Spring Harbor, New York: Cold Spring Harbor Laboratory Press).

Sanders, S.L. and Herskowitz, I. (1996). The Bud4 protein of yeast, required for axial budding, is localized to the mother/bud neck in a cell cycle-dependent manner. *J. Cell Biol.* 134(2), 413-427.

Schultz, L.D., and Friesen, J.D. (1983). Nucleotide sequence of the *TCM1* gene (ribosomal protein L3) of *Saccharomyces cerevisiae*. *J. Bacteriol.* 155, 8-14.

Schwob, E., and Nasmyth, K. (1993). *CLB5* and *CLB6*, a new pair of B cyclins involved in DNA replication in *Saccharomyces cerevisiae*. *Genes Dev.* 7, 1160-1175.



Shapiro, L. (1995). The Bacterial Flagellum: From Genetic Network to Complex Architecture. *Cell* 80, 525-527.

Sikorski, R.S. and Hieter, P. (1989) A system of shuttle vectors and yeast host strains designed for efficient manipulation of DNA in *Saccharomyces cerevisiae*. *Genetics* 122, 19-27.

Sloat, B., Adams, A., and Pringle, J. (1981). Roles for the *CDC24* gene product in cellular morphogenesis during the *Saccharomyces cerevisiae* cell cycle. *J. Cell Biol.* 89, 395-405.

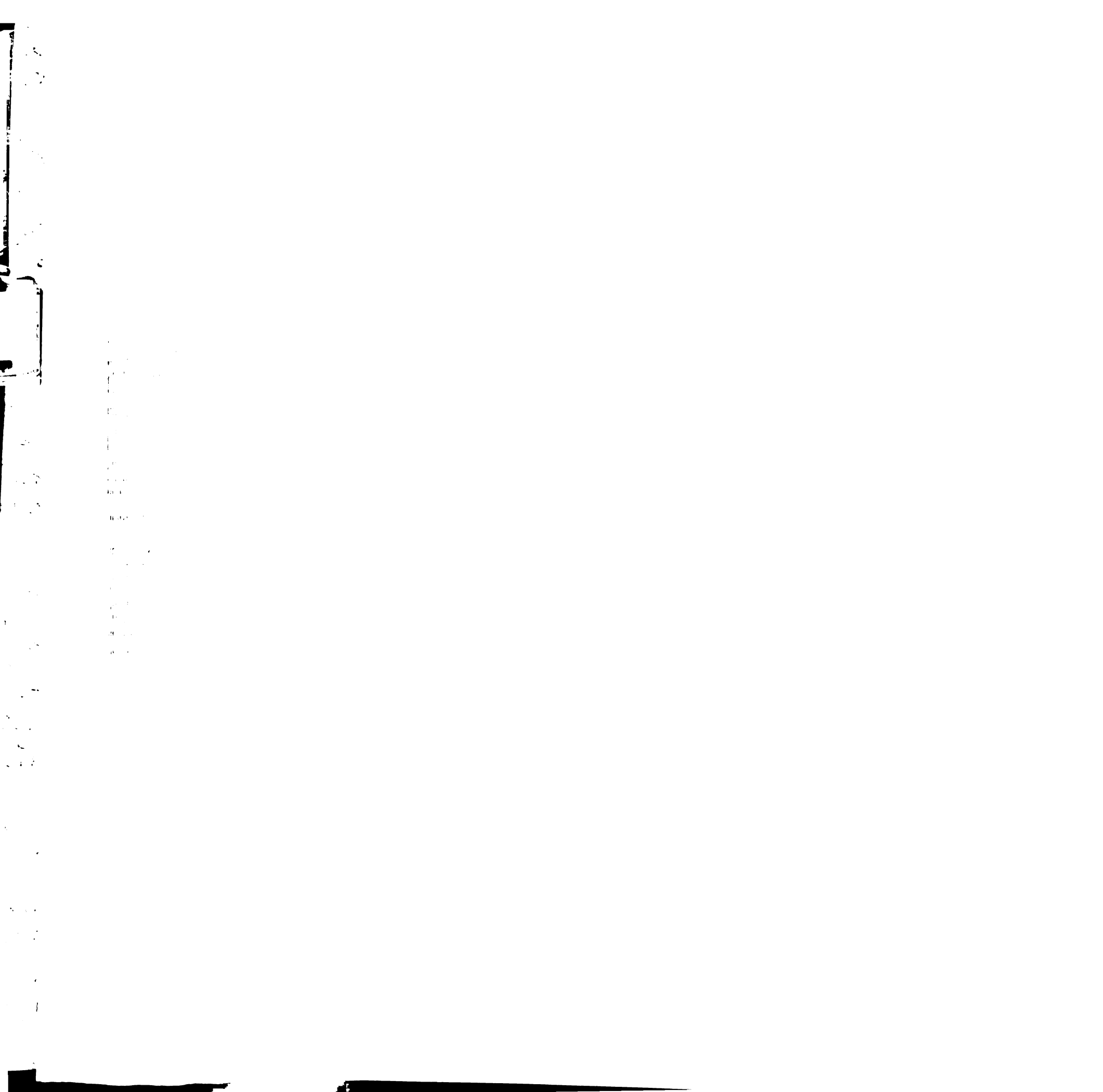
Snyder, M. (1989). The *SPA2* protein of yeast localizes to sites of cell growth. *J. Cell Biol.* 108, 1419-1429.

Snyder, M., Gehrung, S., and Page, B. D. (1991). Studies concerning the temporal and genetic control of cell polarity in *Saccharomyces cerevisiae*. *J. Cell Biol.* 114, 515-532.

St Johnston, D. (1995). The intracellular localization of messenger RNAs. *Cell* 81, 161-170.

Stern, M., Jensen, R., and Herskowitz, I. (1984). Five *SWI* genes are required for expression of the *HO* gene in yeast. *J. Mol. Biol.* 178, 853-868.

Stern, M. (1995). *Genes Controlling the Expression of the HO gene in yeast*: University of California, San Francisco.



Sternberg, P.W., Stern, M.J., Clark, I., and Herskowitz, I. (1987). Activation of the yeast *HO* gene by release from multiple negative controls. *Cell* 48, 567-577.

Stillman, D.J., Bankier, A.T., Seddon, A., Groenhout, E.G., and Nasmyth, K.A. (1988). Characterization of a transcription factor involved in mother cell specific transcription of the yeast *HO* gene. *Embo J.* 7(2):485-94.

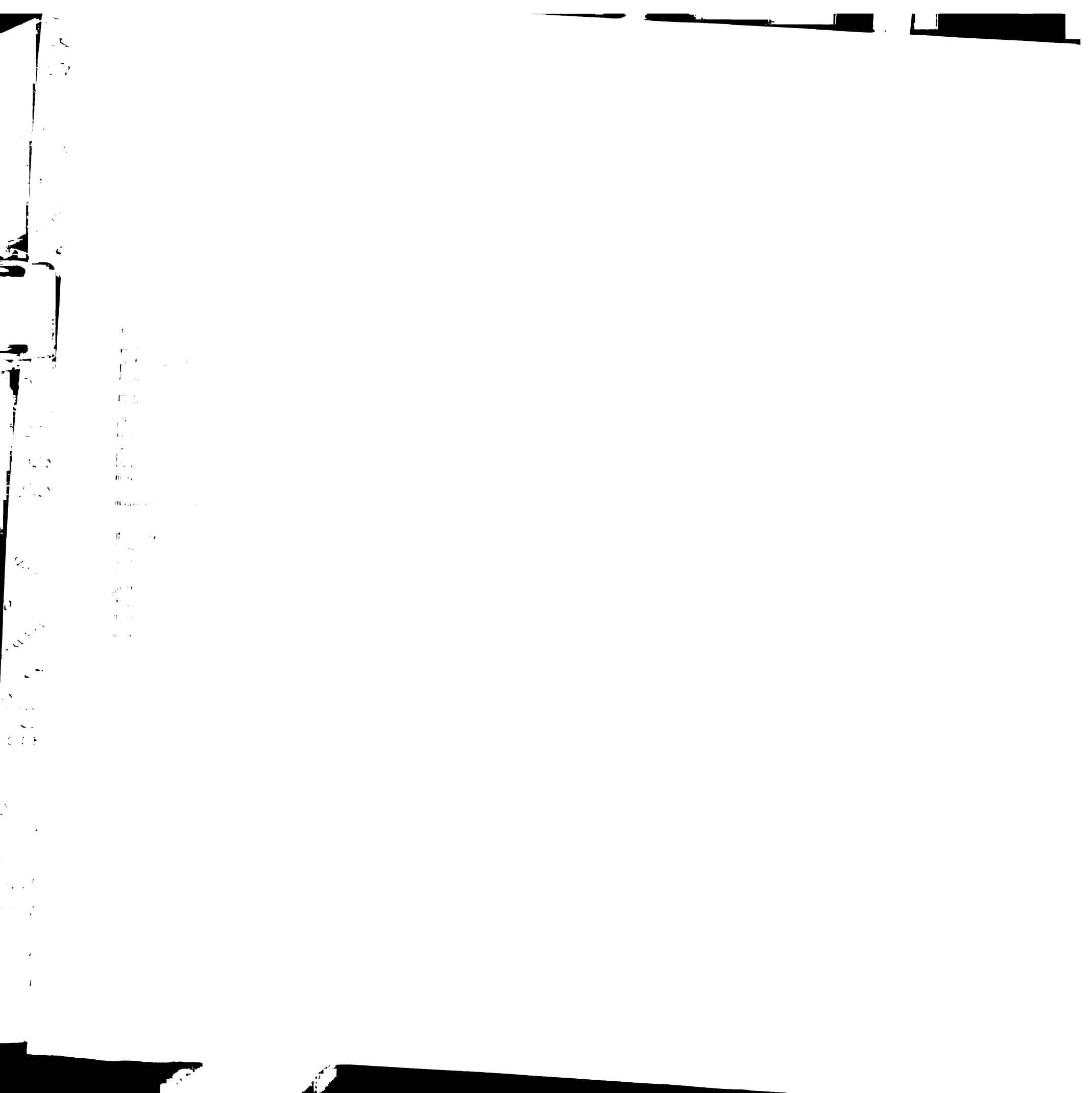
Stragier, P. and Losick, R. (1990). Cascades of sigma factors revisited. *Mol. Microbiol.* 4, 1801-1806.

Strathern, J.N., Blair, L.C., and Herskowitz, I. (1979). Healing of *mat* mutations and control of mating type interconversion by the mating type locus in *Saccharomyces cerevisiae*. *Proc. Natl. Acad. Sci.* 76, 3425-3429.

Strathern, J.N., and Herskowitz, I. (1979). Asymmetry and directionality in production of new cell types during clonal growth: the switching pattern of homothallic yeast. *Cell* 17, 371-381.

Tebb, G., Moll, T., Dowzer, C., and Nasmyth, K. (1993). *SWI5* instability may be necessary but is not sufficient for asymmetric *HO* expression in yeast. *Genes Dev.* 7, 517-528.

Voisard, C., Wang, J., McEvoy, J.L., Xu, P., and Leong, S.A. (1993). *urbs1*, a gene regulating siderophore biosynthesis in *Ustilago maydis*, encodes a protein



similar to the erythroid transcription factor GATA-1. *Mol. Cell. Biol.* 13, 7091-7100.

Wingrove, J.A. and Gober, J.W. (1994). A sigma 54 transcriptional activator also functions as a pole-specific repressor in *Caulobacter*. *Genes Dev.* 8(15), 1839-1852.

Wingrove, J.A. and Gober, J.W. Regulation of Temporal and Spatial Transcription by Asymmetric Localization of a Sensor Histidine Kinase. *Science*, in press.

Wingrove, J.A., Mangan, E.K., and Gober, J.W. (1993). Spatial and temporal phosphorylation of a transcriptional activator regulates pole-specific gene expression in *Caulobacter*. *Genes Dev.* 7(10), 1979-1992.

Zahner, J.E., Harkins, H.A., and Pringle, J.R. (1996). Genetic analysis of the bipolar pattern of bud site selection in the yeast *Saccharomyces cerevisiae*. *Mol. Cell. Biol.* 16(4), 1857-1870.

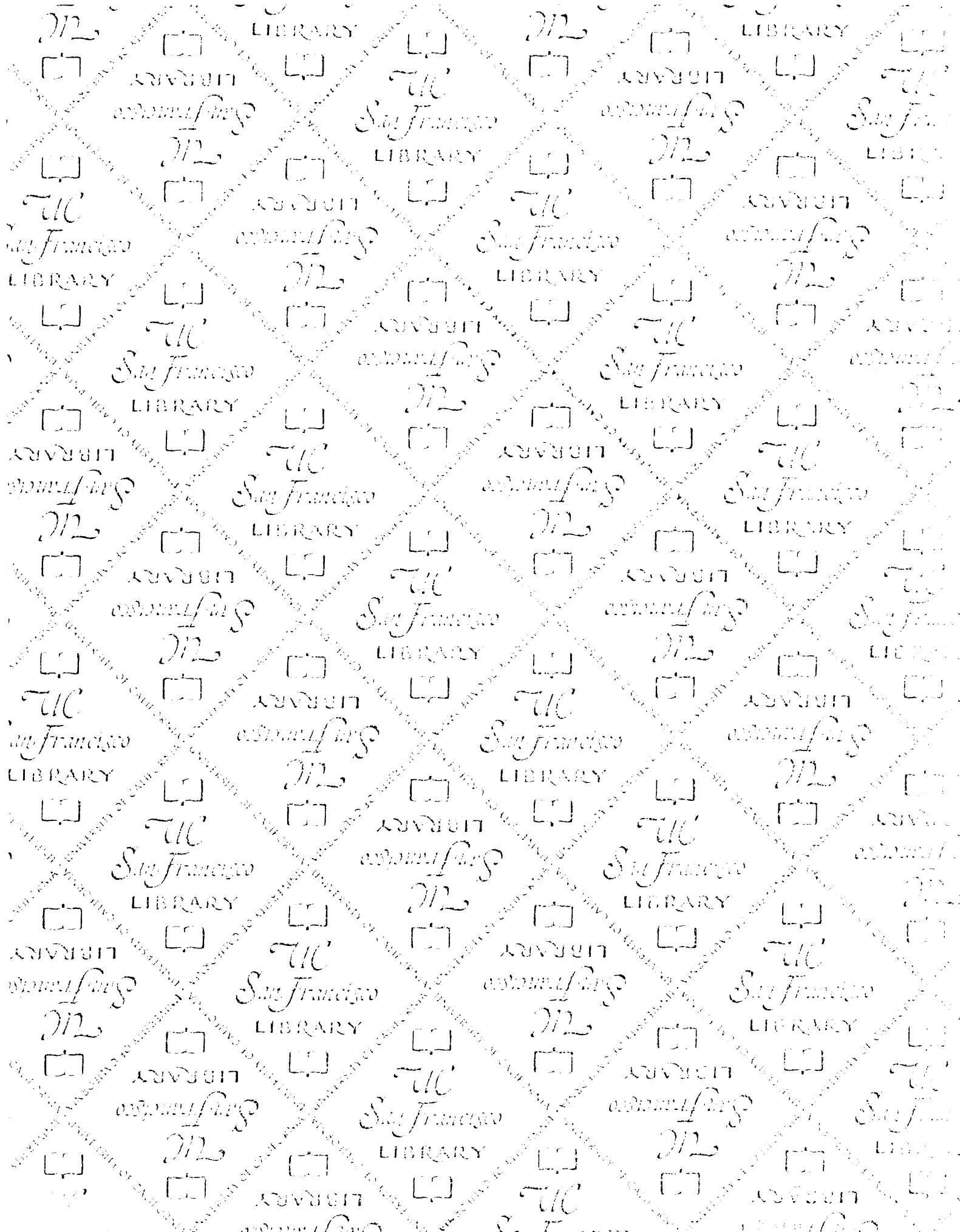
1. The first part of the document is a list of names and addresses of the members of the committee. The names are listed in alphabetical order, and the addresses are given in full. The list includes the names of the members of the committee, the names of the members of the sub-committee, and the names of the members of the advisory committee. The addresses are given in full, including the street, city, and state.

2. The second part of the document is a list of the names and addresses of the members of the committee. The names are listed in alphabetical order, and the addresses are given in full. The list includes the names of the members of the committee, the names of the members of the sub-committee, and the names of the members of the advisory committee. The addresses are given in full, including the street, city, and state.

3. The third part of the document is a list of the names and addresses of the members of the committee. The names are listed in alphabetical order, and the addresses are given in full. The list includes the names of the members of the committee, the names of the members of the sub-committee, and the names of the members of the advisory committee. The addresses are given in full, including the street, city, and state.

1. The first part of the document is a list of names and addresses of the members of the committee. The names are listed in alphabetical order, and the addresses are given in full. The list includes the names of the members of the committee, the names of the members of the sub-committee, and the names of the members of the advisory committee. The addresses are given in full, including the street name, the city, and the state.

2. The second part of the document is a list of the names and addresses of the members of the committee. The names are listed in alphabetical order, and the addresses are given in full. The list includes the names of the members of the committee, the names of the members of the sub-committee, and the names of the members of the advisory committee. The addresses are given in full, including the street name, the city, and the state.



For reference

Not to be taken from the room.

